Scalar-Tensor Theories for Dark Energy and their Cosmological Consequences

Gregory Ian Sculthorpe

School of Mathematics and Statistics

Submitted for the degree of Doctor of Philosophy

February 2014

Supervisor: Professor Carsten van de Bruck

University of Sheffield

Abstract

One of the major outstanding questions in cosmology today is the nature of dark energy, the cause of the observed recent accelerated expansion of the universe. This thesis considers scalar-tensor theories as a possible candidate for dark energy and explores their observational consequences. The evolution equations for perturbation equations of a fluid, either relativistic or non-relativistic, disformally coupled to the scalar field are derived for the first time. A new observational probe for such theories, CMB μ-distortion, is then investigated. The effects of screened models of modified gravity on the CMB angular power spectrum are considered, looking at the potential for these to provide constraints on the models, even after imposing constraints coming from local tests and BBN. Finally, in the context of coupled quintessence, the initial conditions for general perturbation modes are derived with a view to determining whether the constraint on the coupling strength may be relaxed when the assumption of adiabatic initial conditions is lifted.

Preface

The majority of the work contained in this thesis was done by the author.

- Chapter 1 introduces the dark energy problem and reviews relevant material.
- Chapter 2 is based on work done with the author's supervisor and published in [33].
- Chapter 3 is based on work done in collaboration with C. van de Bruck, S. Clesse, P. Brax and A.-C. Davis, and published in [19]. The analytical work was done by the author, S. Clesse and P. Brax. The numerical work was done by the author and S. Clesse. All figures were produced by the author.
- The material in Chapter 4 was done by the author.

The author would like to thank Carsten for his help, encouragement and patience throughout the PhD.

Contents

1 Introduction **1**

1.1 The State of Modern Cosmology 1

1.2 The Standard Model of Cosmology 2

1.3 Cosmological Perturbations 5

1.4 The Dark Energy Problem 8

1.4.1 Observational Evidence for Dark Energy 8

1.4.2 Models of Dark Energy 12

1.5 Outline 25

2 CMB μ–distortion **27**

2.1 Introduction 27

2.2 Evolution of Perturbations in Disformal Theories 28

2.2.1 General Equations 28

2.2.2 Tight-Coupling Approximation 32

2.2.3 Silk Damping 34

2.3 μ-type distortion due to dissipation of acoustic waves 36

2.4 Conclusions 42

3 Screened Modified Gravity and the CMB **45**

3.1 Introduction 45

3.2 Screened Modified Gravity 46

3.3 Perturbations 47

3.4 The models 51

3.4.1 Generalised Chameleons 51

3.4.2 Transition in β 51

3.4.3 BBN Constraint 52

3.4.4 Local tests 54

3.5 Numerical implementation 57

3.6 Numerical results 60
3.6.1 Transition in β 60
3.6.2 Generalised chameleons 69
3.7 Conclusion 69

4 Isocurvature Modes in Coupled Quintessence 72
4.1 Introduction 72
4.2 The Effect of a Coupling on Background Variables 73
4.3 Early Time Perturbation Equations 74
4.4 Mode Solutions 79
4.4.1 Constant Modes 80
4.4.2 Growing Modes 83
4.4.3 Transforming to Synchronous Gauge 84
4.4.4 Initial Conditions for Modes in Synchronous Gauge 85
4.5 Numerical Results for CMB Angular Power Spectrum 92
4.6 Conclusions 93

5 Conclusions 95

Chapter 1

Introduction

§ 1.1 The State of Modern Cosmology

In the last two decades cosmology has entered an era of precision observations of the cosmic microwave background, large scale structure and type 1a supernovae among others. These observations have provided strong evidence for the standard Big Bang model of cosmology in which the universe has expanded and cooled over time and is homogeneous and isotropic on large scales. It has also been established that the universe is spatially flat to high accuracy. However, these observations have also indicated that our understanding of the universe is far from complete. It seems that only 5% of the energy in the universe is in the form of normal matter and radiation which we understand. The remaining 95% is thought to be in the form of dark matter and dark energy neither of which has been directly detected. Dark matter is needed to explain the gravitational behaviour of galaxies and clusters of galaxies. Most problematic, there is now overwhelming evidence that the expansion of the universe is accelerating. If Einstein's equations of General Relativity are correct then this means that the energy density of the universe is currently dominated by a form of energy with negative pressure, known as dark energy. The simplest possibility is a cosmological constant Λ and indeed all observations to date are consistent with this. However, the natural interpretation of Λ would be the quantum mechanical vacuum energy density whose expected value from Quantum Field Theory has been calculated to be around 120 orders of magnitude greater than that inferred from cosmological observations. This is the cosmological constant problem and is one motivation for considering alternative models for dark energy.

§ 1.2 The Standard Model of Cosmology

The geometry of spacetime is described by a metric. The observed nature of the universe (homogeneous, isotropic and expanding) is represented by the Friedmann-Lemaître-Robertson-Walker (FLRW) metric:

$$ds^2 = -dt^2 + a^2(t)\left[\frac{dr^2}{1-\kappa r^2} + r^2(d\theta^2 + \sin^2\theta \mathrm{d}\phi^2)\right], \tag{1.1}$$

where $a(t)$ is the scale-factor which is the ratio of the comoving distance between two points, which remains constant, and the physical distance between them, which grows as the universe expands. Today, $a(t_0) = 1$. κ describes the spatial curvature of the universe where $\kappa = 0$ corresponds to spatial flatness and $\kappa = +1(-1)$ to a closed (open) universe.

General Relativity describes how the distributions of the various forms of energy in the universe determine the geometry of spacetime. This is contained in Einstein's equations:

$$G_{\mu\nu} \equiv R_{\mu\nu} - \frac{1}{2}g_{\mu\nu}R = 8\pi G_N\, T_{\mu\nu}\,, \tag{1.2}$$

where $G_{\mu\nu}$ is the Einstein tensor, G_N is Newton's constant and we have chosen natural units where the speed of light, $c = 1$. $R_{\mu\nu}$ is the Ricci tensor which depends on the metric and its derivatives and is given by

$$R_{\mu\nu} = \partial_\alpha \Gamma^\alpha_{\mu\nu} - \partial_\nu \Gamma^\alpha_{\mu\alpha} + \Gamma^\alpha_{\beta\alpha}\Gamma^\beta_{\mu\nu} - \Gamma^\alpha_{\beta\nu}\Gamma^\beta_{\mu\alpha}\,, \tag{1.3}$$

where

$$\Gamma^\lambda_{\mu\nu} = \frac{g^{\lambda\sigma}}{2}(\partial_\mu g_{\nu\sigma} + \partial_\nu g_{\sigma\mu} - \partial_\sigma g_{\mu\nu}) \tag{1.4}$$

are the Christoffel connection coefficients. R is the Ricci scalar, which is the contraction of the Ricci tensor ($R \equiv g^{\mu\nu}R_{\mu\nu}$). The energy-momentum tensor takes the perfect fluid form,

$$T_{\mu\nu} = (\rho + p)U_\mu U_\nu + p g_{\mu\nu}, \tag{1.5}$$

where ρ, p and U_μ are the total energy density, pressure and four-velocity of the constituents of the universe. Conservation of energy-momentum means that

$$\nabla_\mu T^\mu_\nu = \partial_\mu T^\mu_\nu + \Gamma^\mu_{\mu\lambda}T^\lambda_\nu - \Gamma^\lambda_{\mu\nu}T^\mu_\lambda = 0\,. \tag{1.6}$$

For a perfect fluid with equation of state given by

$$p = w\rho, \tag{1.7}$$

equation (1.6) yields

$$\dot{\rho} = -3\frac{\dot{a}}{a}(1+w)\rho, \tag{1.8}$$

where the dots represent derivatives with respect to time. This equation can be integrated to give

$$\rho \propto a^{-3(1+w)}. \tag{1.9}$$

Using the FRW metric in Eq. (1.1) the following equations for the evolution of the universe may be derived from (1.2):

$$H^2 \equiv \left(\frac{\dot{a}}{a}\right)^2 = \frac{8\pi G}{3}\rho - \frac{\kappa}{a^2}\,, \tag{1.10}$$

$$\frac{\ddot{a}}{a} = -\frac{4\pi G}{3}(\rho + 3p)\,. \tag{1.11}$$

These two equations are often referred to as the Friedmann equation and acceleration equation respectively.

Looking at (1.10), we may define a critical energy density,

$$\rho_{crit} \equiv \frac{3H^2}{8\pi G} \tag{1.12}$$

for which the $\kappa = 0$ and the universe is exactly spatially flat. As previously mentioned observational evidence (see for example [1]) now indicates that the effect of the curvature of the universe today (the last term in (1.10)) is negligible. Although this does not give us the actual value of κ, it means that neglecting the terms involving it is a reasonable approximation at late times, and so for simplicity we will assume $\kappa = 0$ from now on. Under this assumption (1.12) is also the total energy density and we will find it convenient to define the fractional energy densities of the various energy species as

$$\Omega_\alpha \equiv \frac{8\pi G\rho_\alpha}{3H^2}\,. \tag{1.13}$$

The fact that the universe is expanding at all was first discovered by Edwin Hubble in 1929 who found that distant galaxies are receding from us with a velocity proportional to their distance from us [61]. This has become known as Hubble's law, $v = Hd$, H being the Hubble parameter defined in (1.10) and $H_0 = 100h\,\mathrm{km\,s^{-1}Mpc^{-1}}$ is

its value today. Data from the Hubble Space Telescope Key Project [51], PLANCK [1] and other observations constrain $h \approx 0.7$.

If the universe is expanding then it follows that in the past it was smaller, denser and therefore hotter. Also, since the energy density of photons and other relativistic particles decreases as $\rho_r \sim a^{-4}$ whilst that of matter scales as $\rho_m \sim a^{-3}$, the universe was dominated by radiation at early times. Initially the temperature was so great that all the various fundamental particles existed in a plasma, colliding and scattering off one another so frequently that they were in equilibrium, but unable to combine to form nuclei or atoms that would not be destroyed by high energy photons. As the temperature dropped and the photon energies decreased below the binding energies of the nuclei, light elements such as deuterium, helium and lithium were able to form. This occured when the universe was only a few minutes old and is known as Big Bang Nucleosynthesis (BBN). The exact physics of the processes depends on the densities of the particles involved which in turn is determined by the expansion rate. The resulting primordial light element abundances can therefore be predicted and measurements of them, coming from the spectra of distant quasars, confirm the standard Big Bang model. On top of this, the same measurements can be used to calculate the energy density of baryons (normal matter) and provide some of the strongest evidence of the need for dark matter to be consistent with the flatness of the universe.

For around three hundred thousand years after BBN the temperature of the photons was still too high to allow the electrons to combine with nuclei to form atoms. During this time the photons and electrons were tightly coupled via Compton scattering and the protons and electrons by Coulomb scattering so that there existed a photon-baryon plasma. The pull on the baryons from gravitational potentials associated with over-dense regions was counterbalanced by the pressure of the photons resisting compression with the result of acoustic oscillations in the plasma. At the epoch of recombination the temperature dropped sufficiently for the baryons to form atoms and the photons to decouple from them, free-streaming to us from the surface of last scattering. These photons are what we observe today as the cosmic microwave background (CMB). Before last scattering the collisions with the electrons ensured that the photons were in thermal equilibrium and so should have a blackbody spectrum. Observations [75] have confirmed this to high precision, providing further compelling evidence for the Big Bang. Anistropies in the CMB, which correspond to the inhomogeneities in the photon distribution, were first observed by COBE [91] in 1992 and have since been measured to high precision by WMAP [14] and PLANCK [1].

The resulting angular power spectrum contains a series of peaks and troughs, produced by the acoustic oscillations, whose positions and amplitudes depend heavily on the cosmological parameters and so the observational data can be used to constrain them. In particular the position of the first peak indicates that the universe is very close to being spatially flat and therefore the total energy density of the universe is very close to being critical. Since other measurements demonstrate that matter and radiation only make up around 30% of this density, this also contributes to the evidence that there must be another form of energy in the universe.

§ 1.3 Cosmological Perturbations

The inhomogeneities in the distributions of the matter and radiation fluids are represented by perturbations to the energy-momentum tensor. To first order in perturbations, $T^{\mu}_{\ \nu}$ is given by [73]

$$T^0_0 = -(\rho + \delta\rho)\,, \tag{1.14}$$

$$T^0_i = (\rho + p)v_i = -T^i_0\,, \tag{1.15}$$

$$T^i_j = (p + \delta p)\delta^i_j + \Sigma^i_j\,, \quad \Sigma^i_i = 0\,, \tag{1.16}$$

where $v_i \equiv dx^i/d\tau$ is the fluid velocity and Σ^i_j represents the anisotropic stress. We also introduce the density contrast $\delta \equiv \delta\rho/\rho$ which will be much used in later subsequent chapters.

It is convenient to use a different time variable: the distance light could have travelled since $t = 0$, which is called the conformal time and defined as

$$\tau \equiv \int_0^t \frac{dt'}{a(t')}\,. \tag{1.17}$$

Dots will now denote derivatives with respect to τ rather t.

Perturbations to a flat FRW metric can be written most generally as [73]

$$g_{00} = -a^2(\tau)[1 + 2\Psi]\,, \tag{1.18}$$

$$g_{0i} = a^2(\tau)w_i\,, \tag{1.19}$$

$$g_{ij} = a^2(\tau)[(1 - 2\Phi)\delta_{ij} + \chi_{ij}]\,, \quad \chi_{ii} = 0\,, \tag{1.20}$$

where the functions Ψ, Φ, w_i and χ_{ij}, which represent the perturbations to the metric, all depend on space and time. The correspondence between points in the physical spacetime and points in the background defines a choice of gauge. The

two most frequently used gauges in cosmology are the synchronous gauge and the conformal Newtonian gauge. In the synchronous gauge only the spatial part of the metric is perturbed. The line element is given by

$$ds^2 = a^2(\tau)[-d\tau^2 + (\delta_{ij} + h_{ij})dx^i dx^j]\,, \tag{1.21}$$

and for scalar modes the metric perturbation h_{ij} can be written as a Fourier integral [73]

$$h_{ij}(\boldsymbol{x},\tau) \;=\; \int d^3k e^{i\boldsymbol{k}\cdot\boldsymbol{x}}[\hat{\boldsymbol{k}}_i\hat{\boldsymbol{k}}_j h(\boldsymbol{k},\tau) + (\hat{\boldsymbol{k}}_i\hat{\boldsymbol{k}}_j - \tfrac{1}{3}\delta_{ij})6\eta(\boldsymbol{k},\tau)]\,, \tag{1.22}$$

where $h \equiv h_{ii}$ and η are the trace and traceless parts respectively of h_{ij} and $\boldsymbol{k} = k\hat{\boldsymbol{k}}$. In the conformal Newtonian gauge the line element is

$$ds^2 = a^2(\tau)[-(1+2\Psi)d\tau^2 + (1-2\Phi)\gamma_{ij}dx^i dx^j]\,. \tag{1.23}$$

We shall use both gauges in this thesis, the Newtonian for analytical calculations and the synchronous for numerical work. Following [73] we now give the Einstein equations to first order in perturbations for both gauges. In the synchronous gauge they are

$$k^2\eta - \frac{1}{2}H\dot{h} = -4\pi G a^2\delta\rho\,, \tag{1.24}$$

$$k^2\dot{\eta} = 4\pi G a^2(\rho+p)\theta\,, \tag{1.25}$$

$$\ddot{h} + 2H\dot{h} - 2k^2\eta = -24\pi G a^2\delta p\,, \tag{1.26}$$

$$\ddot{h} + 6\ddot{\eta} + 2H(\dot{h} + 6\dot{\eta}) - 2k^2\eta = -24\pi G a^2(\rho+p)\sigma\,, \tag{1.27}$$

where k is the wavenumber of the perturbations, $\theta = ik^j v_j$ is the divergence of the fluid velocity and σ is defined as

$$(\rho+p)\sigma \equiv -(\hat{\boldsymbol{k}}_i\cdot\hat{\boldsymbol{k}}_j - \tfrac{1}{3}\delta_{ij})\Sigma^i_j\,. \tag{1.28}$$

In the conformal Newtonian gauge the four equations are

$$k^2\Phi + 3H(\dot{\Phi} + H\Psi) = -4\pi G a^2 \delta\rho\,, \tag{1.29}$$

$$k^2(\dot{\Phi} + H\Psi) = 4\pi G a^2(\rho + p)\theta\,, \tag{1.30}$$

$$\ddot{\Phi} + H(\dot{\Psi} + 2\dot{\Phi}) + \left(2\frac{\ddot{a}}{a} - H^2\right)\Psi + \frac{k^2}{3}(\Phi - \Psi) = 4\pi G a^2 \delta p\,, \tag{1.31}$$

$$k^2(\Phi - \Psi) = 12\pi G a^2(\rho + p)\sigma\,. \tag{1.32}$$

It should be noted that the perturbation variables $\delta\rho$, δp and θ in one gauge are different from those in the other gauge and are related by gauge transformations given by [73]. The perturbation σ is in fact the same in both gauges.

Relativistic particles cannot accurately be described like a perfect fluid by only their density and velocity [47]. Instead perturbations to the photon distribution are conventionally expressed as the fractional temperature difference, $\Theta(\mathbf{x}, \hat{p}, \tau) \equiv \delta T/T$, which depends on $\hat{p}$, the direction of the photon's propagation, as well as position and time. As above we work in Fourier space defining

$$\Theta(\mathbf{x}, \hat{p}) = \int \frac{d^3k}{(2\pi)^3}\Theta(k, \mu)e^{i\mathbf{k}\cdot\mathbf{x}}\,, \tag{1.33}$$

where

$$\mu = \frac{\mathbf{k}\cdot\hat{\mathbf{p}}}{k}\,. \tag{1.34}$$

The multipole moments are then defined as

$$\Theta_l \equiv \frac{1}{(-i)^l}\int_{-1}^{1}\frac{d\mu}{2}\mathcal{P}_l(\mu)\Theta(\mu)\,, \tag{1.35}$$

where $\mathcal{P}_l$ is the Legendre polynomial of order l.

Observations of the CMB measure temperature anisotropies. These are related to the perturbations in the temperature Θ by expanding in spherical harmonics:

$$\Theta = \sum_{l=1}^{\infty}\sum_{m=-l}^{l} a_{lm}Y_{lm}\,, \tag{1.36}$$

and the coefficients a_{lm} are assumed to be statistically independent with variance $C_l \equiv \langle|a_{lm}|^2\rangle$. This can be expressed in terms of Θ_l by [8]

$$C_l = \frac{2}{\pi}\int_0^{\infty} dk k^2|\Theta_l(k)|^2\,. \tag{1.37}$$

§ 1.4 The Dark Energy Problem

The original evidence for dark energy, coming from observations of type 1a supernovae [89, 81], was that the expansion of the universe is accelerating. This was a major surprise as we can see from looking at equation (1.11). In order for accelerated expansion ($\ddot{a} > 0$) we require $p < -\frac{1}{3}\rho$. That is, the total pressure of the universe is negative. Bearing in mind that the known contituents of the universe, matter and radiation, have equation of state parameters $w = 0$ and $w = \frac{1}{3}$ respectively, this implies the existence of some new, exotic form of energy.

1.4.1 Observational Evidence for Dark Energy

Type Ia Supernovae

Many astronomical observations use the idea of luminosity distance. It is related to the luminosity of the source, L_s, and the energy flux we observe today, F, in the following way

$$d_L^2 \equiv \frac{L_s}{4\pi F}\,. \tag{1.38}$$

Type Ia supernovae (SNe Ia) occur when a white dwarf star in a binary system reaches the Chandrasekhar limiting mass as a result of accreting matter from its companion. In theory, the peak luminosity of SNe Ia is solely determined by their mass and so should be constant. This would mean they could be used as standard candles, objects whose apparent brightness only depends on their distance from us. In practice, however, the peak luminosities vary too much but in the 1990's a correlation was found between the peak luminosity and the rate at which the luminosity declines [54]. Using this it is possible to estimate the intrinsic luminosity accurately enough to measure the luminosity distance. The redshift, z, of the supernovae is measured using their spectra. In a flat universe the luminosity distance and redshift of an object are related through the following expression

$$d_L = (1+z)\int_0^z \frac{dz'}{H(z')}\,. \tag{1.39}$$

Using Eq. (1.10) this leads to

$$d_L = \frac{1+z}{H_0}\int_0^z \frac{dz'}{\sqrt{\sum_i \Omega_i^{(0)}(1+z')^{3(1+w_i)}}}\,, \tag{1.40}$$

where H_0 is the Hubble parameter at the present time and $\Omega_i^{(0)} = \rho_i^{(0)}/\rho_{tot}^{(0)}$ and $w_i = p_i/\rho_i$ are the fractional energy density at the present time and the equation of state respectively, for each energy component. In the 1990's two teams, the Supernova Cosmology Project and the High-z Supernova Search, measured the brightnesses and redshifts of type Ia supernovae and then compared the resulting Hubble diagram plots with theoretical curves for different cosmological models [89, 81]. They found that the more distant supernovae were dimmer than would be expected if the universe contained only matter and radiation and when the results were analysed assuming the universe contained matter and dark energy they required $\Omega_{\rm DE} > 0$ at greater than 99% confidence.

CMB

As mentioned previously the CMB data constrains the geometry of the universe to be very close to spatial flatness and in combination with other observations this suggests that, if General Relativity is correct, the present energy density of the universe is dominated by some form of dark energy. In addition, there are two main ways that dark energy itself affects the CMB spectrum. The first is a change in the locations of the acoustic peaks through the modified expansion rate. The second is the integrated Sachs-Wolfe (ISW) effect.

Just as distances can be related to luminosities, they can also be related to the angular size of features. The angular diameter distance is defined as

$$d_A \equiv \frac{\Delta x}{\Delta\theta}\,, \tag{1.41}$$

where Δx is the size of the object in the direction perpendicular to the line of sight and $\Delta\theta$ is the angle subtended. In a flat universe this leads to

$$d_A = \frac{1}{(1+z)}\int_0^z \frac{dz'}{H(z')}\,. \tag{1.42}$$

The positions of the acoustic peaks depend on the sound horizon at last scattering,

$$r_s(z_{\rm dec}) = \int_{z_{\rm dec}}^{\infty} \frac{c_s}{H(z)} dz, \tag{1.43}$$

where

$$c_s = \frac{1}{\sqrt{3(1+R)}} \tag{1.44}$$

is the effective speed of sound in the photon-baryon plasma and

$$R = \frac{3\rho_b}{4\rho_\gamma}, \tag{1.45}$$

with ρ_b and ρ_γ being the energy densities of baryons and photons respectively. Roughly speaking we expect peaks in the photon temperature distribution when

$$kr_s = n\pi. \tag{1.46}$$

This can be used to define a characteristic angle for the peaks [8]:

$$\theta_A \equiv \frac{r_s(z_{\rm dec})}{d_A^{(c)}(z_{\rm dec})}, \tag{1.47}$$

where $d_A^{(c)}(z) \equiv (1+z)d_A(z)$ is the comoving angular diameter distance and $z_{\rm dec}$ is the redshift of decoupling.

The corresponding multipole is

$$l_A \equiv \frac{\pi}{\theta_A} = \pi \frac{d_A^{(c)}(z_{\rm dec})}{r_s(z_{\rm dec})}. \tag{1.48}$$

The change in the expansion history due to dark energy will result in a different distance back to last scattering which in turn causes a shift in the positions of the peaks. For a fixed value of H_0 the angular diameter distance, like the luminosity distance, becomes larger as $\Omega_{\rm DE}$ is increased. However, in a flat universe, higher $\Omega_{\rm DE}$ means lower Ω_m which makes the sound horizon at last scattering bigger. This second effect is greater than the change to d_A and so l_A is smaller and the peaks move to larger scales. Alternatively, since the CMB spectrum is affected by the parameter $\omega_m \equiv \Omega_m h^2$ and so constrains it, we may choose to keep ω_m and r_s fixed. If so, decreasing Ω_m requires a higher value of h (and H_0). The overall result of increasing $\Omega_{\rm DE}$ is then to make the angular diameter distance smaller and decrease l_A. Either way, dark energy results in a shift of the peaks to larger angular scales.

The ISW effect is caused by the variation of the gravitational potentials since the time of last scattering. On scales larger than the Hubble radius the potentials are constant. Within the Hubble radius particles are in causal contact and the evolution of the potentials depends on the energy content. Since the end of inflation the Hubble radius has increased and so larger physical scales have gradually come inside it over time and perturbations on these scales are then affected by physical processes.

During radiation-domination the gravitational potentials within the Hubble radius decay whereas in a purely matter dominated universe the potentials remain constant. Decoupling occurs not so long after matter-radiation equality and so there is still a non-negligible amount of radiation and inside the Hubble radius the gravitational potentials continue to decay. This is the main contribution to the ISW effect and it results in an enhancement of the anisotropy with the biggest effect on scales around the first acoustic peak which entered the Hubble radius at the time of decoupling. There is also a late-time ISW effect caused by dark energy. As the expansion rate begins to accelerate, the growth of matter perturbations decreases and consequently the gravitational potentials once again decay. This primarily affects the very largest scales which have entered the Hubble radius recently and typically leads to an increase in power.

Large Scale Structure

The acoustic oscillations in the CMB leave their mark on the distibution of galaxies and clusters of galaxies. This leads to similar peaks and troughs in the matter power spectrum, referred to as the baryon acoustic oscillations (BAO), which have been detected by large galaxy surveys such as the Sloan Digital Sky Survey (SDSS). Differences in the cosmological model affect both the angular and redshift separations between galaxies and therefore the wavenumbers of features in the power spectrum both parallel and perpendicular to the line of sight. Ideally we would like to measure these dilations of scales separately but so far insufficient data has been gathered. Instead, [49] define the distance scale

$$D_V(z) \equiv \left[(1+z)^2 d_A^2 \frac{cz}{H(z)}\right]^{1/3}, \tag{1.49}$$

which is the cube root of the product of the dilation along the line of sight and the square of the transverse dilation. This distance is measured at $z = 0.35$, the typical redshift of their sample. A more robust measure comes from the ratio between this distance and the comoving angular diameter distance to last scattering:

$$R_{0.35} \equiv \frac{D_V(0.35)}{d_A^{(c)}(1089)}, \tag{1.50}$$

and [49] find $R_{0.35} \approx 0.0979$ which is consistent with ΛCDM and strongly disfavours a model without dark energy.

Another way in which the matter power spectrum depends on dark energy is through

the turnover scale. This corresponds to the wavenumber of modes entering the horizon at the time of matter-radiation equality which can be expressed as $k_{eq} = 0.073\Omega_m^{(0)}h^2$ Mpc^{-1}. If the universe if dominated by dark energy today then $\Omega_m^{(0)}$ will be smaller and so the power spectrum turns over on larger scales. The results from galaxy surveys favour ΛCDM.

The Age of the Universe

The age of the universe depends on the expansion history and therefore on its energy composition. In a flat universe the age is given by

$$\begin{aligned} t_0 &= \int_0^\infty \frac{dz}{H(1+z)} \\ &= \int_0^\infty \frac{dz}{H_0(1+z)\sqrt{\sum_i \Omega_i(0)(1+z)^{3(1+w_i)}}}\,. \end{aligned} \tag{1.51}$$

In a universe with only matter this reduces to

$$t_0 = \frac{2}{3H_0}\,. \tag{1.52}$$

Using the constraints on H_0 from the Hubble Space Telescope Key project [51] gives $t_0 = 8 - 10$Gyr. However observations [63, 35] have determined that the oldest stars in globular clusters have ages greater than 12Gyr. So these observations are inconsistent with a universe containing only matter. If, however a cosmological constant is included in the Einstein equations then the calculated age is $t_0 = 13.1$Gyr. This is consistent with the globular cluster observations and provides further evidence of the need for some form of dark energy.

To conclude, there is now strong evidence from a variety of observations for a new form of energy with negative pressure. The question is what is it?

1.4.2 Models of Dark Energy

Many models for explaining dark energy have been proposed but they fall into three general groups. The first is just the cosmological constant, the second is scalar fields and the third is modified gravity.

The Cosmological Constant

The cosmological constant was first introduced by Einstein in order for his equations of general relativity to allow for a static universe, as he believed this to be the case. However, after Edwin Hubble's observations of the recession of galaxies indicated that the universe was expanding he famously called the cosmological constant his "greatest blunder". In spite of this the idea didn't die as it turned out that particle physics predicts there to be a vacuum energy density which would correspond to a cosmological constant. When an expected value of the vacuum energy was calculated it was found to be about 121 orders of magnitude greater than the critical density required for a flat universe (see, for example, section 6.3 of [8]). This is known as the cosmological constant problem and many attempts have been made to resolve it.

The discovery of the expansion of the universe is consistent with a very small vacuum energy. When a cosmological constant is included in Einstein's equations the acceleration equation is modified as follows

$$\frac{\ddot{a}}{a} = -\frac{4\pi G}{3}(\rho + 3p) + \frac{\Lambda}{3}\,. \tag{1.53}$$

This has the effect of a negative pressure leading to accelerated expansion. The challenge now is to either explain why the vacuum energy should be so much smaller than theoretically expected or to find a mechanism to make it zero and look for other solutions to the dark energy problem. For example, Supersymmetry, a theory which says that every fermion has a bosonic partner and vice versa, would cancel out the vacuum energy entirely. However this symmetry isn't seen in nature and so it must have been broken. This leads to a vacuum energy the value of which depends on the energy scale at which the symmetry was broken. So far attempts to produce a small enough vacuum energy have failed. Another alterative is to say that there are many disconnected regions in the universe which all have their own vacuum energy value. We inhabit a region with small enough vacuum energy that galaxies have formed and intelligent life can exist. This argument makes use of the anthropic principle which says that the observed values of fundamental constants are restricted to those which permit life to evolve in time to observe them. In [96] Weinberg used this idea to put the following upper bound on the vacuum energy density

$$\rho_\Lambda \lesssim 3 \times 10^{-121} m_{Pl}^4\,, \tag{1.54}$$

which is consistent with the observed value $\rho_\Lambda \approx 10^{-123} m_{Pl}^4$.

Quintessence

Scalar fields are predicted to exist by many theories of particle physics and have for a long time been the most popular means of providing inflation, a period of accelerated expansion in the very early universe required to solve the flatness and horizon problems and provide the initial density perturbations necessary for structure formation. With the discovery of accelerated expansion in the present universe they have natuarally been explored as a possible explanation. There have been many scalar field models proposed (see, for example, [41] for a review) but the simplest is quintessence [34], the Lagrangian of which is

$$\mathcal{L} = -\frac{1}{2}g^{\mu\nu}\nabla_\mu\phi\nabla_\nu\phi - V(\phi)\,, \tag{1.55}$$

which in a flat expanding universe leads to the following energy density and pressure

$$\rho = \frac{1}{2}\dot{\phi}^2 + V(\phi)\,, \qquad p = \frac{1}{2}\dot{\phi}^2 - V(\phi)\,, \tag{1.56}$$

and the equation of state is

$$w_\phi = \frac{\dot{\phi}^2 - 2V(\phi)}{\dot{\phi}^2 + 2V(\phi)}\,. \tag{1.57}$$

Substituting these expressions in the acceleration equation, (1.11), gives

$$\frac{\ddot{a}}{a} = -\frac{8\pi G}{3}(\dot{\phi}^2 - V(\phi))\,. \tag{1.58}$$

It can readily be seen that in order for acceleration to happen we require $V(\phi) > \dot{\phi}^2$. Achieving this depends on the slope of the potential as can be seen from the Klein-Gordon equation,

$$\ddot{\phi} + 3H\dot{\phi} + V_{,\phi} = 0\,, \tag{1.59}$$

which is obtained by varying the action with respect to the field.

A great many different potentials have been investigated. These may be separated into "freezing" and "thawing" models. In the former case the field initially rolls down the potential before slowing, either towards infinity or a minimum, with w_ϕ tending to -1. In the latter case the field is initially frozen by the Hubble friction until its mass $m_\phi > H$ and it starts to roll, giving rise to the present acceleration.

One advantage of quintessence over the cosmological constant is that its energy density doesn't need to be as small at early times so that there is less of a coincidence problem. Exponential potentials may exhibit scaling solutions where the

quintessence energy density is proportional to that of the background. However, if the potential is a simple exponential, that is

$$V(\phi) = V_0 e^{-\lambda\phi}\,, \tag{1.60}$$

with constant λ, it is not possible to exit the scaling regime so as to also generate the accelerated expansion today. In order to do so the potential needs to become shallower or have a minimum so that the field slows down. This can be realised with a double exponential potential [10]. In the context of inflation, [71] showed that multiple scalar fields with potentials steeper than required to individually generate accelerated expansion can together combine to act like one field with a shallower potential. This has been applied to quintessence ("assisted quintessence" [67]) and as with the double exponential scaling solutions can be found.

Another appealing possibility is "tracker" solutions [103] where, from a wide range of initial conditions, the quintessence energy density can track the background density. The condition for the existence of such solutions is

$$\Gamma \equiv \frac{V V_{,\phi\phi}}{V_{,\phi}^2} > 1. \tag{1.61}$$

This can be realised with a inverse power-law potential, $V(\phi) = M^{4+n}\phi^{-n}$, where $n > 0$ and M is the mass scale.

The greatest challenge for quintessence is finding potentials in particle physics that give rise to accelerated expansion. Firstly, the required energy density, $\rho_\phi \sim 10^{-123} m_{Pl}^4$, is very small compared to typical energy scales in particle physics. Secondly, the potential has to be shallow to allow the field to slowly roll, which means that the field has to have a very light mass, $m^2 \sim H_0^2$. This is problematic though because, in the absence of supersymmetry, radiative corrections will tend to increase the mass [69].

From the point of view of observations there are two possible ways of distinguishing between scalar field dark energy and a cosmological constant. These are that the equation of state of scalar fields can vary with time, which would affect the expansion rate, and that scalar fields need not be homogeneous and may instead cluster.

Coupled Quintessence

In order for quintessence to generate accelerated expansion the scalar field must be light. Such a scalar field is expected to couple to other forms of energy unless prevented by some symmetry [36]. Another motivation for considering interactions

between matter and dark energy is the similarity in their energy densities today. One possible form of interaction [5] is

$$\nabla^{\mu} T^{(m)}_{\mu\nu} = \beta \nabla_{\nu} \phi \, T_{(m)}, \tag{1.62}$$

where β is the strength of the coupling. Since this coupling is proportional to the trace of the energy-momentum tensor there is no effect on relativistic particles. Such an interaction arises in scalar-tensor theories as we shall see in section 1.4.2 and these models can be regarded as equivalent but with different interpretations (i.e. dark energy or modified gravity). Eq. (1.62) leads to the following modified equations for the background evolution of matter and quintessence:

$$\ddot{\phi} + 3H\dot{\phi} + V_{,\phi} = -\beta \rho_m \,, \tag{1.63}$$

$$\dot{\rho}_c = -3H\rho_m + \beta \dot{\phi} \rho_m \,. \tag{1.64}$$

Two points may be observed here. Firstly, the field now experiences an effective potential which depends on the matter density and may possess a minimum even when the bare potential does not. This allows for attractor solutions where the field tracks a minimum that gradually moves as the matter density decays [20, 44]. Secondly, matter is no longer conserved and does not follow geodesics. This creates a problem as it has the effect of a fifth force or modification to the gravitational force experienced which could be observed by experimental and solar system tests of General Relativity. Therefore, it is often assumed that the couplings to baryons and dark matter are different or that baryons are simply decoupled. As we shall see in section 1.4.2 an alternative is provided by the chameleon mechanism.

In [5] it was shown that with the exponential potential, (1.60), coupled quintessence can exhibit a scaling solution for a matter dominated era which was labelled ϕMDE during which $\Omega_{\phi} = 2\beta^2/3$. This can be followed by the present accelerated era if $\lambda^2 < 2$ and $\lambda(\beta + \lambda) < 3$ where λ is the slope of the potential (1.60).

In general the densities of matter and the field, and therefore the expansion rate, are modified as a result of the coupling. If significant at early times these changes would create observable effects on the CMB spectrum as noted in [5, 7] among others. Firstly, an increase in the distance to last scattering will shift the peaks to smaller scales. Secondly, for a coupling to just CDM resulting in the density of baryons relative to the total matter density being lower at decoupling, the amplitude of the peaks will be suppressed. In addition to the background evolution, the growth of perturbations is also modified by a coupling and so constraints are also provided by

observations of large scale structure. Observational data has been used to constrain the coupling to be $\beta \lesssim 0.1$.

Scalar-tensor theories

General relativity describes gravity using just one tensor field, the metric $g_{\mu\nu}$. In principle there is no reason why other fields should not also be involved. The simplest possibility is to add a single scalar field. Indeed, attempts to unify gravity with the other fundamental forces, as described by quantum field theory, such as string theory predict the existence of light scalar fields.

A general scalar-tensor theory can be described by the action

$$\mathcal{S} = \frac{1}{16\pi}\int \sqrt{-\tilde{g}}\, d^4x \left[\tilde{\phi}R - \frac{\omega(\tilde{\phi})}{\tilde{\phi}}\tilde{g}^{\mu\nu}(\nabla_\mu\tilde{\phi})(\nabla_\nu\tilde{\phi}) - 2\Lambda(\tilde{\phi})\right] + \mathcal{S}_m(\chi, \tilde{g}_{\mu\nu}), \quad (1.65)$$

where $\omega(\tilde{\phi})$ and $\Lambda(\tilde{\phi})$ are arbitrary functions of $\tilde{\phi}$. Varying (1.65), the following field equations may be derived:

$$\tilde{\phi}G_{\mu\nu} + \left[\tilde{g}^{\mu\nu}\nabla_\mu\nabla_\nu\tilde{\phi} + \frac{1}{2}\frac{\omega}{\tilde{\phi}}\tilde{g}^{\mu\nu}\nabla_\mu\tilde{\phi}\nabla_\nu\tilde{\phi} + \Lambda\right]\tilde{g}_{\mu\nu} - \nabla_\mu\nabla_\nu\tilde{\phi} - \frac{\omega}{\tilde{\phi}}\nabla_\mu\tilde{\phi}\nabla_\nu\tilde{\phi} = 8\pi T_{\mu\nu}\,, \quad (1.66)$$

$$(2\omega+3)\tilde{g}^{\mu\nu}\nabla_\mu\nabla_\nu\tilde{\phi} + \frac{d\omega}{d\tilde{\phi}}\tilde{g}^{\mu\nu}\nabla_\mu\tilde{\phi}\nabla_\nu\tilde{\phi} + 4\Lambda - 2\tilde{\phi}\frac{d\Lambda}{d\tilde{\phi}} = 8\pi T\,. \quad (1.67)$$

This is in the Jordan frame where the energy-momentum tensor is conserved and matter follows geodesics of the metric. However the above equations are rather complicated and inconvenient to use since the metric and scalar modes are mixed. Additionally, there are mathematically singular boundary points and it is difficult to generalise the theory to include more than one scalar field. A popular alternative is the Einstein frame where the Einstein equations take their usual form but matter follows geodesics of the conformally related Jordan metric

$$\tilde{g}_{\mu\nu} = A^2(\phi)g_{\mu\nu}, \quad (1.68)$$

and the new scalar field is related to the old one by

$$\phi = \int \frac{d\tilde{\phi}}{\tilde{\phi}}\sqrt{\frac{3+2\omega(\tilde{\phi})}{16\pi G^*}}\,. \quad (1.69)$$

In this frame the action is

$$\mathcal{S} = \int \sqrt{-g}\, d^4x \left[\frac{R}{16\pi G^*} - \frac{1}{2} g^{\mu\nu} (\nabla_\mu \phi)(\nabla_\nu \phi) - V(\phi) \right] + \mathcal{S}_m(\chi_\alpha, \tilde{g}_{\mu\nu}), \tag{1.70}$$

where G^* is a bare gravitational constant and the energy-momentum tensor is no longer conserved:

$$\nabla^\mu T^{(m)}_{\mu\nu} = \frac{1}{A} \frac{dA}{d\phi} \nabla_\nu \phi\, T. \tag{1.71}$$

The Einstein frame potential $V(\phi)$ is related to the Jordan frame one by

$$V(\phi) = A^2(\phi) \Lambda(\tilde{\phi})\,. \tag{1.72}$$

We shall refer to $A(\phi)$ as the coupling function and define the coupling strength

$$\beta(\phi) = m_{\rm Pl} \frac{\partial \ln A(\phi)}{\partial \phi}. \tag{1.73}$$

The earliest and most famous scalar-tensor theory is Brans-Dicke theory [17] in which ω is a constant and $\Lambda = 0$. However, this case is highly constrained by solar system tests of gravity such as measurements of the time-delay of radio signals from the Cassini spacecraft [16] which require $\omega \gtrsim 40,000$ [40]. In [42] Damour and Nordtvedt demonstrated the existence of an attractor mechanism for more general theories with $\omega(\phi)$ and $\Lambda = 0$.

Screening

Scalar-tensor theories (and others in which a light scalar field drives the accelerated expansion of the universe) have a problem. In the absence of a symmetry to prevent it, scalar fields are expected to couple to matter with gravitational strength. This would lead to an observable fifth force. However, we have not observed such a force and experiments such as those measuring the motions of solar-system bodies [97, 99, 100, 98] constrain the coupling between matter and a scalar field to be smaller than 10^{-5} times that of gravity. To evade these constraints a number of screening mechanisms have been investigated, for example the chameleon, symmetron and dilaton mechanisms.

Chameleons

In the original chameleon model [65, 66, 20] the scalar field has a runaway potential and an exponential coupling function $A(\phi) = e^{\beta\phi}$ (with constant β) which combine to create an effective potential,

$$V_{\text{eff}} = V(\phi) + A(\phi)\rho^* \,, \tag{1.74}$$

with a density-dependent minimum (the value of ϕ which minimises the effective potential depends on the matter density). $\rho^* = \rho/A$ is the conserved matter density. Inside sufficiently massive objects, the field is roughly at the minimum of the effective potential up to close to the object's surface and only varies significantly within a thin outer shell. This means that the resulting force is contributed to only by the mass within the thin shell and is thus suppressed. Less massive objects have no thin shell and the field varies throughout meaning that the object is not screened.

Considering a spherically symmetric body of mass M and radius R with homogeneous density, the field equation reduces to

$$\frac{d^2\phi}{dr^2} + \frac{2}{r}\frac{d\phi}{dr} - \frac{dV_{\text{eff}}(\phi)}{d\phi} = 0 \,, \tag{1.75}$$

with the field moving along the inverted potential $-V_{\text{eff}}$. This potential then has maxima at ϕ_c and ϕ_∞ inside and outside the body respectively (and $\phi_\infty > \phi_c$). Similarly, inside the body the matter density is ρ_c^* and field's mass is m_c and outside they are ρ_∞^* and m_∞. In order to solve equation (1.75) the following boundary conditions are set:

$$\frac{d\phi}{dr} = 0 \quad \text{at} \quad r = 0 \,, \qquad \phi \to \phi_\infty \quad \text{as} \quad r \to \infty \,. \tag{1.76}$$

If the body is massive enough then at $r = 0$ the field will be very close to ϕ_c, the minimum of the effective potential. This means that close to the centre the driving term in (1.75) is negligible compared to the friction term and so the field is frozen. Moving away from the centre, the field will begin to roll down the inverted potential when the driving term becomes dominant at a radius r_s. Since the field moves to larger values of ϕ the effective potential is determined by the coupling term and in the range $r_s < r < R$ (1.75) can be approximated by

$$\frac{d^2\phi}{dr^2} + \frac{2}{r}\frac{d\phi}{dr} \approx \beta\rho_c^* \tag{1.77}$$

where we have assumed $\beta\phi \ll 1$. The solution to this equation is

$$\phi(r) = \frac{\beta\rho_c^* r^2}{6} - \frac{C}{r} + D\,, \tag{1.78}$$

with C and D constants. Outside of the body, as the background density abruptly decreases, the effective potential changes shape, its curvature becoming smaller. The maximum of the inverted potential moves to ϕ_∞ and the field, having gained sufficient kinetic energy between r_s and R, now rolls up the slope towards the new maximum. In the limit $\frac{2}{r}\frac{d\phi}{dr} \gg \frac{dV_{\rm eff}}{d\phi}$ the solution is

$$\phi(r) = \phi_\infty - \frac{E}{r}. \tag{1.79}$$

The full exterior solution for the field profile can be found by matching solutions for the three regions $r < r_s$, $r_s < r < R$ and $r > R$ at $r = r_s$ and $r = R$ [94]:

$$\phi(r) = \phi_\infty - 2\beta\Phi_N R\left[1 - \frac{r_s^3}{R^3} + 3\frac{r_s}{R}\frac{1}{(m_c R)^2}\left(\frac{m_c r_s(e^{m_c r_s} + e^{-m_c r_s})}{e^{m_c r_s} - e^{-m_c r_s}} - 1\right)\right]\frac{e^{-m_\infty(r-R)}}{r}\,, \tag{1.80}$$

where $\Phi_N = G_N M/(8\pi R)$ is the Newtonian potential at the surface of the body. The magnitude of the fifth force experienced by a test particle of unit mass outside a massive body is given by

$$F_\phi = -\beta\nabla\phi\,. \tag{1.81}$$

From (1.80) it can be seen that this force will be suppressed if $\Delta R \equiv R - r_s \ll R$ and $m_c R \gg 1$. The former condition corresponds to the existence of a thin shell and can be expressed as

$$\frac{\Delta R}{R} = \frac{\phi_\infty - \phi_c}{6\beta\Phi_N} \ll 1, \tag{1.82}$$

as long as $m_c R \gg (\Delta R/R)^{-1}$.

Dilatons

Inspired by the Damour-Polyakov mechanism [43], the environmentally dependent dilaton model first proposed in [24] consists of a runaway bare potential,

$$V(\phi) = V_0 e^{-\gamma\phi/M_{Pl}}\,, \tag{1.83}$$

and a coupling function with a minimum at $\phi = \phi_*$, given by

$$A(\phi) = 1 + \frac{A_2}{2}(\phi - \phi_*)^2 \,, \tag{1.84}$$

where $\gamma > 0$ and $A_2 \gg 1$ are constants. Near ϕ_* we have

$$\beta(\phi) \approx A_2(\phi - \phi_*) \,. \tag{1.85}$$

In regions where the matter density is high the effective potential is dominated by the $A(\phi)$ term and its minimum is close to ϕ_* where the strength of the coupling vanishes and so the fifth force is suppressed. On the other hand, in regions of low matter density the minimum of the effective potential is displaced from ϕ_* so the coupling strength is non-vanishing and the effects of modified gravity may be observed.

Symmetrons

The symmetron mechanism [55, 56] works in a similar way to the dilaton. The bare potential has a symmetry-breaking form,

$$V(\phi) = -\frac{1}{2}\mu^2\phi^2 + \frac{1}{4}\lambda\phi^4 \,, \tag{1.86}$$

with a local maximum at $\phi = 0$ and two global minima at $\phi = \pm\mu/\sqrt{\lambda}$, while the coupling function, given by

$$A(\phi) = 1 + \frac{1}{2}\left(\frac{\phi}{M}\right)^2 \,, \tag{1.87}$$

has a minimum at the origin. It is required that $\lambda \ll 1$, $\mu \sim H_0$ and $M \lesssim 10^{-3} M_{Pl}$. In a low density region the effective potential will have the symmetry-breaking feature of the bare potential and the field will fall into one of the minima where the coupling does not vanish. When the matter density exceeds a certain value, $\rho^* > M^2\mu^2$, the effective potential does not break the symmetry, the field goes to the origin where the coupling strength vanishes and there is no fifth force.

Tomography

It has been shown in [28] and [29] that the screened modified gravity models described above satisfy a tomographic description whereby the potential $V(\phi)$ and coupling

function $A(\phi)$ can be reconstructed solely from the knowledge of the density or scale factor dependence of the mass $m(a)$ of fluctuations about the minimum of the effective potential and the coupling strength $\beta(a)$. If the mass of the scalar field is much greater than the Hubble rate, $m \gg H$, then the field is attracted to the minimum of the effective potential where

$$\frac{dV}{d\phi} = -\frac{\beta A \rho^*}{m_{\rm Pl}}, \tag{1.88}$$

and

$$m^2(a) = \frac{d^2 V_{\rm eff}}{d^2\phi} = \frac{d^2 V}{d^2\phi} + \frac{\beta^2 A \rho^*}{m_{\rm Pl}^2} + \frac{A\rho^*}{m_{\rm Pl}}\frac{d\beta}{d\phi} \tag{1.89}$$

Differentiating Eq. (1.88) with respect to conformal time,

$$\frac{d^2 V}{d^2\phi}\dot{\phi} = -\left(A\rho^*\frac{d\beta}{d\phi} + \beta\rho^*\frac{dA}{d\phi}\right)\frac{\dot{\phi}}{m_{\rm Pl}} - \frac{\beta A \dot{\rho}^*}{m_{\rm Pl}}, \tag{1.90}$$

and then using Eq. (1.89) we find

$$\dot{\phi} = \frac{3H\beta A\rho^*}{m^2(a) m_{\rm Pl}}, \tag{1.91}$$

and so, given $\rho^* = \rho_0^*/a^3$,

$$\phi(a) = \phi_c + \frac{3\rho_0^*}{m_{\rm Pl}}\int_{a_i}^{a} \frac{\beta(a)}{a^4 m^2(a)} da, \tag{1.92}$$

where ϕ_c is the field value at the minimum corresponding to the density $\rho^*(a_i)$ and we have taken $A \approx 1$ (as required by the constraint on the time variation of fermion masses). Eq. (1.88) also implies that

$$V(a) = V_0 - \frac{3(\rho_0^*)^2}{m_{\rm Pl}}\int_{a_i}^{a} \frac{\beta^2(a)}{a^7 m^2(a)} da, \tag{1.93}$$

yielding an implicit definition of $V(\phi)$.

$f(R)$ Theories

Rather than introducing extra fields, an alternative way to modify gravity is to replace the Ricci scalar in the Einstein-Hilbert action with a general function of it, $f(R)$:

$$\mathcal{S} = \frac{1}{16\pi G^*}\int d^4x\sqrt{-g} f(R) + \mathcal{S}_m(g_{\mu\nu}, \chi), \tag{1.94}$$

where G^* is a bare gravitational constant which will generally differ from its observed value. The energy-momentum tensor of the matter fields χ is conserved in the standard way so $g_{\mu\nu}$ is the Jordan frame metric. Varying (1.94) with respect to the metric in the usual way [1] yields

$$f_{,R}R_{\mu\nu} - \frac{1}{2}f(R)g_{\mu\nu} - \nabla_\mu\nabla_\nu f_{,R} + g_{\mu\nu}\Box f_{,R} = 8\pi G T_{\mu\nu}\,, \tag{1.95}$$

where $f_{,R} \equiv \partial f/\partial R$. If $f(R) = R$ then the standard Einstein equations are retrieved while the choice $f(R) = R - 2\Lambda$ corresponds to the inclusion of a cosmological constant (ΛCDM).

Using the flat FRW metric and assuming the perfect fluid form for $T_{\mu\nu}$, (1.95) yields

$$H^2 = \frac{8\pi G}{3f_{,R}}\left[\rho + \frac{Rf_{,R} - f(R)}{2} - 3H\dot{R}f_{,RR}\right]\,, \tag{1.96}$$

$$2\dot{H} + 3H^2 = -\frac{8\pi G}{f_{,R}}\left[p + \dot{R}^2 f_{,RRR} + 2H\dot{R}f_{,RR} + \ddot{R}f_{,RR} + \frac{f(R) - Rf_{,R}}{2}\right]\,. \tag{1.97}$$

One can define an effective density and pressure for the modified curvature terms,

$$\rho^{\text{eff}} = \frac{Rf_{,R} - f(R)}{2f_{,R}} - \frac{3H\dot{R}f_{,RR}}{f_{,R}}\,, \tag{1.98}$$

$$p^{\text{eff}} = \frac{\dot{R}^2 f_{,RRR} + 2H\dot{R}f_{,RR} + \ddot{R}f_{,RR} + \frac{f(R)-Rf_{,R}}{2}}{f_{,R}}\,, \tag{1.99}$$

which give

$$w^{\text{eff}} = \frac{\dot{R}^2 f_{,RRR} + 2H\dot{R}f_{,RR} + \ddot{R}f_{,RR} + \frac{f(R)-Rf_{,R}}{2}}{\frac{Rf_{,R}-f(R)}{2} - 3H\dot{R}f_{,RR}}\,, \tag{1.100}$$

for the effective equation of state parameter. To have accelerating expansion we require $w < -1/3$ so (1.100) shows that this is possible depending on the choice of $f(R)$. In order to be viable, models have to satisfy a variety of other conditions including consistency with the observed cosmological evolution, compatibility with local tests of gravity and the avoidance of ghosts or instabilities. Successful models include those of [9] and [57].

Taking the trace of (1.95) gives

$$3\Box f_{,R} + f_{,R}R - 2f(R) = 8\pi T\,, \tag{1.101}$$

[1] Unlike in GR, different field equations are found depending upon the variational approach chosen [92]

where $T = g^{\mu\nu}T_{\mu\nu}$. In general $f_{,R}$ is a function of R so $\Box f_{,R}$ does not vanish and (1.101) governs the dynamics of this new scalar degree of freedom, $\varphi \equiv f_{,R}$ (called "scalaron" by [93]). In fact $f(R)$ theories have been shown to be equivalent to a type of scalar-tensor theory. To see this we start by introducing a new scalar field ψ and writing (1.94) in an equivalent form:

$$\mathcal{S} = \frac{1}{16\pi G^*}\int d^4x\sqrt{-g}[f(\psi) + f_{,\psi}(R-\psi)] + \mathcal{S}_m(g_{\mu\nu},\chi)\,. \tag{1.102}$$

Varying this action with respect to ψ we obtain

$$f_{,\psi\psi}(R-\psi) = 0 \tag{1.103}$$

which means that, as long as $f_{,\psi\psi} \neq 0$, $\psi = R$. Now, defining $\phi = f_{,\psi}$ and

$$\Lambda(\phi) = \frac{1}{2}\left[\phi\psi(\phi) - f(\psi(\phi))\right]\,, \tag{1.104}$$

the action (1.102) becomes

$$\mathcal{S} = \frac{1}{16\pi}\int \sqrt{-g}\, d^4x\, [\phi\mathcal{R} - 2\Lambda(\phi)] + \mathcal{S}_m(\chi, g_{\mu\nu}),\,, \tag{1.105}$$

which is the action of a scalar-tensor theory in the Jordan frame, (1.65), with $\omega = 0$. However, this violates the constraint $\omega > 40,000$ [40] coming from solar-system tests of gravity. As with scalar-tensor theories generally, we can switch to the Einstein frame by making a conformal transformation. For $f(R)$ theories the transformation is

$$g^E_{\mu\nu} = f_{,R}\, g^J_{\mu\nu}\,, \tag{1.106}$$

and the scalar field is redefined as

$$\phi = \sqrt{\frac{3}{16\pi G}}\ln(f_{,R})\,. \tag{1.107}$$

The Einstein frame action can then be written as

$$\mathcal{S} = \int \sqrt{-g}\, d^4x \left[\frac{R}{16\pi G} - \frac{1}{2}g^{\mu\nu}(\nabla_\mu\phi)(\nabla_\nu\phi) - V(\phi)\right] + \mathcal{S}_m(\chi_\alpha, g^J_{\mu\nu}), \tag{1.108}$$

where

$$V(\phi) = \frac{Rf_{,R} - f(R)}{16\pi G(f_{,R})^2}\,. \tag{1.109}$$

In order to compare with scalar-tensor theories in Einstein frame as descibed in section 1.4.2 we can combine (1.106) and (1.107) to write

$$g^J_{\mu\nu} = A^2(\phi) g^E_{\mu\nu} = e^{-\sqrt{\frac{16\pi G}{3}}\phi}\, g^E_{\mu\nu}\,, \tag{1.110}$$

which gives $\beta = -1/\sqrt{6}$.

As already mentioned there appears to be a conflict with local tests of gravity. However, since we have just shown that $f(R)$ theories are a subclass of scalar-tensor theories this conflict may be alleviated by the chameleon mechanism described in section 1.4.2. The effective potential is

$$V_{\text{eff}} = V(\phi) + e^{-\sqrt{\frac{4\pi G}{3}}\phi}\rho^*\,, \tag{1.111}$$

where, as before, ρ^* is the conserved matter density in the Einstein frame. In order for there to be a minimum we need $V_{,\phi} > 0$ which, by differentiating (1.109), can be shown to translate into the requirement $2f(R) > Rf_{,R}$. A number of authors have investigated the chameleon mechanism in $f(R)$ theories, for example [32, 76, 50, 23].

§ 1.5 Outline

In this thesis, we consider models of dark energy that can be written as scalar-tensor theories and address two questions. Firstly, what effects might such models have on observables in the early universe, particularly the CMB, both its angular power spectrum and spectral distortions. Secondly, how are the constraints that have been placed on such models affected if we relax assumptions typically made about the early universe.

In Chapter 2 we investigate scalar-tensor theories in modified gravity. Firstly we consider a general disformal relation between the physical and gravitational metrics and derive perturbation equations for a general fluid coupled to the scalar field. We then specialise to a coupling to baryons and derive the equations describing the acoustic oscillations in the photon-baryon plasma and an expression for the modified sound-speed. These are then used to consider the possibility of probing modified gravity with the CMB μ-distortion. In Chapter 3 we restrict ourselves to theories with a purely conformal coupling of the field to matter that allow for a screening mechanism. The possible effects of these models on the CMB angular power spectrum are then considered and we explore the potential for these to provide constraints on the models, even after imposing constraints coming from local tests

and BBN. In Chapter 4 we consider coupled quintessence models and whether the constraints on a coupling between the scalar field and CDM might be relaxed if the assumption of adiabatic initial conditions is lifted. Initial conditions for general perturbation modes (adiabatic and isocurvature) are derived and CMB spectra for these modes are produced. In Chapter 5 we summarise.

Chapter 2

CMB μ–distortion

§ 2.1 Introduction

We have already seen that a number of theories to explain dark energy can be written in the form of a scalar-tensor theory and all the models considered in this thesis are of this form. These theories result in couplings between the scalar field and one or more matter species. The majority of work so far has focussed on conformal couplings but in [13] Bekenstein showed that the most general relation between the physical and gravitational metrics is disformal. This possibility has recently attracted growing attention as it has been realised that many types of modified gravity can have this relation, for example, models violating Lorentz invariance [18], massive gravity [88] and Galileons [104].

Unfortunately, it has recently been shown that disformal couplings are difficult to constrain with local experiments (see e.g. [18, 78, 25]). Therefore it is worthwhile considering alternatives and to this end we have studied the consequences of modifications of gravity in the radiation dominated epoch. In this Chapter, we find a generic expression for the sound-speed of the tightly coupled photon-baryon fluid in theories with conformal and disformal couplings and calculate the distortion of the cosmic microwave background (CMB) caused by the dissipation of acoustic waves. As is well known, the dissipation of acoustic waves injects energy into the photons and therefore gives rise to slight deviations from the blackbody spectrum by producing a positive chemical potential μ. The deviations are small; the chemical potential created by the dissipation of acoustic waves is of order $\mu \approx 10^{-8}$ in the standard inflationary scenario and does not violate the current constraint $|\mu| < 9 \times 10^{-5}$ (for work on these issues, see e.g.[59, 58, 64, 38, 80] and references therein). Proposed experiments such as PIXIE, however, would reach this sensitivity to search

for deviations of the order $\mu \approx 10^{-8}$ [68]. These observations probe the primordial power spectrum at very small scales and constrain the inflationary epoch [46, 37]. We point out that, in general, modifications of gravity alter the spectral distortions because of the different sound-speed of the coupled photon-baryon plasma. For theories in which the field is very heavy the sound-speed is smaller than in General Relativity and thus an absence of a μ-type distortion in the CMB spectrum could be explained by a lower sound-speed during the epoch in which the distortion was created ($5 \times 10^4 < z < 2 \times 10^6$). However, the sound horizon is well constrained by measurements of the CMB anisotropies (e.g. the position of the first peak is well known), and, as we will see, this further constrains the type of modified gravity theories which are allowed. It is worth pointing out that the μ–distortion is the earliest direct probe of modifications of gravity.

§ 2.2 Evolution of Perturbations in Disformal Theories

2.2.1 General Equations

In this section we derive the equations governing the evolution of perturbations for a scalar-tensor theory with both conformal and disformal couplings. As we shall see the disformal relation gives rise to much more complicated couplings between the scalar field and matter. We will consider scalar-tensor models whose action in the Einstein frame is

$$\mathcal{S} = \int \sqrt{-g}\, d^4x \left[\frac{\mathcal{R}}{16\pi G} - \frac{1}{2} g^{\mu\nu} (\nabla_\mu \phi)(\nabla_\nu \phi) - V(\phi) \right] + \mathcal{S}_m(\chi_\alpha, \tilde{g}^{(\alpha)}_{\mu\nu}), \tag{2.1}$$

where

$$\mathcal{S}_m = \int \sqrt{-\tilde{g}}\, d^4x\, \mathcal{L}_m(\chi_\alpha, \tilde{g}^{(\alpha)}_{\mu\nu}), \tag{2.2}$$

and $\mathcal{R}$ is the Ricci scalar, χ_α are the matter fields in the theory (relativistic and non-relativistic), ϕ is an additional scalar degree of freedom and the metrics $\tilde{g}^{(\alpha)}$ are related to the metric g by

$$\tilde{g}^{(\alpha)}_{\mu\nu} = C^{(\alpha)}(\phi) g_{\mu\nu} + D^{(\alpha)}(\phi) \partial_\mu \phi \partial_\nu \phi \ . \tag{2.3}$$

To obtain the field equations we vary the action with respect to the scalar field

$$\delta_\phi \mathcal{S} = \int d^4x \left[\delta_\phi(\sqrt{-g}\mathcal{L}_\phi) + \delta_\phi(\sqrt{-\tilde{g}}\mathcal{L}_m) \right] = 0. \tag{2.4}$$

The first term is

$$\delta_\phi(\sqrt{-g}\mathcal{L}_\phi) = \sqrt{-g}(g^{\mu\nu}\nabla_\mu\nabla_\nu\phi - V')\delta\phi, \tag{2.5}$$

where the prime denotes a derivative with respect to the field. The second term can be rewritten as

$$\delta_\phi(\sqrt{-\tilde{g}}\mathcal{L}_m) = \frac{\delta(\sqrt{-\tilde{g}}\mathcal{L}_m)}{\delta g_{\alpha\beta}}\frac{\delta g_{\alpha\beta}}{\delta\tilde{g}_{\mu\nu}}\,\delta_\phi(\tilde{g}_{\mu\nu}), \tag{2.6}$$

and then using the definition of the energy-momentum tensor

$$T_m^{\mu\nu} = \frac{2}{\sqrt{-g}}\frac{\delta(\sqrt{-\tilde{g}}\mathcal{L}_m)}{\delta g_{\mu\nu}} \tag{2.7}$$

we obtain

$$\delta_\phi(\sqrt{-\tilde{g}}\mathcal{L}_m) = \sqrt{-g}Q\delta\phi, \tag{2.8}$$

where

$$Q = \frac{C'}{2C}g_{\mu\nu}T_m^{\mu\nu} - \nabla_\nu\left(\frac{D}{C}\partial_\mu\phi T_m^{\mu\nu}\right) + \frac{D'}{2C}\partial_\mu\phi\partial_\nu\phi T_m^{\mu\nu}. \tag{2.9}$$

Then substituting for both terms in Eq. (2.4) gives

$$g^{\mu\nu}\nabla_\mu\nabla_\nu\phi - \frac{dV}{d\phi} + Q = 0. \tag{2.10}$$

Owing to the coupling to matter, the energy-momentum tensor of the scalar field,

$$T_{\mu\nu}^{(\phi)} = \nabla_\mu\phi\nabla_\nu\phi - \tfrac{1}{2}g_{\mu\nu}g^{\rho\sigma}\nabla_\rho\phi\nabla_\sigma\phi - g_{\mu\nu}V(\phi), \tag{2.11}$$

is not conserved:

$$\nabla^\mu T_{\mu\nu}^{(\phi)} = (g^{\mu\nu}\nabla_\mu\nabla_\nu\phi - V')\nabla_\nu\phi = -Q\nabla_\nu\phi, \tag{2.12}$$

where the last equality uses Eq. (2.10). Since $\nabla^\mu(T_{\mu\nu}^{(\phi)} + T_{\mu\nu}^{(m)}) = 0$, the previous equation gives us

$$\nabla^\mu T_{\mu\nu}^{(m)} = Q\nabla_\nu\phi. \tag{2.13}$$

As noted in [104], the coupling as expressed in (2.9) contains terms in $\nabla^\mu T_{\mu\nu}^{(m)}$ and $\nabla_\mu\nabla_\nu\phi$. In order to solve both Eq. (2.10) and Eq. (2.13) we can use the latter to eliminate $\nabla^\mu T_{\mu\nu}^{(m)}$ from Q in the former. Raising the indices in (2.13) and then contracting with $\nabla_\nu\phi$ we have

$$\nabla_\nu\phi\nabla_\mu T^{\mu\nu} = Q\nabla_\nu\phi\nabla^\nu\phi. \tag{2.14}$$

Expanding the second term in (2.9) gives us

$$Q = \frac{C'}{2C} g_{\mu\nu} T_m^{\mu\nu} - \frac{D}{C} T_m^{\mu\nu} \nabla_\mu \nabla_\nu \phi + \left(\frac{C'D}{C^2} - \frac{D'}{2C} \right) T_m^{\mu\nu} \nabla_\mu \phi \nabla_\nu \phi - \frac{D}{C} \nabla_\nu \phi \nabla_\mu T^{\mu\nu}, \quad (2.15)$$

which, after using (2.14) and rearranging, can be rewritten as

$$Q = \frac{1}{C + D \nabla_\nu \phi \nabla^\nu \phi} \left[\frac{C'}{2} g_{\mu\nu} - D \nabla_\mu \nabla_\nu \phi + \left(\frac{C'D}{C} - \frac{D'}{2} \right) \nabla_\mu \phi \nabla_\nu \phi \right] T_m^{\mu\nu}. \quad (2.16)$$

Inserting this in Eq. (2.10) and rearranging we get

$$\mathcal{M}^{\mu\nu} \nabla_\mu \nabla_\nu \phi - V' + \frac{C}{C + D \nabla_\nu \phi \nabla^\nu \phi} \mathcal{Q}_{\mu\nu} T_m^{\mu\nu} = 0, \quad (2.17)$$

where

$$\mathcal{M}^{\mu\nu} \equiv g^{\mu\nu} - \frac{D}{C + D \nabla_\nu \phi \nabla^\nu \phi} T_m^{\mu\nu}, \quad (2.18)$$

and

$$\mathcal{Q}_{\mu\nu} \equiv \frac{C'}{2C} g_{\mu\nu} + \left(\frac{C'D}{C^2} - \frac{D'}{2C} \right) \nabla_\mu \phi \nabla_\nu \phi. \quad (2.19)$$

This corresponds to equation (47) of [104] for the case of a canonical scalar field. Now using Eq. (2.17) and Eq. (2.13) we can obtain the following equations for the background evolution

$$\ddot{\phi} + 2\mathcal{H}\dot{\phi} + a^2 V' = a^2 Q_0, \quad (2.20)$$

$$\dot{\rho}_i = -3\mathcal{H}(1 + w_i)\rho_i - Q_0 \dot{\phi}, \quad (2.21)$$

where $\mathcal{H} = \dot{a}/a$ is the Hubble rate, w is the equation of state parameter, Q_0 is the zero-order part of Q,

$$Q_0 = -\frac{a^2 C'(1 - 3w_i) - 2D(3\mathcal{H}\dot{\phi}(1 + w_i) + a^2 V' + \frac{C'}{C}\dot{\phi}^2) + D'\dot{\phi}^2}{2(a^2 C + D(a^2 \rho_i - \dot{\phi}^2))} \rho_i \,, \quad (2.22)$$

and the subscript i denotes the species to which the field is coupled. Eq. (2.22) agrees with [104] for the case $w_i = 0$. Perturbing (2.13) and (2.17) in the conformal

Newtonian gauge yields the following equations

$$\dot{\delta}_i = -(1+w_i)(\theta_i - 3\dot{\Phi}) - 3\mathcal{H}\left(\frac{\delta p_i}{\delta\rho_i} - w_i\right)\delta_i + \frac{Q_0}{\rho_i}\dot{\phi}\,\delta_i - \frac{Q_0}{\rho_i}\delta\dot{\phi} - \frac{\dot{\phi}}{\rho_i}\delta Q, \tag{2.23}$$

$$\dot{\theta}_i = -\mathcal{H}(1-3w_i)\theta_i - \frac{\dot{w}_i}{1+w_i}\theta_i + k^2\Psi + \frac{\delta p_i/\delta\rho_i}{1+w_i}k^2\delta_i - k^2\sigma_i + \frac{Q_0}{\rho_i}\dot{\phi}\theta_i - \frac{Q_0}{(1+w_i)\rho_i}k^2\delta\phi, \tag{2.24}$$

$$\delta\ddot{\phi} + 2\mathcal{H}\delta\dot{\phi} + (k^2 + a^2V'')\delta\phi = \dot{\phi}(\dot{\Psi} + 3\dot{\Phi}) - 2a^2(V' - Q_0)\Psi + a^2\delta Q\,, \tag{2.25}$$

where k is the perturbation wavenumber, Φ and Ψ are the potentials in the conformal Newtonian gauge (see (1.23)), $\delta \equiv \delta\rho/\rho$ is the density contrast, δp is the pressure perturbation, θ is the velocity perturbation and σ is the anisotropic stress perturbation defined in (1.28). The perturbation of Q is

$$\delta Q = -\frac{\rho_i}{a^2C + D(a^2\rho_i - \dot{\phi}^2)}[\mathcal{B}_1\delta_i + \mathcal{B}_2\dot{\Phi} + \mathcal{B}_3\Psi + \mathcal{B}_4\delta\dot{\phi} + \mathcal{B}_5\delta\phi], \tag{2.26}$$

where

$$\mathcal{B}_1 = \frac{a^2C'}{2}\left(1 - 3\frac{\delta p_i}{\delta\rho_i}\right) - 3D\mathcal{H}\dot{\phi}\left(1 + \frac{\delta p_i}{\delta\rho_i}\right) - Da^2(V' - Q_0) - D\dot{\phi}^2\left(\frac{C'}{C} - \frac{D'}{2D}\right), \tag{2.27}$$

$$\mathcal{B}_2 = 3D\dot{\phi}(1+w_i), \tag{2.28}$$

$$\mathcal{B}_3 = 6D\mathcal{H}\dot{\phi}(1+w_i) + 2D\dot{\phi}^2\left(\frac{C'}{C} - \frac{D'}{2D} + \frac{Q_0}{\rho_i}\right), \tag{2.29}$$

$$\mathcal{B}_4 = -3D\mathcal{H}(1+w_i) - 2D\dot{\phi}\left(\frac{C'}{C} - \frac{D'}{2D} + \frac{Q_0}{\rho_i}\right), \tag{2.30}$$

$$\mathcal{B}_5 = \frac{a^2C''(1-3w_i)}{2} - Dk^2(1+w_i) - Da^2V'' - D'a^2V' - 3D'\mathcal{H}\dot{\phi}(1+w_i) - D\dot{\phi}^2\left(\frac{C''}{C} - \left(\frac{C'}{C}\right)^2 + \frac{C'D'}{CD} - \frac{D''}{2D}\right) + (a^2C' + D'a^2\rho_i - D'\dot{\phi}^2)\frac{Q_0}{\rho_i}. \tag{2.31}$$

For the rest of this chapter we will consider the scalar field to be coupled to baryons only. In the next Section we examine the dynamics of the tightly coupled photon-baryon fluid, deriving the effective coupling between the scalar field and baryons and the effective sound-speed for the photon-baryon fluid. In Section 3 we calculate the resulting $\mu-$distortion for some simple examples in which the field is heavy and the coupling is purely conformal. We are treating photons and baryons as fluids, coupled

via Thomson scattering. For photons and baryons, Eqns. (2.23) and (2.24) become

$$\dot{\delta}_\gamma = -\tfrac{4}{3}\theta_\gamma + 4\dot{\Phi}, \tag{2.32}$$

$$\dot{\theta}_\gamma = \tfrac{1}{4}k^2\delta_\gamma - k^2\sigma_\gamma + k^2\Psi + an_e\sigma_T(\theta_b - \theta_\gamma), \tag{2.33}$$

$$\dot{\delta}_b = -\theta_b + 3\dot{\Phi} + \frac{Q_0}{\rho_b}\dot{\phi}\,\delta_b - \frac{Q_0}{\rho_b}\delta\dot{\phi} - \frac{\dot{\phi}}{\rho_b}\delta Q, \tag{2.34}$$

$$\dot{\theta}_b = -\mathcal{H}\theta_b + k^2\Psi + \frac{an_e\sigma_T}{R}(\theta_\gamma - \theta_b) + \frac{Q_0}{\rho_b}\dot{\phi}\theta_b - \frac{Q_0}{\rho_b}k^2\delta\phi\ , \tag{2.35}$$

where we have added the interaction terms for Thomson scattering in which n_e is the electron number density, σ_T is the Thomson scattering cross-section and $R = 3\rho_b/4\rho_\gamma$.

2.2.2 Tight-Coupling Approximation

We are interested in scales much smaller than the horizon and on time-scales much smaller than the Hubble expansion rate. To derive a second order differential equation for δ_γ, we ignore therefore terms which involve the Hubble expansion rate, the time-evolution of the background scalar field, and the time-derivatives of the scalar field perturbations and the gravitational potential. In this limit, the relevant equations read

$$\dot{\delta}_\gamma = -\tfrac{4}{3}\theta_\gamma, \tag{2.36}$$

$$\dot{\theta}_\gamma = \tfrac{1}{4}k^2\delta_\gamma - k^2\sigma_\gamma + k^2\Psi + an_e\sigma_T(\theta_b - \theta_\gamma), \tag{2.37}$$

$$\dot{\delta}_b = -\theta_b, \tag{2.38}$$

$$\dot{\theta}_b = k^2\Psi + \frac{an_e\sigma_T}{R}(\theta_\gamma - \theta_b) - \frac{Q_0}{\rho_b}k^2\delta\phi, \tag{2.39}$$

$$(k^2 + a^2V'')\delta\phi = a^2\delta Q, \tag{2.40}$$

where

$$Q_0 = \frac{2DV' - C'}{2(C + D\rho_b)}\rho_b, \qquad \delta Q = -\frac{\rho_b}{a^2(C + D\rho_b)}[\mathcal{B}_1\delta_b + \mathcal{B}_5\delta\phi], \tag{2.41}$$

and

$$\mathcal{B}_1 = \frac{a^2C'}{2} - Da^2(V' - Q_0), \tag{2.42}$$

$$\mathcal{B}_5 = \frac{a^2C''}{2} - Dk^2 - Da^2V'' - D'a^2V' + a^2(C' + D'\rho_b)\frac{Q_0}{\rho_b}. \tag{2.43}$$

From equation (2.40) we find

$$\delta\phi = -\frac{\mathcal{B}_1\rho_b}{(C+D\rho_b)(k^2+a^2V'')+\mathcal{B}_5\rho_b}\delta_b. \tag{2.44}$$

To leading order in the tight-coupling approximation $\frac{1}{\tau_c} \equiv an_e\sigma_T \to \infty$ which implies

$$\theta_\gamma \approx \theta_b, \tag{2.45}$$

and therefore

$$\delta_b \approx \tfrac{3}{4}\delta_\gamma. \tag{2.46}$$

Additionally it can be shown (e.g. [82]) that

$$\sigma_\gamma = \frac{16\tau_c}{45}\theta_\gamma, \tag{2.47}$$

and so we can neglect the anisotropic stress. Using equation (2.45) on the left-hand side of equation (2.39) we have

$$\frac{(\theta_\gamma-\theta_b)}{\tau_c} = R\left(\dot\theta_\gamma - k^2\Psi + \frac{Q_0}{\rho_b}k^2\delta\phi\right), \tag{2.48}$$

which can be inserted in equation (2.37) to get

$$\dot\theta_\gamma = \tfrac{1}{4}k^2\delta_\gamma + k^2\Psi + R\left(\dot\theta_\gamma - k^2\Psi + \frac{Q_0}{\rho_b}k^2\delta\phi\right). \tag{2.49}$$

Rearranging and using equation (2.36) we find

$$\ddot\delta_\gamma = -\frac{k^2}{3(1+R)}\delta_\gamma - \frac{4}{3}k^2\Psi + \frac{Q_0}{\rho_b}\frac{4Rk^2}{3(1+R)}\delta\phi. \tag{2.50}$$

We can then substitute for $\delta\phi$ using equations (2.44) and (2.46) and this leads to

$$\ddot\delta_\gamma + (1+3R\mathcal{F})k^2c_s^2\delta_\gamma = -\frac{4}{3}\Psi, \tag{2.51}$$

where $c_s = 1/\sqrt{3(1+R)}$ is the standard sound-speed and

$$\mathcal{F} = \frac{Q_0\mathcal{B}_1}{(C+D\rho_b)(k^2+a^2V'')+\mathcal{B}_5\rho_b}. \tag{2.52}$$

From this equation we can read off the modified sound-speed

$$\tilde{c}_s^2 = c_s^2(1 + 3R\mathcal{F}), \tag{2.53}$$

which reduces to the expression given in [27] for the purely conformal case.

2.2.3 Silk Damping

An important feature of the CMB spectrum is that perturbations on small scales are damped. This is known as Silk damping and is a result of the fact that the photons and baryons do not behave exactly as a single fluid. The tight-coupling approximation breaks down on small scales because the photons travel a finite distance between each scatter off an electron. In the course of a Hubble time, H^{-1}, a photon moves on average a distance λ_D. This means that perturbations on scales smaller than λ_D become smoothed out.

To account for Silk damping it is necessary to go beyond leading order in the tight-coupling approximation. We follow the method outlined in [47]. Damping occurs on very small scales on which the gravitational potentials are very small but the photon quadrupole is relevant. We assume that all the perturbation variables vary as $e^{i\int \omega d\tau}$ so that

$$\delta_b = -\frac{\theta_b}{i\omega} \qquad \text{and} \qquad \delta_\gamma = -\frac{4\theta_\gamma}{3i\omega}. \tag{2.54}$$

Equation (2.39) then becomes

$$i\omega\theta_b = \frac{(\theta_\gamma - \theta_b)}{\tau_c R} - \frac{k^2\mathcal{F}}{i\omega}\theta_b. \tag{2.55}$$

Rearranging, we find to second order in τ_c

$$\begin{aligned}\theta_b &= \left[1 + i\omega\tau_c R\left(1 - \frac{k^2\mathcal{F}}{\omega^2}\right)\right]^{-1}\theta_\gamma \\ &\approx \left[1 - i\omega\tau_c R\left(1 - \frac{k^2\mathcal{F}}{\omega^2}\right) - (\omega\tau_c R)^2\left(1 - \frac{k^2\mathcal{F}}{\omega^2}\right)^2\right]\theta_\gamma\ .\end{aligned} \tag{2.56}$$

Inserting this in equation (2.37) gives

$$i\omega = -\frac{k^2}{3i\omega} - \frac{16k^2\tau_c}{45} + \frac{1}{\tau_c}\left(\left[1 - i\omega\tau_c R\left(1 - \frac{k^2\mathcal{F}}{\omega^2}\right) - (\omega\tau_c R)^2\left(1 - \frac{k^2\mathcal{F}}{\omega^2}\right)^2\right] - 1\right) \tag{2.57}$$

and after collecting terms we obtain

$$\omega^2 = k^2 c_s^2(1+3R\mathcal{F}) + i\omega k^2 c_s^2 \tau_c \left[\frac{16}{15} + \frac{3\omega^2 R^2}{k^2} - 6R^2\mathcal{F} + \frac{3k^2R^2}{\omega^2}\mathcal{F}^2\right]. \tag{2.58}$$

We can recognise the first term on the right-hand side as $k^2\tilde{c}_s^2$. Using this, we now get ω by taking the first two terms of the binomial expansion in τ_c of the square root of (2.58) which allows us to write

$$\begin{aligned}\omega &= k\tilde{c}_s + \frac{i\omega k c_s^2 \tau_c}{2\tilde{c}_s}\left[\frac{16}{15} + \frac{3\omega^2R^2}{k^2} - 6R^2\mathcal{F} + \frac{3k^2R^2}{\omega^2}\mathcal{F}^2\right] \\ &= k\tilde{c}_s + \frac{ik^2c_s^2\tau_c}{2}\left[\frac{16}{15} + \frac{R^2}{1+R}\left(1 - 3(2+R)\mathcal{F} + \frac{3(1+R)}{\tilde{c}_s^2}\mathcal{F}^2\right)\right],\end{aligned} \tag{2.59}$$

where, in the second equality, we have inserted the zeroth order part of the τ_c expansion ($\omega_0 = k\tilde{c}_s$) into the first order correction. Now using this expression in our ansatz for δ_γ we find

$$\begin{aligned}\delta_\gamma \propto e^{i\int\omega d\tau} &= e^{ik\int\tilde{c}_s d\tau} e^{i\int\delta\omega d\tau} \\ &= e^{ik\tilde{r}_s} e^{-k^2/\tilde{k}_D^2}\end{aligned} \tag{2.60}$$

where $\delta\omega$ is the second term in (2.59),

$$\tilde{r}_s = \int_0^\tau \tilde{c}_s d\tau' \tag{2.61}$$

is the sound horizon (which in general differs from its value in General Relativity) and $\tilde{k}_D$ is the modified damping wavenumber:

$$\frac{1}{\tilde{k}_D^2} = \int_z^\infty \frac{dz(1+z)}{6H(1+R)n_e\sigma_T}\left[\frac{16}{15} + \frac{R^2}{1+R}\left(1 - 3(2+R)\mathcal{F} + \frac{3(1+R)}{\tilde{c}_s^2}\mathcal{F}^2\right)\right]. \tag{2.62}$$

It can be seen that the additional terms are multiplied by $R^2/(1+R)$. Deep in the radiation dominated epoch when $\rho_\gamma \gg \rho_b$ these terms will be totally insignificant. We found that these modifications are irrelevant for the μ–distortion considered in the next section.

The evolution of $\tilde{c}_s$ depends on the details of the coupling functions $C(\phi)$ and $D(\phi)$ and can be very complicated, even in purely conformal theories ($D = 0$). Potentially, $\tilde{c}_s^2$ can become negative, signalling instabilities but we will not study the consequences of an imaginary sound-speed during the radiation dominated epoch. Note that $\tilde{c}_s$ is

k–dependent, which means that each mode k has its own propagation speed and so each mode has traveled a different distance at a given redshift. Therefore, $\tilde{r}_s$ is also k–dependent.

There are several observables which depend on the sound-speed and can therefore be used to search for deviations from General Relativity. In this chapter we consider two of them, namely the sound horizon at decoupling and the μ–distortion. The sound horizon at decoupling determines, for example, the position of the peaks in the anisotropy spectrum. Since the position of the first peak is well known, $\tilde{r}_s(z_{\rm dec})$ cannot vary too much from its value in General Relativity. As an integral of $\tilde{c}_s$ over time, $\tilde{r}_s(z_{\rm dec})$ is dependent mostly on the evolution of $\tilde{c}_s$ for redshifts below 10^5 or so. The μ–distortion of the CMB blackbody spectrum is created in the redshift range $5 \times 10^4 \leq z \leq 2 \times 10^6$ and probes length scales of order $k \approx 10$ Mpc^{-1} to $k \approx 10^4$ Mpc^{-1} . As such, μ not only provides useful information about the primordial curvature perturbation and therefore about inflationary physics, but also about modifications of gravity. In fact, the μ–distortion of the CMB spectrum is the earliest possible direct probe of modifications of gravity available to us. We therefore turn our attention to calculate μ in the next section.

§ 2.3 μ-type distortion due to dissipation of acoustic waves

The evolution of the μ–distortion is given by [59, 58]

$$\frac{d\mu}{dt} = -\frac{\mu}{t_{\rm DC}(z)} + 1.4\frac{d\mathcal{Q}/dt}{\rho_\gamma}, \tag{2.63}$$

where the last term describes the change of μ due to the input of energy into the coupled photon-baryon fluid and the first term describes the thermalization process with $t_{\rm DC}$ being the double Compton scattering time scale. We will give the expression for $\mathcal{Q}$ below.

The solution of this equation is

$$\begin{aligned}\mu &= 1.4\int_{t(z_1)}^{t(z_2)} dt \frac{d\mathcal{Q}/dt}{\rho_\gamma} e^{-(z/z_{\rm DC})^{5/2}} \\ &= 1.4\int_{z_1}^{z_2} dz \frac{d\mathcal{Q}/dz}{\rho_\gamma} e^{-(z/z_{\rm DC})^{5/2}},\end{aligned} \tag{2.64}$$

where

$$z_{\rm DC} = 1.97 \times 10^6 \left(1 - \frac{1}{2}\left(\frac{Y_p}{0.24}\right)\right)^{-2/5} \left(\frac{\Omega_b h^2}{0.0224}\right)^{-2/5}, \tag{2.65}$$

and Y_p is the primordial helium mass fraction.

To calculate the energy input, we follow [38, 80] who showed that the energy density of an acoustic wave in the photon-baryon plasma can be written as

$$\mathcal{Q} = \rho_\gamma \frac{c_s^2}{1+w_\gamma} \left\langle \delta_\gamma^2(\vec{x}) \right\rangle_P , \tag{2.66}$$

where we here ignore the baryon density (which is much smaller than the energy density in photons ρ_γ), c_s is the sound-speed of the wave, δ_γ is the photon density contrast, $w_\gamma = p_\gamma/\rho_\gamma = \frac{1}{3}$ and the average $\langle ... \rangle_P$ denotes an average over one period of oscillation. The expression (2.66) differs by a factor of 3/4 from that given in [58] who used the formula for the average energy density in acoustic waves in massive particles applied to photons. The correction we use here was found by [38] who derived it using the full Boltzmann equation. We have

$$\left\langle \delta_\gamma^2(\vec{x}) \right\rangle_P = \int \frac{d^3k}{(2\pi)^3} P_\gamma(k), \tag{2.67}$$

where $P_\gamma(k)$ is the power spectrum of the photon density contrast. The power spectrum $P_\gamma(k)$ for scales well within the horizon can be related to the primordial power spectrum $P_\gamma^i(k)$ by

$$P_\gamma(k) = \Delta_\gamma^2(k) P_\gamma^i(k), \tag{2.68}$$

where Δ_γ is the transfer function. In General Relativity, the transfer function reads

$$\Delta_\gamma(k) = 3\cos(k\tilde{r}_s) e^{-k^2/k_D^2}, \tag{2.69}$$

where $\tilde{r}_s = \int \tilde{c}_s d\tau$ is the sound horizon and k_D is the diffusion scale. The factor of 3 takes into account the fact that the potential is decaying on super-horizon scales, leading to an enhancement in δ_γ [60, 38]. It is here that modifications of gravity could play an important role too: if the field is light ($m < H$) the enhancement might be larger or smaller, depending on the coupling functions C and D. On the other hand, in theories such as chameleon theories, the mass of the scalar degree of freedom is much larger than the Hubble expansion rate H and the field is short ranged. This is the case we consider here and so we expect the factor of 3 to be a very good approximation.

The primordial power spectrum for photons can be written [64]

$$P_\gamma^i(k) \approx 1.45 P_\zeta = 1.45 A_\zeta \frac{2\pi^2}{k^3} \left(\frac{k}{k_0}\right)^{n_s - 1 + \frac{1}{2}\alpha \ln\left(\frac{k}{k_0}\right)} \tag{2.70}$$

where P_ζ is the primordial power spectrum for the curvature perturbation in the comoving gauge, $A_\zeta = 2.4 \times 10^{-9}$, $k_0 = 0.002 \mathrm{Mpc}^{-1}$, n_s is the spectral index and

$$\alpha \equiv dn_s/d\ln k \tag{2.71}$$

is the running of the index.

In the standard case $\tilde{c}_s$ is independent of the wavenumber k, but as we have seen, the interaction of the baryons with the scalar field causes $\tilde{c}_s$ to be dependent on the wavenumber. We are interested in scales much smaller than the interaction range of the scalar field ($k \gg m(a)a$) and $\tilde{c}_s$ is only varying very slowly in time. Using equation (2.66) for a wave with a given wave vector $\vec{k}$, one can derive the energy density of that wave. Then using (2.68) in (2.67) and including the modified sound speed in the integral over all waves gives the total energy density

$$\mathcal{Q} = \tfrac{3}{4}\rho_\gamma \int \frac{d^3k}{(2\pi)^3} \tilde{c}_s^2(k) \Delta_\gamma^2(k) P_\gamma^i(k) \ . \tag{2.72}$$

Then using the fact that the average over one oscillation of $\cos^2(x)$ is $1/2$ and treating the photon density as effectively constant over the timescales considered we can obtain the energy release per unit redshift

$$\frac{d\mathcal{Q}/dz}{\rho_\gamma} = 1.1745 \times 10^{-8} \int \frac{dk}{k} \left(\frac{k}{k_0}\right)^{n_s - 1 + \frac{1}{2}\alpha_s \ln\left(\frac{k}{k_0}\right)} \frac{d}{dz}\left(\tilde{c}_s^2(k) e^{-2k^2/k_D^2}\right). \tag{2.73}$$

We can then use this expression to evaluate equation (2.64).

For the models considered here the effect of modified gravity on μ comes solely from the modified sound-speed. How $\tilde{c}_s$ deviates from its evolution in General Relativity depends on the coupling functions $C(\phi)$ and $D(\phi)$ and the potential $V(\phi)$. Therefore, a plethora of possibilities could be explored. To keep things simple however we shall focus on the purely conformal case for which (with $C = e^{2\beta\phi}$ and $D = 0$) the effective sound-speed can be written as

$$\tilde{c}_s^2 = c_s^2 \left(1 - \frac{9\Omega_b \beta^2 R \mathcal{H}^2}{k^2 + m^2 a^2 + 3\mathcal{H}^2 \beta' \Omega_b)}\right), \tag{2.74}$$

where Ω_b is the fractional energy density of baryons and $\beta' = d\beta/d\phi$. In this case the effective sound-speed is smaller than in General Relativity. Precisely when and how much smaller is dictated by how the coupling strength β and the mass ($m^2 = d^2V/d\phi^2$) evolve in time. It is instructive to estimate the deviation of $\tilde{c}_s^2$ from its value in General Relativity. When the coupling strength is constant, we find

$$\mathcal{A} \equiv \frac{9\Omega_b\beta^2 R\mathcal{H}^2}{k^2 + m^2a^2} = \frac{27\Omega_{b,0}^2 H_0^2\beta^2}{4\Omega_{\gamma,0}(k^2 + m^2a^2)}. \tag{2.75}$$

Looking at a regime for which $m^2a^2 \ll k^2$ and $k = 100$ Mpc^{-1}, we find $\mathcal{A} = 10^{-3}$ for $\beta = 10^3$, and $\mathcal{A} = 0.15$ for $\beta = 10^4$. Therefore, rather large couplings are needed in this case for the sound-speed to deviate significantly from its value in General Relativity. As mentioned above, for such a theory to be consistent with the observed CMB anisotropies, the sound horizon cannot be modified very much. Therefore $\mathcal{A}$ has to become small before decoupling which requires that either β decreases or m increases well before decoupling. In the following we focus on the former case for which β becomes smaller in time and as a concrete example we consider

$$\beta = b\left[1 + \tanh\left(d(z - z_0)\right)\right], \tag{2.76}$$

where z_0 is a redshift after which the coupling becomes rapidly smaller, and b and d are constants. For the mass we assume that

$$m(z) = m_{\rm rat}H(z), \tag{2.77}$$

with $m_{\rm rat}$ being a constant. In Fig. 2.1 we show the evolution of $\tilde{c}_s$ for a couple of choices of b, d, z_0 and $m_{\rm rat}$. In the first case, the sound-speed deviates from its value in General Relativity at high redshifts ($z > 10^6$), but approaches the standard value quickly for $z < 10^6$. In the second case, the deviation is quite large for $z > 400000$, so $\tilde{c}_s$ approaches c_s at a later time than in the first example and the maximum deviation is greater in this case. In both cases the sound-speed approaches its standard value in General Relativity. A motivation for the behaviour of β could be that General Relativity is an attractor in the radiation dominated epoch (see e.g. [42] for early ideas on such models).

The corresponding results for the μ–distortion as a function of spectral index n_s and running α (defined in (2.71)) for the evolution of $\tilde{c}_s$ are shown in Fig. 2.2, where we also show the predictions for General Relativity which agree with [46], but with the relativistic correction of 3/4 taken into account. As expected, the predicted μ

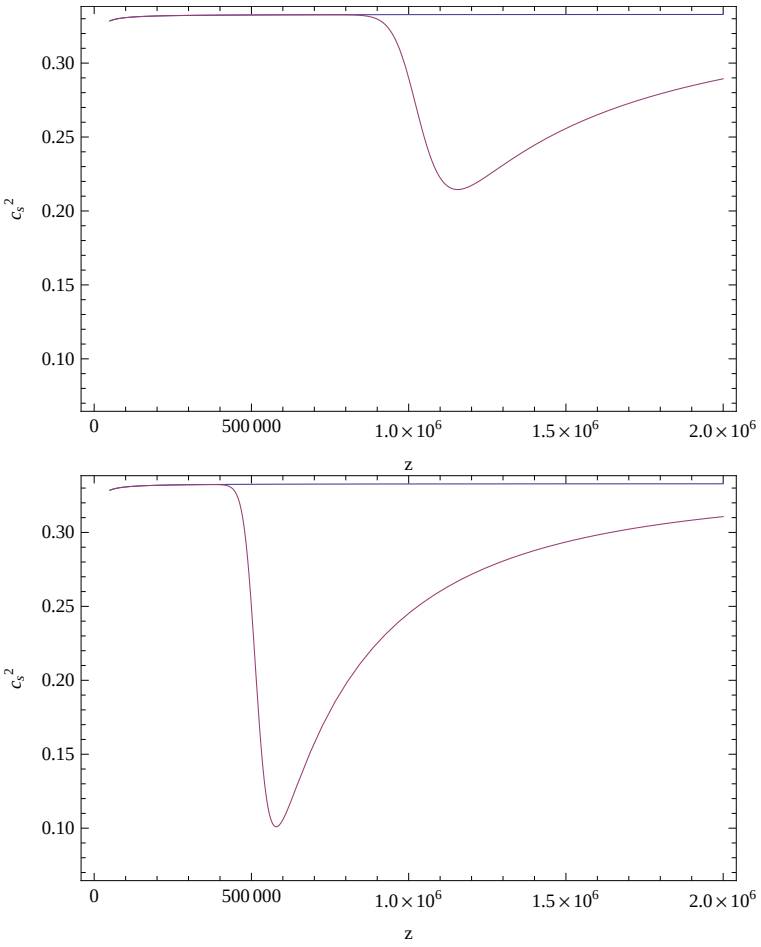

Figure 2.1: These graphs show the evolution of the effective sound-speeds, with $k = 100$ Mpc^{-1}, for two examples. In the top plot we have taken $b = 7 \times 10^4$, $d = 10^{-5}$, $z_0 = 10^6$ and $m_{\rm rat} = 350$. In the bottom plot we have taken $b = 5 \times 10^4$, $d = 2 \times 10^{-5}$, $z_0 = 5 \times 10^5$ and $m_{\rm rat} = 350$. We also plot the evolution of the standard sound-speed (upper curve in both graphs).

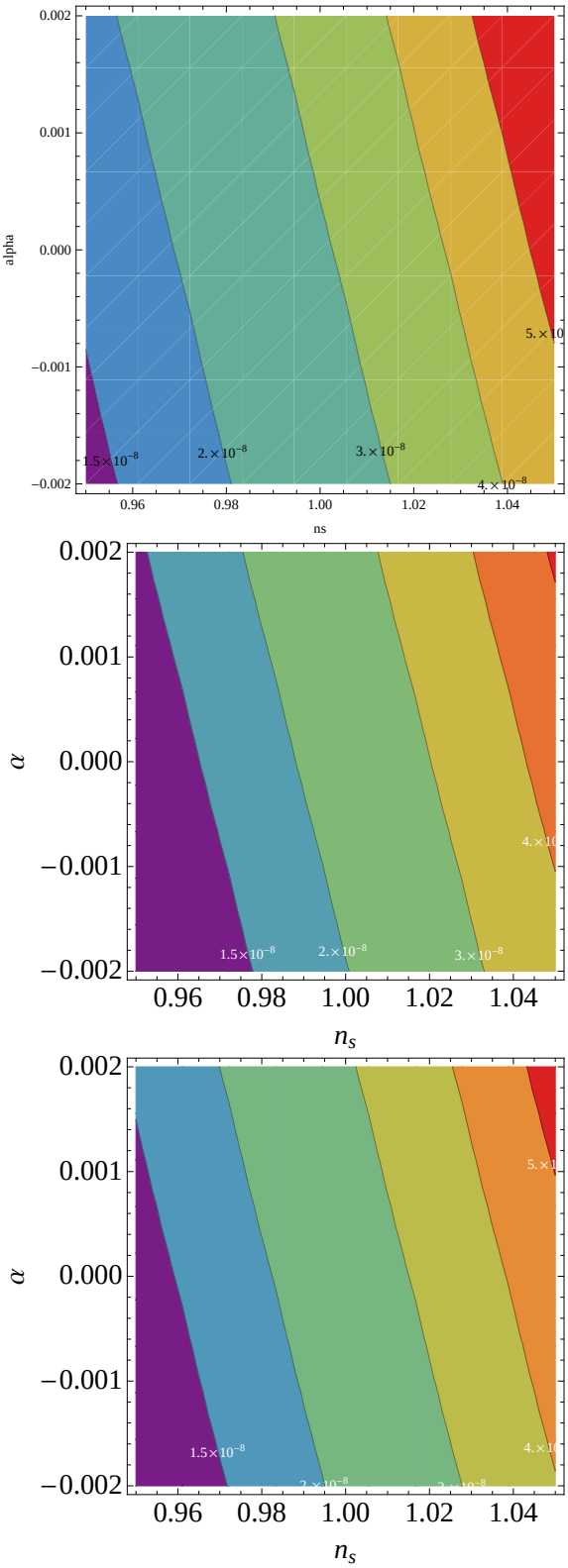

Figure 2.2: The upper graph shows the predictions for the μ–distortion in the case of General Relativity as a function of the spectral index n_s and the running α. The two lower graphs show the predictions for two examples of modified gravity, with the parameters taken as in Fig. 2.1. Since in our case the sound-speed $\tilde{c}_s$ is smaller than in the standard case, μ is predicted to be smaller for a given n_s and α.

is smaller than in General Relativity since $\tilde{c}_s$ is smaller. For the examples shown we see that the predictions for μ are very similar, although the evolution of the sound-speed is significantly different. The sound horizon for both cases deviates less than a percent from its value in General Relativity for all relevant k–values. For the examples studied here the effects of the coupling of ϕ to baryons on μ are of order 10^{-9}, similar to other, less exotic contributions. Thus the predictions for the μ–distortion depend on the details of the evolution of the coupled photon-baryon fluid and therefore provide a window for modifications of gravity.

In Fig. 2.3 we show a case for which the deviations of the effective sound-speed from c_s are significant for $z > 150000$, but not below. In this case the predictions for μ are very similar to in General Relativity, but the prediction for the sound horizon deviates by 17 percent for $k < 0.1$ Mpc^{-1}. This example is ruled out by observations of the CMB anisotropies and the matter power spectrum and was added just for illustration. What becomes clear from these considerations (and from Eq. (2.75)) is that it is the interplay between β and m (both their magnitude and evolution) which determines the predictions for μ and $\tilde{r}_s$. Even in the case of purely conformal couplings, with different choices for β and m a range of possible deviations in either $\tilde{r}_s$ or μ (or both) can be obtained. If we were to allow for a disformal coupling as well ($D \neq 0$), the results for μ and $\tilde{r}_s$ would also depend on the first derivative of the potential and, in general, the evolution of ϕ, at which point general statements about predictions and trends are no longer useful but instead concrete models (i.e. concrete choices for $C(\phi)$, $D(\phi)$ and $V(\phi)$) have to be studied. However, the results above show that the μ–distortion of the CMB is a useful tool to constrain modifications of gravity further.

§ 2.4 Conclusions

In this Chapter, we have derived the general coupling of a fluid (relativistic or non-relativistic) to a scalar field, whose influence is described by the effective metric given in Eq. (2.3). We allowed not only for conformal but also disformal couplings and these expressions are generic when the scalar field is coupled to one species only, whose equation of state is w_i. It is clear that even in this case the evolution of the effective coupling (Q_0/ρ_i in equation (2.22) for the background evolution) can be rather complicated. The evolution of its perturbation (given in Eq. (2.26)) is even more complicated. Therefore, in these scenarios, the coupling is in general a function of time. This opens the door to a rich phenomenology. Considering the case of a

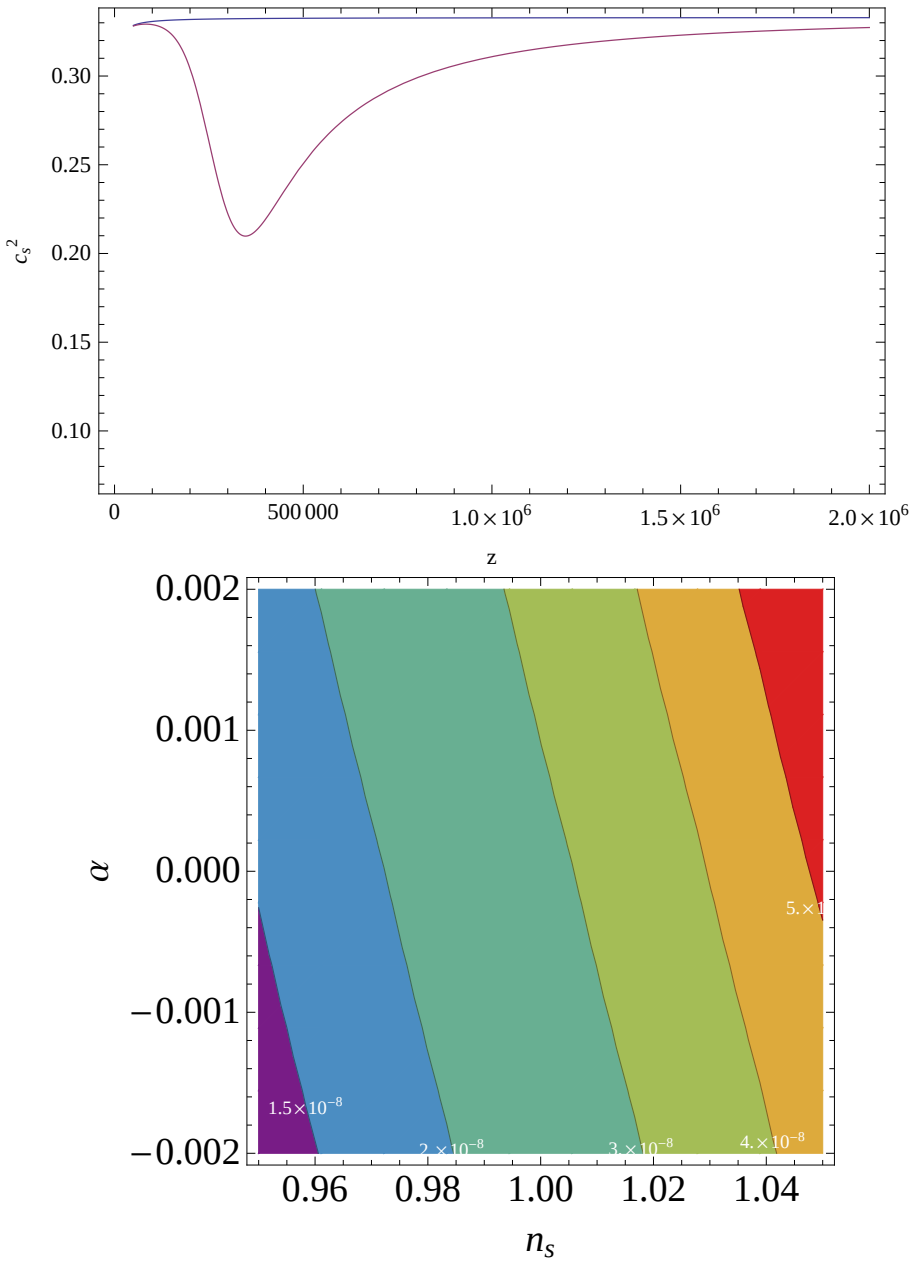

Figure 2.3: In this example we have taken $b = 2.5\times10^4$, $d = 10^{-5}$, $z_0 = 2.5\times10^5$ and $m_{\rm rat} = 350$ (and $k = 100$ Mpc^{-1} to calculate $\tilde{c}_s$ in the upper plot). As can be seen, the sound-speed approaches its standard value only for $z < 150000$ and the deviation of μ from its value in General Relativity is very small. However, the sound horizon deviates from its value in General Relativity by 17 percent for $k < 0.1$ Mpc^{-1}. This case is not compatible with other cosmological observations and is shown only for illustration.

scalar field coupled to baryons, we have derived the expression for the effective sound-speed of the tightly coupled photon-baryon fluid, which differs from the expression in General Relativity. As we have pointed out, the μ–distortion of the CMB can be used to constrain the evolution of $\tilde{c}_s$ and therefore constrain modifications of gravity at very high redshifts ($5 \times 10^4 \leq z \leq 2 \times 10^6$) and small length scales ($k > 50$ Mpc^{-1}). At these times the universe was less than 1Mpc in diameter. Therefore we have calculated the μ–distortion for some simple examples in which the coupling becomes smaller as time progresses. In these cases the μ–distortion is smaller than in General Relativity because the sound-speed is smaller. Determining whether this is generic would require a comprehensive analysis of different choices for the functions $C(\phi)$, $D(\phi)$ and $V(\phi)$.

The μ–distortion of the CMB spectrum is a useful additional probe for testing gravity and not only for the primordial power spectrum of perturbations. As we have seen, for theories with conformal couplings the coupling has to be large ($\beta > 10^3$) for μ to deviate significantly from its value in General Relativity.

Chapter 3

Screened Modified Gravity and the CMB

§ 3.1 Introduction

As previously discussed, a number of models of screened modified gravity satisfy a tomographic description [28, 29]. These models cannot be distinguished from ΛCDM at the background level because the field remains close to the minimum of the effective potential since before BBN. However the evolution of perturbations in these models may be sufficiently modified that deviations from ΛCDM could be observed. The evolution of perturbations on scales outside the Compton wavelength of the scalar field is expected to differ only slightly from ΛCDM but on smaller scales deviations may be significant. The interaction range usually changes with the cosmological expansion in these models as can the coupling strength, but usually local constraints today impose that in the present universe the range of interaction is less than 1 Mpc. Therefore to test these models with cosmological observations, predictions for structure formation at small length scales need to be studied in detail using N-body simulations [22, 31, 30, 45]. Larger scales affected by linear perturbation theory can show deviations which are smaller but could still be within reach by precision cosmology. In the future, besides the large scale structure surveys at low redshifts, the 21-cm signal from the reionisation or the late dark ages may provide complementary constraints [87, 52, 39, 26]. A typical result of screening is that the effects of the scalar field are greater at later times and in lower densities and so it is natural that previous work has concentrated on predictions for corresponding observations. However, it is worth considering what effects these models could have in earlier epochs both to provide a cross-check for other observations and to extend

our knowledge of the phenomenology of modified gravity generally. In this chapter we address the following questions: i) How can screened gravity affect the evolution of linear perturbations before recombination? And ii) imposing the BBN and local test constraints on screened modified gravity, can we find new regimes/models for which those effects leave observable imprints on the CMB as well as the matter power spectrum? These questions are considered for two classes of screened gravity models: generalised chameleons [28, 29], to which the $f(R)$, dilaton and chameleon models belong, and a new phenomenological model where the coupling of the scalar field to matter undergoes a transition before the time of last scattering. For this purpose, we use the fact that models of screened modified gravity can be described by two functions of the scale-factor a: the effective mass $m(a)$ of the scalar field and the couplings to matter $\beta(a)$. This tomographic approach has the advantage that several models are described within one framework via different $m(a)$ and $\beta(a)$ functions. We shall see that there can be significant deviations from ΛCDM in the CMB spectrum for the transition models where the modifications of gravity are significant before recombination. These manifest themselves as both enhancements and reductions of power on different scales. It is possible to choose parameters such that these differences are at the percent level while preserving structure formation and evading local tests of gravity. In contrast we find that, for generalised chameleon models with couplings that are stronger at earlier rather than later times, the constraint on the variation over time of particle masses is violated before we observe effects on the CMB. For these models it would seem that large scale structure is the best cosmological test. Therefore we conclude that the signatures of the generalised chameleons and the early transition models are sufficiently different to envisage the possibility of distinguishing different models of modified gravity using CMB data if they were ever to be observed.

§ 3.2 Screened Modified Gravity

In the Einstein frame the Einstein equations are preserved and depend on the energy momentum tensor of the scalar field:

$$R_{\mu\nu} - \frac{1}{2} g_{\mu\nu} R = 8\pi G_N \left(\sum_\alpha T^{(\alpha)}_{\mu\nu} + T^{(\phi)}_{\mu\nu} \right) , \tag{3.1}$$

where

$$T^{(\phi)}_{\mu\nu} = \partial_\mu \phi \partial_\nu \phi - g_{\mu\nu} \left(\frac{1}{2} (\partial\phi)^2 + V \right) . \tag{3.2}$$

In these models the relation between the metrics is conformal,

$$g^{(\alpha)}_{\mu\nu} = A^2_\alpha(\phi) g_{\mu\nu}, \quad \alpha = b, c \tag{3.3}$$

and we allow for the possibility of a different coupling to each matter species which are defined as

$$\beta_\alpha(\phi) = m_{\rm Pl} \frac{\partial \ln A_\alpha(\phi)}{\partial \phi} \tag{3.4}$$

where $m_{\rm Pl}^{-2} \equiv 8\pi G_N$ is the reduced Planck mass. Due to the interaction with the scalar field, matter is not conserved and satisfies

$$\nabla_\mu T^{\mu\nu}_{(\alpha)} = \frac{\beta_\alpha}{m_{\rm Pl}} (\partial^\nu \phi) T_{(\alpha)}. \tag{3.5}$$

where $T^{\mu\nu}_{(\alpha)}$ is the energy momentum tensor of the species α and $T_{(\alpha)}$ its trace. As a result of the conformal relation radiation is not affected by the presence of the coupled scalar field. The effective potential for the scalar field in the matter era is modified by the presence of matter as a consequence of the non-trivial matter couplings

$$V_{\rm eff}(\phi) = V(\phi) + \sum_\alpha (A_\alpha(\phi) - 1) \rho^*_\alpha \tag{3.6}$$

where the sum is taken over the non-relativistic species and ρ^*_α is the conserved energy density of the fluid α, related to the normal Einstein frame matter density by $\rho^* = \rho/A$. The potential acquires a slowly varying minimum $\phi(\rho^*_\alpha)$ as long as the mass $m^2 = \frac{d^2 V_{\rm eff}}{d^2\phi}|_{\phi(\rho^*_\alpha)}$ is larger than the Hubble rate. We will always assume that this is the case in the following.

§ 3.3 Perturbations

In this section, we study the evolution of perturbations with analytical methods, to gain an understanding of the physics involved. From now on we will work in natural units where $8\pi G_N = 1$. We are interested in the first order perturbations of the Einstein equation and the conservation equations. In the absence of anisotropic stress, the metric can be described in the conformal Newton gauge

$$ds^2 = a(\tau)(-(1+2\Phi)d\tau^2 + (1-2\Phi)\gamma_{ij} dx^i dx^j), \tag{3.7}$$

where Φ is Newton's potential. In this gauge the relevant Einstein equations are (in Fourier space)

$$k^2\Phi + 3\mathcal{H}(\dot{\Phi} + \mathcal{H}\Phi) = -a^2\sum_\alpha \delta\rho_\alpha - a^2\left(\frac{\dot{\phi}^2}{a^2}\Phi - \frac{\dot{\phi}}{a^2}\delta\dot{\phi} - V_{,\phi}\delta\phi\right) \tag{3.8}$$

and

$$k^2(\dot{\Phi} + \mathcal{H}\Phi) = a^2\sum_\alpha (1+w_\alpha)\theta_\alpha + k^2\dot{\phi}\delta\phi \ , \tag{3.9}$$

where $\delta\rho_\alpha = \rho_\alpha\delta_\alpha$. The Hubble rate is $\mathcal{H} = \dot{a}/a$ and the equation of state of each species is w_α. We have defined the divergence of the velocity field of each species $\theta = \partial_i v^i$. The perturbed Klein-Gordon equation reads

$$\begin{aligned}\delta\ddot{\phi} + 2\mathcal{H}\delta\dot{\phi} + (k^2 + a^2V_{,\phi\phi})\delta\phi + 2\Phi a^2 V_{\text{eff},\phi} - 4\dot{\Phi}\dot{\phi} + a^2\left(\beta_c\delta\rho_c + \beta_b\delta\rho_b\right) \\ + a^2\left(\beta_{c,\phi}\rho_c + \beta_{b,\phi}\rho_b\right)\delta\phi = 0 \ .\end{aligned} \tag{3.10}$$

We now consider the perturbation equations in CDM, baryons and radiation. The conservation equation for CDM leads to the coupled equations

$$\dot{\delta}_c = -(\theta_c - 3\dot{\Phi}) + \beta_{c,\phi}\dot{\phi}\delta\phi + \beta_c\delta\dot{\phi}, \tag{3.11}$$

and

$$\dot{\theta}_c = -\mathcal{H}\theta_c + k^2\Phi + k^2\beta_c\delta\phi - \beta_c\dot{\phi}\theta_c. \tag{3.12}$$

For the baryons we get

$$\dot{\delta}_b = -\theta_b + 3\dot{\Phi} + \beta_{b,\phi}\dot{\phi}\delta\phi + \beta_b\delta\dot{\phi}, \tag{3.13}$$

and

$$\dot{\theta}_b = -\mathcal{H}\theta_b + \frac{an_e\sigma_T}{R}(\theta_\gamma - \theta_b) + k^2\Phi + \beta_b k^2\delta\phi - \beta_b\dot{\phi}\theta_b, \tag{3.14}$$

where we have added the interaction term to account for the coupling to photons via Thompson scattering in which n_e is the electron number density, σ_T is the Thomson scattering cross-section and $R = 3\rho_b/4\rho_\gamma$.

The Thompson scattering cross section depends on the electron mass m_e which is field dependent due to the conformal rescaling of the metric, i.e. m_e is proportional to $A_b(\phi)$. However, since the scalar field tracks the minimum of the effective potential, the time variation of the electron mass in one Hubble time is suppressed by $\mathcal{O}(\frac{H^2}{m^2}) \ll 1$ and can therefore be neglected.

To describe the photons we shall work in the fluid approximation and since the Boltzmann hierarchy is not altered by the presence of a scalar field we have

$$\dot{\delta}_\gamma = -\frac{4}{3}\theta_\gamma + 4\dot{\Phi} \tag{3.15}$$

and

$$\dot{\theta}_\gamma = \frac{k^2}{4}\delta_\gamma + k^2\Phi + an_e\sigma_T(\theta_b - \theta_\gamma). \tag{3.16}$$

We also need to specify the initial conditions for all the perturbations. We will be interested in modes which will enter the horizon before radiation-matter equality. Adiabatic initial conditions are determined by $\delta_c^i = \delta_b^i = \frac{3}{4}\delta_\gamma^i$ and $\delta_b^i = -\frac{3}{2}\Phi^i$.

On subhorizon scales and neglecting the time variation of ϕ, the equations simplify:

$$\dot{\delta}_c = -\theta_c, \tag{3.17}$$

$$\dot{\theta}_c = -\mathcal{H}\theta_c + k^2\Phi + k^2\beta_c\delta\phi. \tag{3.18}$$

$$\dot{\delta}_b = -\theta_b, \tag{3.19}$$

$$\dot{\theta}_b = -\mathcal{H}\theta_b + \frac{an_e\sigma_T}{R}(\theta_\gamma - \theta_b) + k^2\Phi + \beta_b k^2\delta\phi, \tag{3.20}$$

$$\dot{\delta}_\gamma = -\frac{4}{3}\theta_\gamma \tag{3.21}$$

$$\dot{\theta}_\gamma = \frac{k^2}{4}\delta_\gamma + k^2\Phi + an_e\sigma_T(\theta_b - \theta_\gamma). \tag{3.22}$$

To leading order in the tight-coupling approximation $an_e\sigma_T \to \infty$ which implies $\theta_b \approx \theta_\gamma$, and therefore the photon and baryon density contrasts are linked by $\delta_b \approx \frac{3}{4}\delta_\gamma$. This leads to

$$\ddot{\delta}_b = -\frac{\dot{R}}{(1+R)}\dot{\delta}_b - k^2c_s^2\delta_b - k^2\Phi - \frac{R}{(1+R)}\beta_b k^2\delta\phi, \tag{3.23}$$

where $c_s = 1/\sqrt{3(1+R)}$ is the standard sound-speed. The Klein-Gordon equation in the subhorizon limit is

$$\delta\phi = -\frac{\beta_c\delta\rho_c + \beta_b\delta\rho_b}{\frac{k^2}{a^2} + V_{,\phi\phi} + \beta_{c,\phi}\rho_c + \beta_{b,\phi}\rho_b}. \tag{3.24}$$

Using this and approximating the Poisson equation with $2k^2\Phi = -a^2\delta\rho_c$, and then

defining $\delta_b = (1+R)^{-1/2}\delta$ yields

$$\ddot{\delta} + c_s^2 k^2 \left(1 - \frac{9\Omega_b \beta_b^2 R\mathcal{H}^2}{k^2 + a^2 V_{,\phi\phi} + 3\mathcal{H}^2(\beta_{c,\phi}\Omega_c + \beta_{b,\phi}\Omega_b)}\right)\delta$$
$$= -k^2(1+R)^{1/2}\left(1 + \frac{2\beta_b\beta_c}{1 + \frac{a^2 V_{,\phi\phi} + 3\mathcal{H}^2(\beta_{c,\phi}\Omega_c + \beta_{b,\phi}\Omega_b)}{k^2}}\frac{R}{R+1}\right)\Phi. \tag{3.25}$$

This can be simplified by introducing

$$\tilde{\delta} = \delta + (1+R)^{1/2}\left(1 + \frac{2\beta_b\beta_c}{1 + \frac{a^2 V_{,\phi\phi} + 3\mathcal{H}^2(\beta_{c,\phi}\Omega_c + \beta_{b,\phi}\Omega_b)}{k^2}}\frac{R}{R+1}\right)\frac{\Phi}{\tilde{c}_s^2}, \tag{3.26}$$

where the effective speed of sound is

$$\tilde{c}_s^2 = c_s^2\left(1 - \frac{9\Omega_b \beta_b^2 R\mathcal{H}^2}{k^2 + a^2 V_{,\phi\phi} + 3\mathcal{H}^2(\beta_{c,\phi}\Omega_c + \beta_{b,\phi}\Omega_b)}\right). \tag{3.27}$$

This leads to

$$\ddot{\tilde{\delta}} + \tilde{k}^2 c_s^2 \tilde{\delta} = 0, \tag{3.28}$$

and using the WKB method the solution is

$$\tilde{\delta} = \tilde{c}_s^{-1/2} B \cos k\tilde{r}_s, \tag{3.29}$$

where B is set by the initial conditions and $\tilde{r}_s(\tau) = \int_0^\tau \tilde{c}_s d\tau$ is the modified sound horizon. We can relate this to back to the baryon perturbation,

$$\delta_b = \frac{\tilde{\delta}}{(1+R)^{1/2}} - \left(1 + \frac{2\beta_b\beta_c}{1 + \frac{a^2 V_{,\phi\phi} + 3\mathcal{H}^2(\beta_{c,\phi}\Omega_c + \beta_{b,\phi}\Omega_b)}{k^2}}\frac{R}{R+1}\right)\frac{\Phi}{\tilde{c}_s^2}. \tag{3.30}$$

We should note that the WKB approximation is only valid if the time variation of $\tilde{c}_s$ is smooth. This will be violated for a short period in the models with a transition in β. As implied above the evolution of the Newtonian potential before last scattering is dominated by that of the CDM perturbations. Equations (3.17) and (3.18) therefore lead to the growth equation for CDM

$$\ddot{\delta}_c + \mathcal{H}\dot{\delta}_c - \frac{3}{2}\mathcal{H}^2\Omega_c\left(1 + \frac{2\beta_c^2}{1 + \frac{a^2 V_{,\phi\phi} + 3\mathcal{H}^2(\beta_{c,\phi}\Omega_c + \beta_{b,\phi}\Omega_b)}{k^2}}\right)\delta_c$$
$$- \frac{3\mathcal{H}^2\Omega_b\beta_b\beta_c}{1 + \frac{a^2 V_{,\phi\phi} + 3\mathcal{H}^2(\beta_{c,\phi}\Omega_c + \beta_{b,\phi}\Omega_b)}{k^2}}\delta_b = 0 \tag{3.31}$$

As noted in [27] we can identify three possible sources of modification to the CMB angular power spectrum. These are the modified sound horizon which could cause a shift in the peak positions, the modified evolution of the Newtonian potential due to anomalous growth of the CDM perturbations, and an extra contribution to the growth of the baryon perturbations proportional to Φ and the couplings to both baryons and CDM.

§ 3.4 The models

To be concrete, we will consider two models which we will now describe.

3.4.1 Generalised Chameleons

In our first model the scalar field mass and the couplings to baryons and dark matter evolve effectively like power-laws in the scale factor,

$$m(a) = m_0 a^{-p}, \qquad \beta_\alpha(a) = \beta_{0\alpha} a^{-b} \ . \tag{3.32}$$

Such a model corresponds to generalised chameleons. Setting $p = 3$, $b = 0$ and $\beta_{b0} = \beta_{c0} = 1/\sqrt{6}$, one recovers the $f(R)$ model [28, 29].
We focus here on the case $b > 0$, for which the coupling to matter is very large during the tight coupling regime but smaller at later times. As we shall discuss in section 3.4.4, the local tests will impose different constraints on m_0 and β_0 for different combinations of the exponents p and b. One also requires $p \geq 3/2$ during the matter dominated era, and $p > 2$ during the radiation era, so that the scalar field mass is always much larger than the Hubble rate, guaranteeing a ΛCDM background expansion.

3.4.2 Transition in β

In the second model we consider that the Universe undergoes a smooth but rapid transition from an epoch of strong coupling between the scalar field and matter to one when the coupling is small and has negligible effect on the growth of perturbations. Using the tomographic maps allowing one to reconstruct $V(\phi)$ and $\beta(\phi)$, one finds that the potential is an inverse power law both before and after a transition point $\phi_{\rm trans}$ where the potential decreases abruptly. The effective potential, both before and after the transition, has a minimum with a large mass where the field gets trapped. Dynamically, the field undergoing the transition jumps from the minimum

before the transition to the minimum after the transition where it will oscillate a few times before being rapidly (the amplitude decreases like $a^{-3/2}$) stuck at the minimum again. We will neglect these decaying oscillations in the following and consider that the field tracks the minimum at all times (for a similar type of phenomenon, see the analysis of the transition in [21]). In order to satisfy the constraints imposed by local tests we are considering very high masses and this will ensure that the field remains close to the minimum through the transition.

We can parameterise this behaviour with the function

$$\beta_{c,b}(a) = \beta_0 + \frac{\beta_i}{2}\left[1 + \tanh(C(a_{\rm trans} - a))\right] \ , \tag{3.33}$$

where the parameter C controls the duration of the transition. We choose the effective mass of the scalar field to evolve like a power-law

$$m(a) = m_0 a^{-p}. \tag{3.34}$$

By setting the transition prior to last scattering, we ensure that all the effects on the CMB angular power spectrum and on the matter power spectrum are caused by the modification of gravity before recombination. Note however that the linear perturbations at recombination, which can be used as initial conditions for the growth of the matter perturbations, are modified and thus can lead to a different evolution compared to the ΛCDM model, even if there is no direct effect of modified gravity on the growth of structures. For the parameters we have considered, values of $\beta_0 \lesssim m_0$ do not lead to any visible modification in the growth of perturbations after last scattering. Since we are considering rather high masses this means a strong coupling even up to the present epoch is not ruled out.

3.4.3 BBN Constraint

It is convenient to introduce the total coupling functions A and β defined such that

$$\beta A \rho = \sum_\alpha \beta_\alpha A_\alpha \rho_\alpha \tag{3.35}$$

where $\rho = \sum_\alpha \rho_\alpha$ is the total conserved energy density of non-relativistic species. In all the models that we consider the masses of fundamental particles vary as

$$m_\psi = A(\phi) m_{\rm bare}, \tag{3.36}$$

where $m_{\rm bare}$ is the bare mass appearing in the matter Lagrangian. The measurements of primordial light element abundances place a tight constraint on the time variation of fermion masses since BBN [79, 12, 15, 77]

$$\frac{\Delta m_\psi}{m_\psi} = \frac{\Delta A}{A} \lesssim 0.1. \tag{3.37}$$

Therefore we must require that $A \approx 1$ since BBN. Using (3.4) and (1.91) we get

$$\frac{dA}{da} = \frac{3\beta^2\rho}{am^2 m_{\rm Pl}^2}, \tag{3.38}$$

and so

$$\Delta A = 9\Omega_m^{(0)} H_0^2 \int_{a_{\rm BBN}}^{a_0} \frac{\beta^2(a)}{a^4 m^2(a)} da \lesssim 0.1. \tag{3.39}$$

For chameleon models this is

$$\frac{9\Omega_m^{(0)} H_0^2 \beta_0^2}{m_0^2} \frac{(a_0^{2p-2b-3} - a_{\rm BBN}^{2p-2b-3})}{2p-2b-3} \lesssim 0.1. \tag{3.40}$$

For the case $2p - 2b - 3 > 0$ this yields

$$\frac{\beta_0}{m_0} \lesssim \left(\frac{2p-2b-3}{90\Omega_m^{(0)} H_0^2} \right)^{1/2} \lesssim \mathcal{O}(10^3) \text{ Mpc}, \tag{3.41}$$

while for $2p - 2b - 3 = 0$

$$\frac{\beta_0}{m_0} \lesssim (90\Omega_m^{(0)} H_0^2 \ln 10^9)^{-1/2} \lesssim \mathcal{O}(10^2) \text{ Mpc}. \tag{3.42}$$

However if $2p - 2b - 3 < 0$ we find

$$\frac{\beta_0}{m_0} \lesssim \left(\frac{|2p-2b-3|}{9\Omega_m^{(0)} H_0^2} \right)^{1/2} 10^{\frac{9(2p-2b-3)-1}{2}} \lesssim \mathcal{O}(10^{\frac{6+9(2p-2b-3)}{2}}) \text{ Mpc}, \tag{3.43}$$

which results in a much tighter constraint on $\frac{\beta_0}{m_0}$ than that coming from the local tests.

For the model with a transition in β the constraint is

$$\frac{9\Omega_m^{(0)} H_0^2}{m_0^2(2p-3)} [\beta_{\rm ini}^2 (a_{\rm trans}^{2p-3} - a_{BBN}^{2p-3}) + \beta_0^2 (a_0^{2p-3} - a_{\rm trans}^{2p-3})] \lesssim 0.1. \tag{3.44}$$

We shall only consider cases where $2p-3>0$ so that

$$\frac{9\Omega_m^{(0)}H_0^2\beta_{\rm ini}^2}{m_0^2(2p-3)}a_{\rm trans}^{2p-3}\lesssim 0.1, \tag{3.45}$$

and if we let $a_{\rm trans}=10^{-t}$ we find

$$\frac{\beta_{\rm ini}}{m_0}\lesssim\left(\frac{2p-3}{9\Omega_m^{(0)}H_0^2}\right)^{-1/2}10^{\frac{t(2p-3)-1}{2}}\lesssim\mathcal{O}(10^{3+t(p-\frac{3}{2})})\text{ Mpc}. \tag{3.46}$$

Typically, we will see that this constraint is superseded by the local constraints.

3.4.4 Local tests

We will now examine the constraints on our two models coming from local tests of gravity. We focus on three tests which can yield strong constraints on screened models. The first comes from the requirement that the Milky Way should be screened in order to avoid large, disruptive effects on its dynamics [86, 62]. The second is the laboratory tests of gravity involving spherical bodies which should not feel a large fifth force [4, 3]. The last one follows from the lunar ranging experiment [99, 97, 100, 98] which looks for violations of the strong equivalence principle, and which turns out to be the strongest constraint for the models we have chosen.
The screening condition is a simple algebraic relation

$$|\phi_{\rm in}-\phi_{\rm out}|\leq 2\beta_{\rm out}m_{\rm Pl}\Phi_N\ , \tag{3.47}$$

where Φ_N is Newton's potential at the surface of a body and $\phi_{\rm in,out}$ are the values of the field inside and outside the body. Using the tomography equation (1.92), we find the relation

$$\frac{|\phi_{\rm in}-\phi_{\rm out}|}{m_{\rm Pl}}=\frac{3}{m_{\rm Pl}^2}\int_{a_{\rm in}}^{a_{\rm out}}\frac{\beta(a)}{am^2(a)}\rho(a)da, \tag{3.48}$$

where $a_{\rm in,out}$ are defined by $\rho(a_{\rm in,out})=\rho_{\rm in,out}$ This condition expresses the fact that the effective modification of Newton's constant felt by an unscreened body in the presence of a screened object due to the scalar field goes from $2\beta^2$ to $2\beta^2\frac{|\phi_{\rm in}-\phi_{\rm out}|}{2\beta m_{\rm Pl}\Phi_N}$. When two screened bodies such as the moon and the earth fall in the gravitational field of the sun, the scalar field induces a relative acceleration between them which is measured by the square of their scalar charges

$$Q=\frac{|\phi_{\rm in}-\phi_{\rm out}|}{m_{\rm Pl}\Phi_N} \tag{3.49}$$

and the lunar ranging experiment requires that the earth's charge $Q_\oplus \leq 10^{-7}$ where $\phi_\oplus \sim 10^{-9}$.

For the Milky Way, the density inside the galaxy is typically 10^6 times the cosmological matter density now, i.e. $a_G \sim 10^{-2}$. The value outside the galaxy is the cosmological one (if it is in a dense cluster then $a_{\rm out} < 1$ and the screening condition is less stringent) so the screening condition reads

$$\frac{|\phi_{\rm G} - \phi_0|}{m_{\rm Pl}} = \frac{3}{m_{\rm Pl}^2}\int_{a_G}^{a_0} \frac{\beta(a)}{am^2(a)}\rho(a)da \leq 2\beta_G\Phi_G \tag{3.50}$$

where $\Phi_G \sim 10^{-6}$. For the generalised chameleon model, this is

$$\frac{9\Omega_m^{(0)}\beta_0 H_0^2}{(2p-b-3)m_0^2}(a_0^{2p-b-3} - a_G^{2p-b-3}) \leq 2\beta_G\Phi_G \ . \tag{3.51}$$

When $2p-b-3<0$, the contribution from a_G dominates and one gets

$$\frac{m_0^2}{H_0^2} \gtrsim \frac{9\Omega_m^{(0)}}{2|2p+b-3|\Phi_G} a_G^{2p-3} \gtrsim \mathcal{O}(10^{6-2(2p-3)}) \ . \tag{3.52}$$

If on the other hand $2p-b-3>0$, the contribution from a_0 dominates and, setting $a_0 \equiv 1$ as usual, one has

$$\frac{m_0^2}{H_0^2} \gtrsim \frac{9\Omega_m^{(0)}}{2(2p-b-3)\Phi_G} \gtrsim \mathcal{O}(10^6) \ . \tag{3.53}$$

For the transition model with $a_{\rm trans} < a_G$, one gets a similar constraint,

$$\frac{m_0^2}{H_0^2} \gtrsim \frac{9\Omega_m^{(0)}}{2(2p-3)\Phi_G} \gtrsim \mathcal{O}(10^6) \ . \tag{3.54}$$

which is independent of the value of β_0.

Tests of gravity in cavities involve spherical bodies of order $L \sim 10$ cm, with a Newtonian potential of order $\Phi_c \sim 10^{-27}$ and a density $\rho_c \sim 10$ g [66]. This density is the cosmological density before BBN when the scalar field must have settled at the minimum of the effective potential. Outside, in the cavity, the scalar field takes a value such that its mass is of order $m_{\rm cav}L \sim 1$ corresponding to a scale factor $a_{\rm cav} = (Lm_0)^{1/p}$. The constraint reads

$$\frac{|\phi_{\rm c} - \phi_{\rm cav}|}{m_{\rm Pl}} = \frac{3}{m_{\rm Pl}^2}\int_{a_c}^{a_{\rm cav}} \frac{\beta(a)}{am^2(a)}\rho(a)da \leq 2\beta_c\Phi_c \ , \tag{3.55}$$

which for the chameleon model with $2p - b - 3 > 0$ is

$$\frac{m_0^2}{H_0^2} \gtrsim \frac{9\Omega_m^{(0)}}{2\Phi_c} \frac{a_{\rm cav}^{2p-b-3}}{2p-b-3} a_c^b \gtrsim \mathcal{O}(10^2) \ . \tag{3.56}$$

For the transition model we find

$$\frac{m_0^2}{H_0^2} \gtrsim \frac{9\Omega_m^{(0)}}{2\Phi_c} \frac{a_{\rm cav}^{2p-3}}{2p-3} \gtrsim \mathcal{O}(10^8) \ , \tag{3.57}$$

which is a tighter constraint than that coming from the screening of the Milky Way.

A much more stringent condition follows from the lunar ranging experiment,

$$\frac{3}{m_{\rm Pl}^2} \int_{a_c}^{a_G} \frac{\beta(a)}{a m^2(a)} \rho(a) da \leq Q_\oplus \Phi_\oplus \ , \tag{3.58}$$

where $Q_\oplus \Phi_\oplus \sim 10^{-16}$ and a_c is associated with the densities inside the earth. For the generalised chameleon model the case $2p - b - 3 < 0$ leads to

$$\frac{m_0^2}{H_0^2} \gtrsim \frac{9\Omega_m^{(0)} \beta_0}{|2p-b-3| Q_\oplus \Phi_\oplus} a_c^{2p-b-3} \ . \tag{3.59}$$

Since $a_c \ll 1$, considering values for which $2p - b - 3 \lesssim -1$ implies an extremely stringent constraint on the ratio m_0^2/β_0 that precludes any visible cosmological signature of the model. We therefore focus on the opposite case $2p - b - 3 > 0$ for which one gets

$$\frac{m_0^2}{H_0^2} \gtrsim \frac{9\Omega_m^{(0)} \beta_0}{Q_\oplus \Phi_\oplus} \frac{a_G^{2p-b-3}}{2p-b-3} \gtrsim \beta_0 \mathcal{O}(10^{16-2(2p-b-3)}) \ . \tag{3.60}$$

For cases where $\beta_0 \sim \mathcal{O}(1)$, $b \simeq 0$ and $p \gtrsim 3$, the lunar ranging bound on m_0 is weaker than the constraint from the Milky Way. For the transition model, assuming $a_{\rm trans} < a_G$ and $2p - 3 > 0$, the condition is

$$\frac{m_0^2}{H_0^2} \gtrsim \frac{9\Omega_m^{(0)} \beta_i}{Q_\oplus \Phi_\oplus} \frac{a_{\rm trans}^{2p-3}}{2p-3} \gtrsim \beta_i a_{\rm trans}^{2p-3} \mathcal{O}(10^{16}) \ . \tag{3.61}$$

For the case $p = 3$, $\beta_i = 10^{13}$ and $z_{\rm trans} = 1090$, this gives the constraint $m_0 \gtrsim 10^{10} H_0$.

§ 3.5 Numerical implementation

We have implemented the linear perturbation dynamics for two models of screened gravity within a modified version of the CAMB code [70]. In this section we give details of the modifications that were required.

CAMB solves the perturbation equations in the synchronous gauge. To account for screened modified gravity it was necessary to add the perturbed Klein Gordon equation which, after using Eq. (1.89) to write $V_{,\phi\phi}$ in terms of the effective mass $m(a)$, can be written

$$\delta\ddot{\phi} + 2\mathcal{H}\delta\dot{\phi} + (k^2 + a^2m^2 - a^2\beta_c^2\rho_c - a^2\beta_b^2\rho_b)\delta\phi + \tfrac{1}{2}\dot{h}\dot{\phi} = -a^2\left(\beta_c\delta\rho_c + \beta_b\delta\rho_b\right), \quad (3.62)$$

and also the evolution equation for θ_c

$$\dot{\theta}_c = -\mathcal{H}\theta_c + k^2\beta_c\delta\phi - \beta_c\dot{\phi}\theta_c \ , \quad (3.63)$$

which, in the presence of modified gravity, is no longer generally vanishing in the synchronous gauge. These equations can be found by perturbing Eqs. (2.10) and (2.13) using the synchronous gauge metric given in (1.21) and (1.22). Extra terms also had to be included in the equations for δ_c, δ_b and θ_b.

Before last scattering modified gravity also introduces new terms in the calculation of the slip, defined as $\dot{\theta}_b - \dot{\theta}_\gamma$. In the synchronous gauge the evolution equations for θ_b and θ_γ are

$$\dot{\theta}_b = -\mathcal{H}\theta_b + c_{sb}^2k^2\delta_\mathrm{b} - \frac{an_e\sigma_T}{R}(\theta_b - \theta_\gamma) + f_\mathrm{MG}, \quad (3.64)$$

and

$$\dot{\theta}_\gamma = \frac{k^2}{4}\delta_\gamma - k^2\sigma_\gamma + an_e\sigma_T(\theta_b - \theta_\gamma), \quad (3.65)$$

where c_{sb}^2 is the adiabatic sound speed of the baryons (not to be confused with c_s^2, the sound speed of the coupled baryon-photon fluid) and we have introduced the notation

$$f_\mathrm{MG} \equiv \beta_\mathrm{b}k^2\delta\phi - \beta_b\dot{\phi}\theta_\mathrm{b} \quad (3.66)$$

corresponding to the additional terms due to screened gravity. During the tight coupling regime the Thomson drag terms in Eqs. (3.64) and (3.65) take very large values making these equations difficult to integrate numerically. In CAMB an alternative form of these equations is used which is valid in the regime $\tau_c \ll \tau$ and $k\tau_c \ll 1$ where $\tau_c \equiv 1/an_e\sigma_T$. In the following we follow [73] to derive the equivalent set of equations in the presence of screened modified gravity. The first step is to use Eq.

(3.65) to write

$$(\theta_{\rm b}-\theta_\gamma)/\tau_{\rm c} = -\dot{\theta}_\gamma + k^2\left(\frac{1}{4}\delta_\gamma - \sigma_\gamma\right), \tag{3.67}$$

and then substitute the corresponding term into Eq. (3.64). One gets

$$\dot{\theta}_b = -\frac{\dot{a}}{a}\theta_{\rm b} + c_{sb}^2 k^2\delta_{\rm b} - R\dot{\theta}_\gamma + Rk^2\left(\frac{1}{4}\delta_\gamma - \sigma_\gamma\right) + f_{\rm MG}\ . \tag{3.68}$$

Then one can rewrite $\dot{\theta}_\gamma = \dot{\theta}_{\rm b} + (\dot{\theta}_\gamma - \dot{\theta}_b)$ in Eq. (3.67), and replace $(\dot{\theta}_\gamma - \dot{\theta}_b)$ by using Eq. (3.68). By defining the functions

$$f \equiv \frac{\tau_{\rm c}}{1+R} \tag{3.69}$$

and

$$g \equiv -\frac{\dot{a}}{a}\theta_{\rm b} + c_{sb}^2 k^2\delta_{\rm b} - R\dot{\theta}_\gamma + Rk^2(\frac{1}{4}\delta_\gamma - \sigma_\gamma) + f_{\rm MG}\ , \tag{3.70}$$

one obtains

$$\theta_{\rm b} - \theta_\gamma = f\left[g - (\dot{f}g)\right] + \mathcal{O}(\tau_{\rm c}^3)\ , \tag{3.71}$$

in which the $\tau_{\rm c}^3$ terms can be conveniently neglected. Differentiating this equation gives

$$\dot{\theta}_b - \dot{\theta}_\gamma = \frac{\dot{f}}{f}(\theta_{\rm b}-\theta_\gamma) + f(\dot{g}\dot{f}g - 2\dot{f}\dot{g} - \ddot{g}f)\ , \tag{3.72}$$

with

$$\dot{g} = -\mathcal{H}\dot{\theta}_b - \dot{\mathcal{H}}\theta_{\rm b} + k^2\left[(\dot{c_{sb}^2})\delta_{\rm b} + c_{sb}^2\dot{\delta_{\rm b}} - \frac{1}{4}\dot{\delta}_\gamma + \dot{\sigma}_\gamma\right] + \dot{f}_{\rm MG}\ . \tag{3.73}$$

The next step involves the following trick. First, one can add $-\mathcal{H}\dot{\theta}_b + \mathcal{H}\dot{\theta}_b$ to the right hand side of the last equation. Then Eq. (3.64) can be used to express the $+\mathcal{H}\dot{\theta}_b$ term. Finally one can rewrite $-\mathcal{H}\dot{\theta}_b = -\mathcal{H}(\dot{\theta}_b - \dot{\theta}_\gamma) - \mathcal{H}\dot{\theta}_\gamma$ and use Eq. (3.65) to express the last term. After using $(\dot{c_{sb}^2}) = -c_{sb}^2\mathcal{H}$, one can obtain

$$\begin{aligned}\dot{g} \;=\; & -2\mathcal{H}(\dot{\theta}_b - \dot{\theta}_\gamma) - \frac{\ddot{a}}{a}\theta_{\rm b} + k^2\left[-\frac{1}{2}\mathcal{H}\delta_\gamma + 2\mathcal{H}\sigma_\gamma + c_{sb}^2\dot{\delta_{\rm b}} - \frac{1}{4}\dot{\delta}_\gamma + \dot{\sigma}_\gamma\right] + \dot{f}_{\rm MG} \\ & + \left(\frac{\mathcal{H}R + 2\mathcal{H}}{\tau_{\rm c}}\right)(\theta_\gamma - \theta_{\rm b})\ .\end{aligned} \tag{3.74}$$

Finally, keeping only the terms in $\mathcal{O}(\tau_c)$, Eq. (3.72) reads

$$\begin{aligned}\dot{\theta}_b - \dot{\theta}_\gamma &= \left(\frac{\dot{\tau}_\mathrm{c}}{\tau_\mathrm{c}} - \frac{2\mathcal{H}}{1+R}\right)(\theta_\mathrm{b} - \theta_\gamma) \\ &\quad + \frac{\tau_\mathrm{c}}{1+R}\left[-\frac{\ddot{a}}{a}\theta_\mathrm{b} - \frac{1}{2}\frac{\dot{a}}{a}k^2\delta_\gamma + k^2(c_{sb}^2\dot{\delta}_\mathrm{b} - \frac{1}{4}\delta_\gamma) + \dot{f}_\mathrm{MG} + \mathcal{H}f_\mathrm{MG}\right] \quad (3.75)\end{aligned}$$

During the tight coupling regime θ_b is obtained by integrating

$$\dot{\theta}_b = \frac{1}{1+R}\left[-\frac{\dot{a}}{a}\theta_\mathrm{b} + c_{sb}^2k^2\delta_\mathrm{b} + k^2R(\frac{1}{4}\delta_\gamma - \sigma_\gamma) + f_\mathrm{MG}\right] + \frac{R}{1+R}(\dot{\theta}_b - \dot{\theta}_\gamma)\ , \quad (3.76)$$

which is derived directly from the Eq. (3.68) and in which the slip is given by Eq. (3.75).

Compared to the standard general relativistic case we get two contributions from modified gravity. The first is the term f_MG in Eq. (3.76) and the second comes from an additional $\tau_\mathrm{c}(\dot{f}_\mathrm{MG} + \mathcal{H}f_\mathrm{MG})/(1+R)$ term in the slip.

The derivative of f_MG is given by

$$\begin{aligned}\dot{f}_\mathrm{MG} &= \dot{\beta}_\mathrm{b}k\delta\phi + \beta_\mathrm{b}k\delta\dot{\phi} - \dot{\beta}_\mathrm{b}\dot{\phi}\theta_\mathrm{b} - \beta_\mathrm{b}\ddot{\phi}\theta_\mathrm{b} - \beta_\mathrm{b}\dot{\phi}\dot{\theta}_b \\ &= \dot{\beta}_\mathrm{b}k\delta\phi + \beta_\mathrm{b}k\delta\dot{\phi} - \dot{\beta}_\mathrm{b}\dot{\phi}\theta_\mathrm{b} - \beta_\mathrm{b}\ddot{\phi}\theta_\mathrm{b} \\ &\quad -\beta_\mathrm{b}\dot{\phi}(-\frac{\dot{a}}{a}\theta_\mathrm{b} + c_{sb}^2k^2\delta_\mathrm{b} + f_\mathrm{MG}) + \frac{R}{\tau_\mathrm{c}}\beta_\mathrm{b}\dot{\phi}(\theta_\mathrm{b} - \theta_\gamma)\ , \quad (3.77)\end{aligned}$$

where the last equation is obtained after using Eq. (3.64).

To get an equation for $\dot{\theta}_\gamma$ we can use Eq. (3.64) to express the drag term as

$$(\theta_\mathrm{b} - \theta_\gamma)/\tau_\mathrm{c} = -R(\dot{\theta}_b + \mathcal{H}\theta_b - c_{sb}^2k^2\delta_\mathrm{b} - f_\mathrm{MG}) \quad (3.78)$$

and then substitute this in Eq. (3.65) to obtain

$$\dot{\theta}_\gamma = \frac{k^2}{4}\delta_\gamma - k^2\sigma_\gamma - R(\dot{\theta}_b + \mathcal{H}\theta_b - c_{sb}^2k^2\delta_\mathrm{b} - f_\mathrm{MG}). \quad (3.79)$$

This last equation is used at all times in CAMB with $\dot{\theta}_b$ determined by Eq. (3.76) during the tight-coupling regime and by Eq. (3.64) otherwise.

The CMB spectra are calculated as a time integral over the product of a geometrical term containing Bessel functions and a source term which is expressed in terms of the photon, baryon and metric perturbations. In CAMB the two parts are separated to reduce the computational time required. This is possible because the source term

depends on the cosmological model but is independent of the multipole moment l whereas for the geometrical term the opposite is the case (see [90] for more details). We have also modified this source term to account for modified gravity. However, we find that this does not have any visible effects on the CMB angular power spectrum for the models and parameters we have considered.
Finally, in order to avoid the time-consuming numerical integration of the field perturbations at early times when they oscillate quickly, we have introduced the approximation

$$\delta\phi = -\frac{\beta_c\delta\rho_c + \beta_b\delta\rho_b}{\frac{k^2}{a^2} + m^2 - \beta_c^2\rho_c - \beta_b^2\rho_b} \tag{3.80}$$

when the condition

$$(k^2 + a^2m^2 - a^2\beta_c^2\rho_c - a^2\beta_b^2\rho_b)\delta\phi \gg |2\mathcal{H}\delta\dot{\phi} + \tfrac{1}{2}\dot{h}\dot{\phi}| \tag{3.81}$$

is satisfied.

§ 3.6 Numerical results

3.6.1 Transition in β

For the transition model we observe deviations from ΛCDM in both the CMB angular power spectrum and the matter power spectrum which increase with increasing β_i/m_0. Keeping the ratios β_i/m_0 and β_0/m_0 constant (with the other parameters fixed) results in identical effects. In the CMB the nature of the deviations varies with l and there are alternating periods of enhancement and reduction of power. We see no shift in the positions of the peaks (see Figs. 3.1 and 3.2). This is because the sound horizon is virtually unchanged. Consequently there is also no shift in the position of the baryon acoustic peaks in the matter power spectrum.
The exact effects of the transition model on the angular power spectrum are different depending on when the transition occurs. In Fig. 3.3 we illustrate this with 4 different transition redshifts. For a transition at last scattering ($z_{\rm trans} = 1090$) we see clear oscillations in the relative difference of the C_l's whose amplitude increases with increasing l. This corresponds to enhanced amplitudes of the odd peaks and troughs and reduced amplitudes of the even peaks and troughs as can be seen in Fig. 3.1. For $\beta_i/m_0 = 5 \times 10^6$ Mpc the deviations exceed the percent level. In the cases $z_{\rm trans} = 3000$ and $z_{\rm trans} = 5000$ we see apparently periodic alternation of enhancement and reduction of power. Increasing the transition redshift lengthens these periods. This can be seen in Fig. 3.2 which shows that for $z_{\rm trans} = 3000$ two

consecutive peaks are enhanced. On average the deviations are greater on smaller scales and the enhancements larger than the reductions. There are also oscillatory features within the intervals of increased and decreased power. Values of $\beta_i/m_0 = 5\times10^7$ Mpc for $z_{\rm trans} = 3000$ and $\beta_i/m_0 = 1.67\times10^8$ Mpc for $z_{\rm trans} = 5000$ produce deviations of around 1%. Finally, for $z_{\rm trans} = 10000$ there is only a slight oscillating enhancement of the relative difference for $l \lesssim 400$ (just before the first trough) and then a more significant reduction in power for $l \gtrsim 400$ with irregular oscillations in the relative difference. At this redshift the deviations approach the percent level for $\beta_i/m_0 = 5\times10^8$ Mpc.

Fig. 3.3 also displays the relative importance of the couplings to CDM and baryons for the effects on the CMB. If we set $\beta_b = 0$ the deviations are smaller (generally no more than half a percent) but visible. The oscillations in the relative difference are out of phase with those of the $\beta_b = \beta_c$ case but there is a greater similarity between the effects for different transition redshifts than with $\beta_b = \beta_c$. On the other hand if we set $\beta_c = 0$ the deviations are completely negligible in all cases. These results suggest that the dominant contribution to the modified effects is the term in Eq. (3.30) which contains both β_c and β_b and causes the modifications to the growth of the baryon perturbations before last scattering.

The simplest case to understand is that of the transition at last scattering since the evolution of perturbations is governed by the same modified equations right up to the creation of the CMB. In Fig. 3.4 we show the effect of modified gravity on the transfer functions. Superimposed on the oscillations in the photon transfer function that lead to the CMB anisotropies is an enhancement of power which increases with k. The peaks and troughs in the angular power spectrum correspond to those in δ_γ^2 (shown in Fig. 3.5). We see that the odd peaks, corresponding to maxima in δ_γ, are enhanced with respect to ΛCDM whilst the even ones, corresponding to minima in δ_γ, are reduced. So far this agrees with what we observe in the C_l's for the $z_{\rm trans} = 1090$ case. The troughs in δ_γ^2 come from the zeros in δ_γ and so at these points the difference with ΛCDM vanishes. However, as we observed above the troughs in the C_l's are alternately enhanced and reduced just like the peaks. We can understand this by noting that the C_l troughs, unlike those in δ_γ^2, are not zeros. This is because the anisotropy at a given l is created by many modes with wavenumbers greater than that of the principal corresponding k-mode. The biggest contribution though will come from modes with only slightly larger k which explains why the troughs preceding odd peaks are also higher and those preceding even peaks are also lower.

When the transition occurs before last scattering the picture is more complicated. The periods of enhancement and reduction of power in the C_l's are different. As can be seen in Fig. 3.4 the effect of modified gravity on the photon transfer function at last scattering is no longer positive on all scales. There are instead oscillations in the difference with ΛCDM and these are out of phase with those in the transfer function itself. This results in a more complicated and unpredictable pattern of enhancements and reductions of power on different scales in the δ_γ^2 spectrum (see Fig. 3.5, right) and therefore the CMB. If however we look at the photon transfer functions at $z_{\rm trans}$ (Fig. 3.5, left) we see that they are always enhanced compared to the ΛCDM case and the effects on δ_γ^2 are the same as those for the transition at last scattering. The only exception to this is the case with $z_{\rm trans} = 5000$ where, because on small scales the maxima as well as the minima in the photon transfer function at $z_{\rm trans}$ are negative, the heights of the corresponding peaks in δ_γ^2 are reduced. Therefore the different effects on the CMB of the models with earlier transitions are not the result of modified gravity as such, but rather the period of effectively ΛCDM evolution following the transition during which the perturbations in δ_γ will have undergone oscillations. For example, a mode which has a maximum in δ_γ at the transition might have become a minimum by recombination. As the maximum would have been higher compared to the ΛCDM case so the minimum would be lower and this would generate an enhanced even peak in the C_l's.

As can be seen in Fig. 3.6 the effect on the linear matter power spectrum is an increase of power on small scales which is greater for higher values of β_i/m_0. This is due to the enhanced growth on small scales of the CDM (and to a lesser extent baryon) perturbations before last scattering (see Fig. 3.4) which occurs despite the fact that, as a result of the very high effective mass of the field, effectively all scales ($k \lesssim 10^{12}$ Mpc^{-1}) are always outside the Compton wavelength. This is because before the transition the couplings to matter are so strong that the factors containing β's in Eq. (3.31) are still significant. The deviations from ΛCDM become noticeable at lower k values for later transitions. Roughly speaking, for cases with $\sim 1\%$ deviation in the C_l's, the relative difference in $P(k)$ only becomes much more than 1% at about $k = 0.1h$ Mpc^{-1}. One should expect non-linear effects to become important on smaller scales.

It should be noted that for the cases shown, for which $\beta_0 = 1$, the effect of the coupling after the transition is negligible and the observed modifications to the matter power spectrum are entirely due to the anomalous growth before the transition at $z_{\rm trans}$ after which the equations governing the evolution of linear perturbations

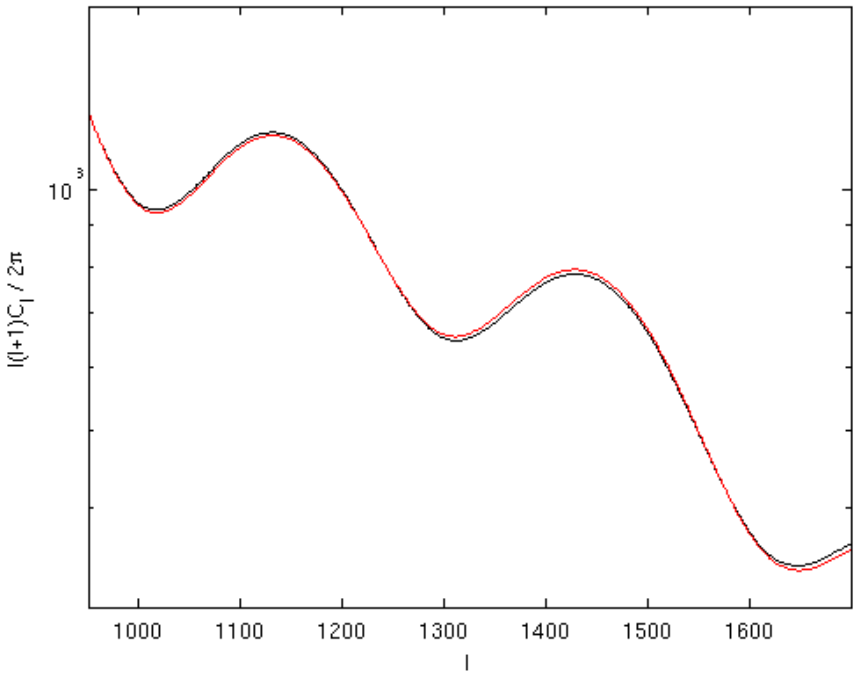

Figure 3.1: CMB angular power spectra of the transition model with $z_{\rm trans} = 1090$ and $\beta_i/m_0 = 5 \times 10^6$ Mpc (red) and a ΛCDM model (black), zooming in on the 4th and 5th peaks.

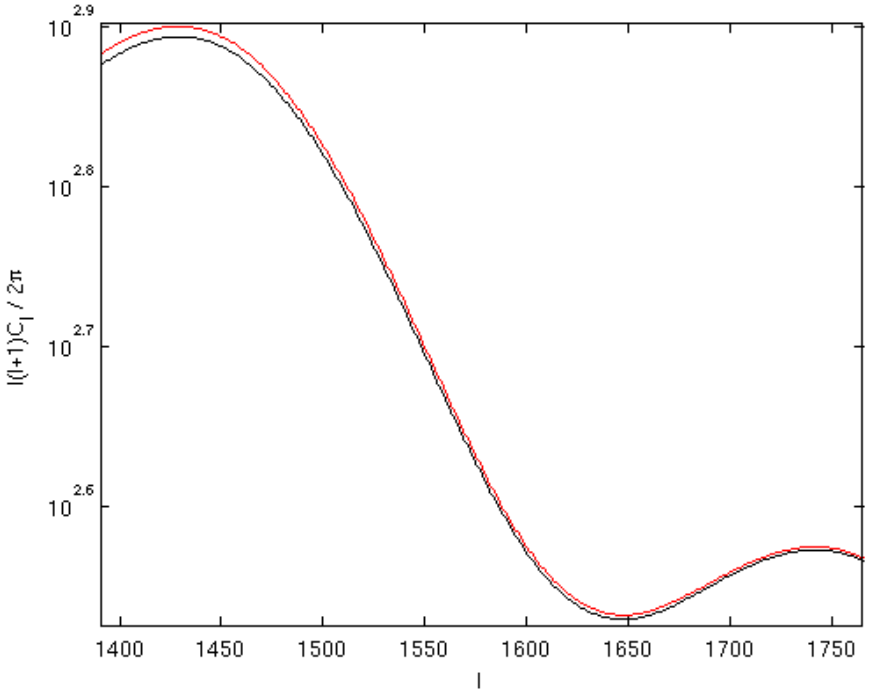

Figure 3.2: CMB angular power spectra of the transition model with $z_{\rm trans} = 3000$ and $\beta_i/m_0 = 5 \times 10^7$ Mpc (red) and a ΛCDM model (black), zooming in on the 5th and 6th peaks.

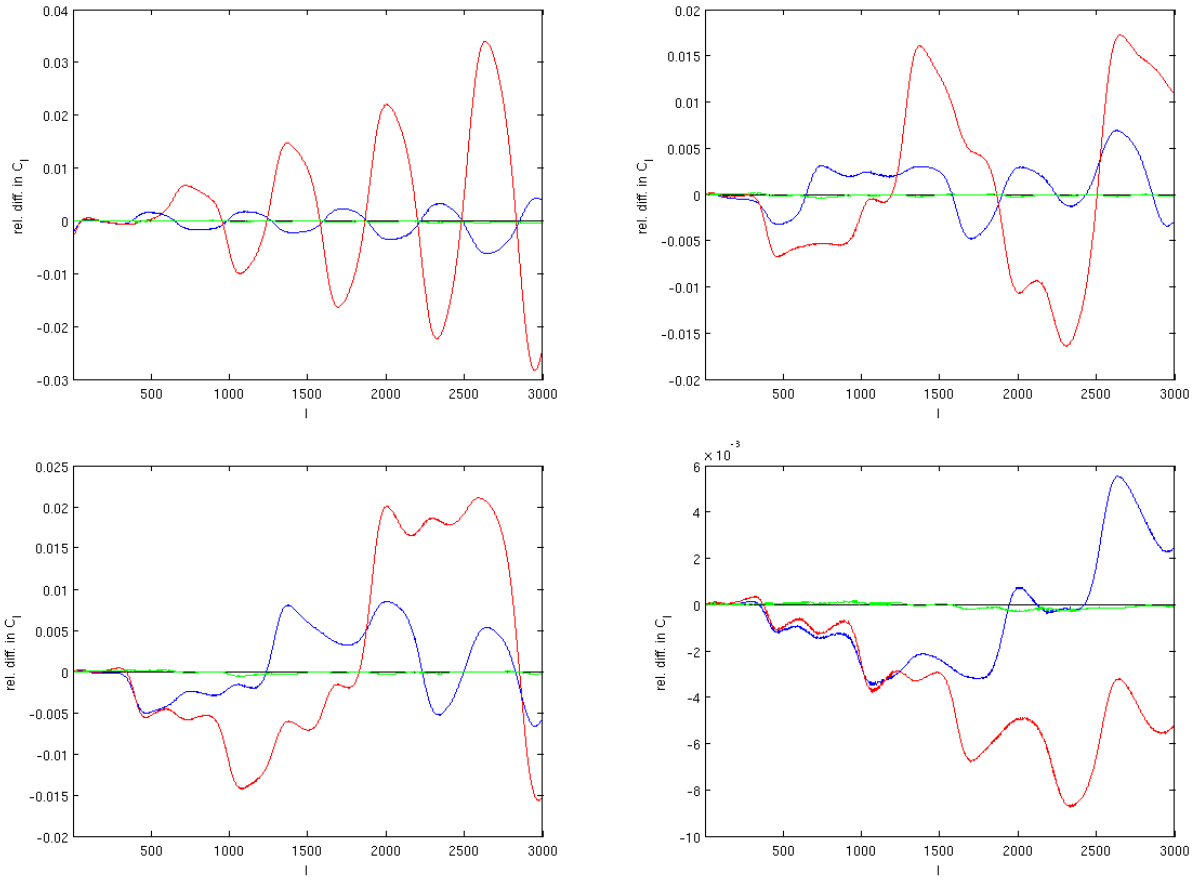

Figure 3.3: Relative differences between the C_l's of the transition models and that of a ΛCDM model. Red: $\beta_b = \beta_c$, blue: $\beta_b = 0$, green: $\beta_c = 0$. Top left: $z_{\rm trans} = 1090$ and $\beta_i/m_0 = 5 \times 10^6$ Mpc; top right: $z_{\rm trans} = 3000$ and $\beta_i/m_0 = 5 \times 10^7$ Mpc; bottom left: $z_{\rm trans} = 5000$ and $\beta_i/m_0 = 1.67 \times 10^8$ Mpc; bottom right: $z_{\rm trans} = 10^4$ and $\beta_i/m_0 = 5 \times 10^8$ Mpc. For all curves $\beta_0 = 1$, $p = 3$ and $C = 10 z_{\rm trans}$ (constant in Eq. (3.33)).

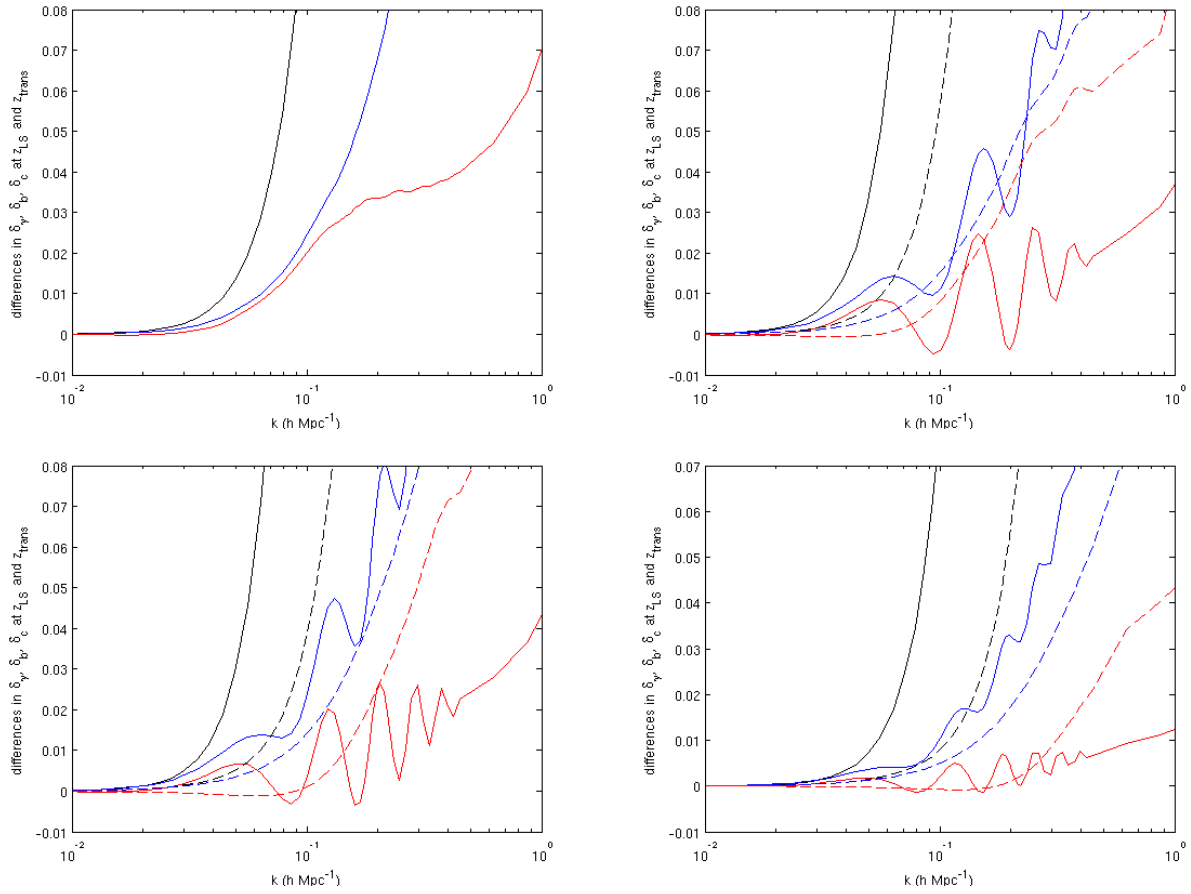

Figure 3.4: Differences between the photon (red), baryon (black) and CDM (blue) transfer functions at $z_{\rm trans}$ (dashed) and $z_{LS} = 1090$ (solid) of the transition models and a ΛCDM model. Top left: $z_{\rm trans} = 1090$ and $\beta_i/m_0 = 5 \times 10^6$ Mpc, top right: $z_{\rm trans} = 3000$ and $\beta_i/m_0 = 5 \times 10^7$ Mpc, bottom left: $z_{\rm trans} = 5000$ and $\beta_i/m_0 = 1.67 \times 10^8$ Mpc, bottom right: $z_{\rm trans} = 10^4$ and $\beta_i/m_0 = 5 \times 10^8$ Mpc. For all curves $\beta_0 = 1, p = 3$ and $C = 10 z_{\rm trans}$ (constant in Eq. (3.33)).

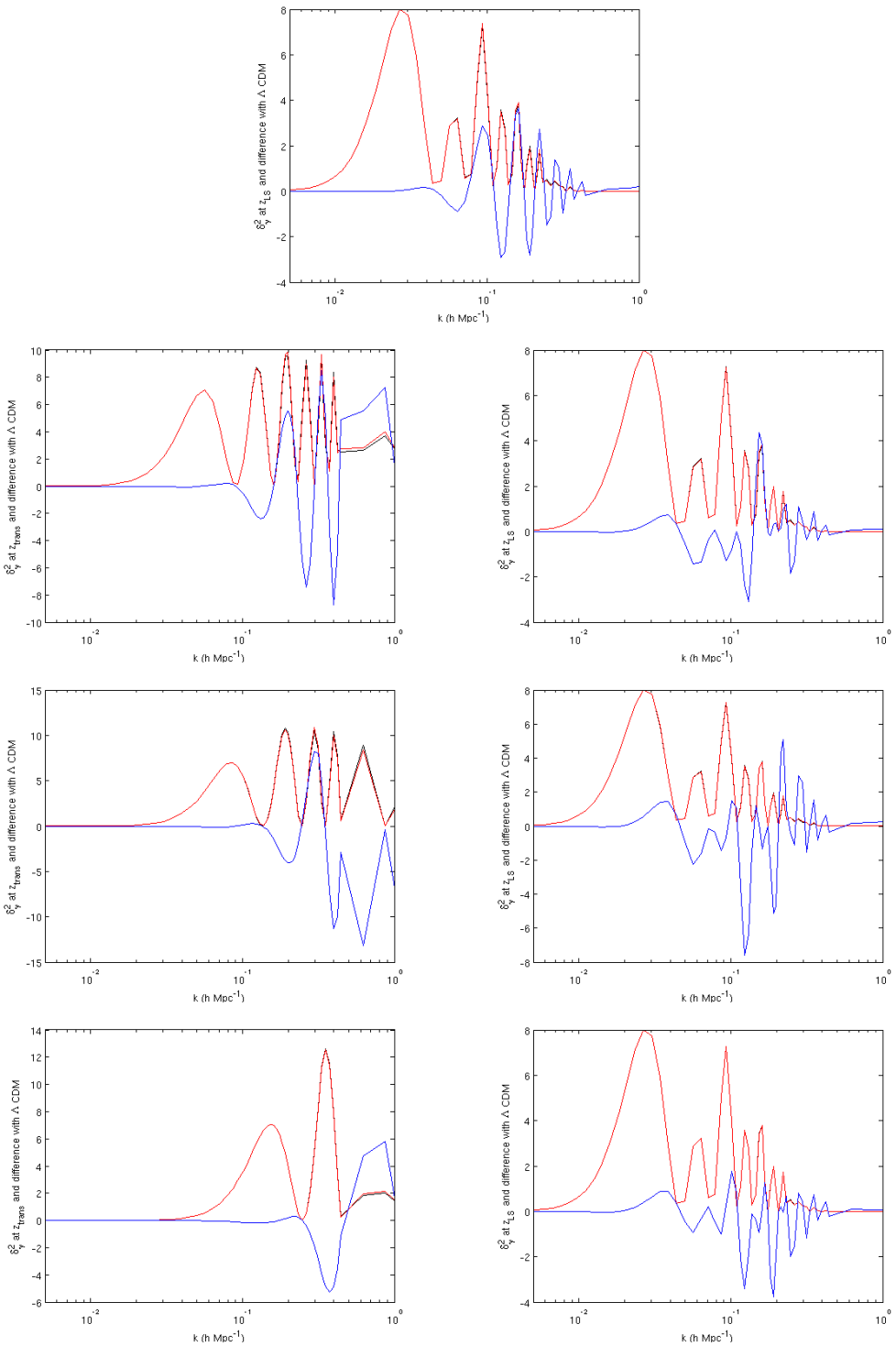

Figure 3.5: δ_γ^2 for the transition models (red) and a ΛCDM model (black) at $z_{\rm trans}$ (left column) and z_{LS} (right column) and the magnified difference with ΛCDM (blue). The red curves are almost entirely superimposed onto the black ones demonstrating how small the deviations from ΛCDM are. Top: $z_{\rm trans} = 1090$ and $\beta_i/m_0 = 5 \times 10^6$ Mpc, second row: $z_{\rm trans} = 3000$ and $\beta_i/m_0 = 5 \times 10^7$ Mpc, third row: $z_{\rm trans} = 5000$ and $\beta_i/m_0 = 1.67 \times 10^8$ Mpc, bottom row: $z_{\rm trans} = 10^4$ and $\beta_i/m_0 = 5 \times 10^8$ Mpc. For all curves $\beta_0 = 1, p = 3$ and $C = 10 z_{\rm trans}$ (constant in Eq. (3.33)).

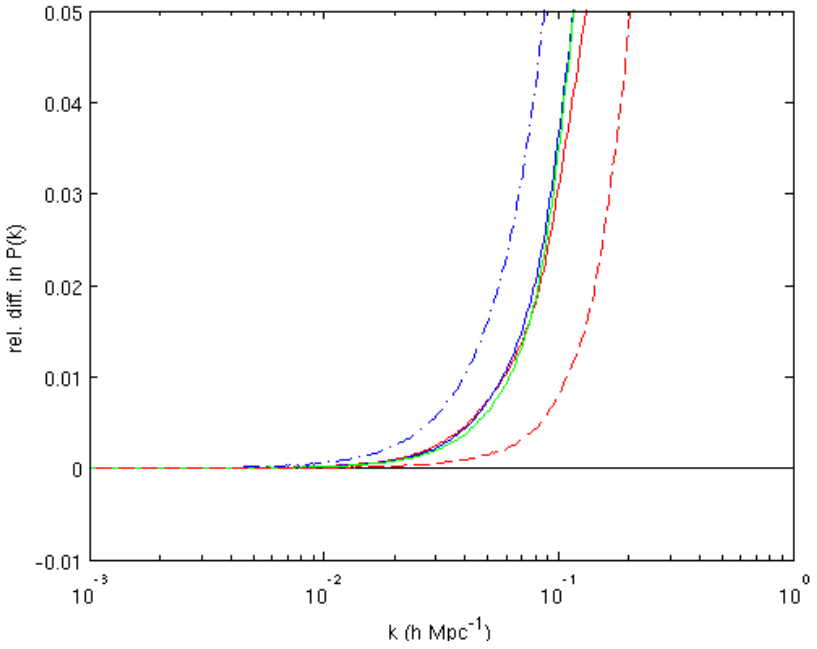

Figure 3.6: Relative differences between the matter power spectra of the modified gravity models and that of a ΛCDM model. Transition models: $z_{\rm trans} = 1090$ and $\beta_i/m_0 = 5 \times 10^6$ Mpc (red), $z_{\rm trans} = 3000$ and $\beta_i/m_0 = 5 \times 10^7$ Mpc (blue), $z_{\rm trans} = 5000$ and $\beta_i/m_0 = 1.67 \times 10^8$ Mpc (green), $z_{\rm trans} = 10^4$ and $\beta_i/m_0 = 5 \times 10^8$ Mpc (red dashed) and a generalised chameleon model with $m_0 = 10^8, \beta_0 = 9 \times 10^7, p = 3$ and $b = 2$ (blue dash-dotted).

are effectively those of a ΛCDM model. We also note that reducing the value of C (while keeping the other parameters fixed), and therefore extending the duration of the transition, results in smaller deviations from ΛCDM, particularly on smaller scales.

Compared to the constraints coming from the local tests and the variation of particle masses, the CMB probes a different part of the parameter space of the model. For values of the coupling β of order of unity and masses of the order of 1 Mpc^{-1}, there is no effect on the CMB whereas the parameters are excluded by lunar ranging tests. However, if the coupling can take very large values prior to recombination (e.g. $\beta \sim 10^{14}$ for $z_{\mathrm{trans}} \sim 10^4$) then the CMB constrains the model more strongly than all the local tests.

3.6.2 Generalised chameleons

For the generalised chameleon models we find that for parameters satisfying the constraints given in sections 3.4.3 and 3.4.4 there are no visible effects on the CMB but the matter power spectrum is affected in the usual way. In Figs. 3.6 and 3.7 we can show results for an example case ruled out by the BBN constraint. The enhanced growth in $P(k)$ on small scales is greater than each of the transition examples but the effects on the C_l's are much smaller. However, we also see that as the difference in the photon transfer function is always positive the amplitude of the peaks in δ_γ^2 is alternately enhanced and reduced and the oscillations in the relative difference of the C_l's are in phase with those of the model with a transition at last scattering. This shows that the effects have the same origin.

In contrast to the transition models, we therefore find that the CMB does not provide complementary, additional constraints on generalised chameleons.

§ 3.7 Conclusion

We have studied models of modified gravity where the screening effects at late time and locally in the solar system still allow for observable effects on cosmological perturbations prior to the recombination era. We have investigated two types of models: the generalised chameleons with an increasing coupling to matter in the past and a new transition model where the coupling to matter is significantly larger before recombination compared to late times. We have presented analytical estimates and full numerical results using a modified version of CAMB which takes into account the effects of modified gravity. We find that even when the constraints from local

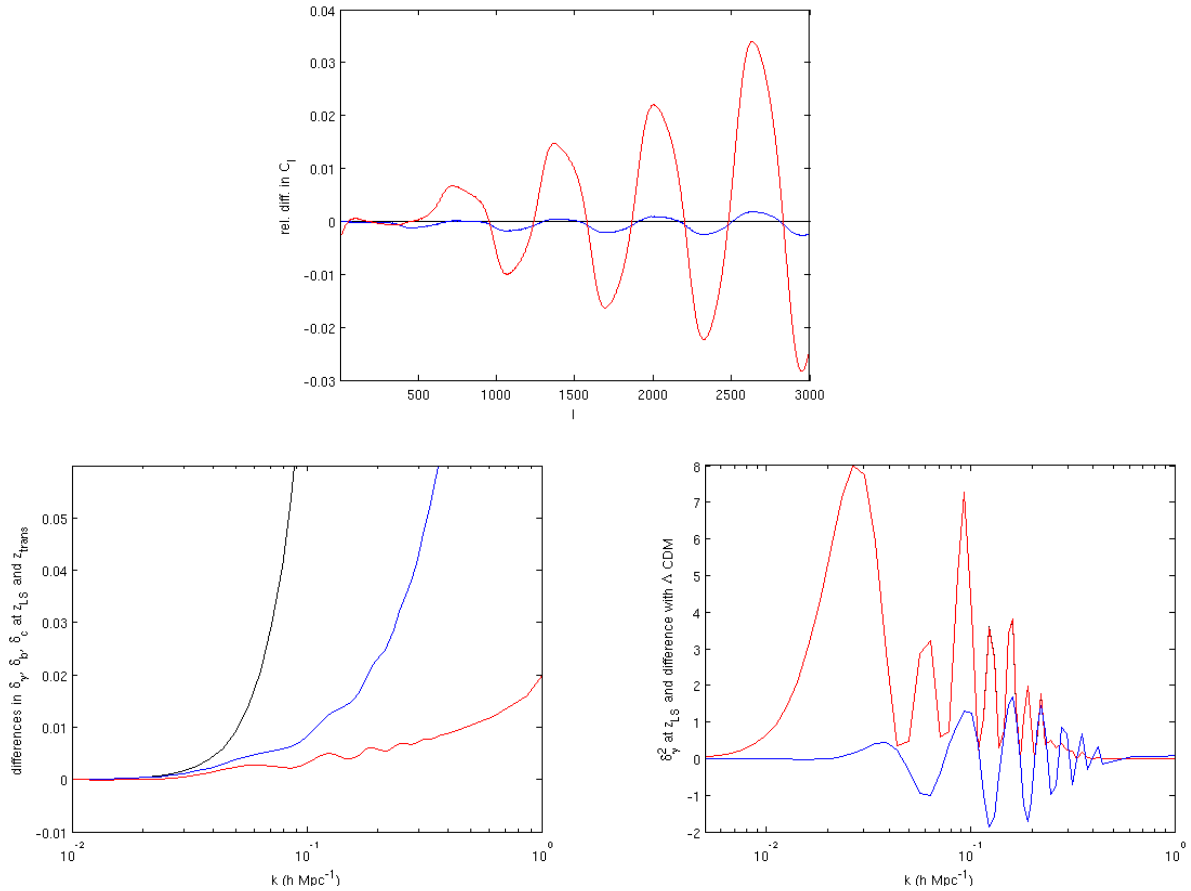

Figure 3.7: Generalised chameleon model with $m_0 = 10^8, \beta_0 = 9\times10^7, p = 3$ and $b = 2$. Top: relative difference between the modified C_l's and those of a ΛCDM model for the generalised chameleon model (blue) compared with the transition model with $z_{\rm trans} = 1090$ (red). Bottom left: differences between the photon (red), baryon (black) and CDM (blue) transfer functions at z_{LS} for the generalised chameleon and those a ΛCDM model. Bottom right: δ_γ^2 for the generalised chameleon (red) and a ΛCDM model (black) at z_{LS} and the magnified difference with ΛCDM (blue).

tests are satisfied the transition model can produce percent level deviations from ΛCDM in the CMB angular power spectrum and that these deviations take the characteristic form of alternating enhancements and reductions of power. For the generalised chameleons though it appears that models satisfying the BBN and local test constraints cannot leave observable signatures in the CMB. Therefore it may be possible to distinguish different models of modified gravity using the CMB.

Chapter 4

Isocurvature Modes in Coupled Quintessence

§ 4.1 Introduction

If dark energy is a scalar field then it is natural that it should couple to matter. However, the resulting interactions would cause a variety of deviations from General Relativity, both cosmological and local, which have not been observed and so observational data put constraints on such couplings. The constraints are much stronger for a coupling to baryons so it is often assumed to be vanishing. In this chapter we only allow for a coupling to dark matter. Even in this case though the strength of the coupling has been significantly constrained by CMB data and other observations, [6, 11, 101, 84, 83, 102]. Most recently [102] found that Planck alone constrains the coupling to dark matter to be $\beta < 0.102$, while combining with polarisation data from WMAP, and also BAO and type Ia supernovae measurements yields $\beta < 0.052$, both at 95% confidence level. However, in this and other work purely adiabatic initial conditions are assumed for the primordial perturbations. The simplest (single field) models of inflation generate only adiabatic (or curvature) perturbations but generally most others involving more than one field tend to also produce isocurvature (or entropy) perturbations [72, 85, 53]. Non-adiabatic perturbations are themselves constrained by the CMB data [2, 95] but scenarios involving a mixture of adiabatic and subdominant isocurvature modes are entirely possible. The constraint on a coupling between quintessence and CDM may be altered if isocurvature perturbations are included. Therefore, in this chapter we shall derive the initial conditions for the various possible perturbation modes in a coupled quintessence model so that these may be used to constrain the strength of the coupling with the available observational

data.

§ 4.2 The Effect of a Coupling on Background Variables

Coupled quintessence is described by a scalar-tensor action, as given in Eq. (2.1), with a purely conformal coupling between the scalar field and CDM ($\beta = \frac{1}{2C}\frac{dC}{d\phi}$) which we will assume to be constant. In this case the Klein-Gordon equation is

$$g^{\mu\nu}\nabla_\mu\nabla_\nu\phi - \frac{dV}{d\phi} = -\beta\, T_{(c)}\,, \tag{4.1}$$

where $T_{(c)}$ is the trace of the CDM energy momentum tensor. At the background level this is

$$\ddot{\phi} + 2H\dot{\phi} + a^2\frac{dV}{d\phi} = -a^2\beta\rho_c\,. \tag{4.2}$$

Many different forms of the quintessence potential $V(\phi)$ have been suggested but here we restrict ourselves to exponential potentials, both single and double:

$$V(\phi) = V_0 e^{-\lambda\phi}, \qquad \text{and} \qquad V(\phi) = V_0[e^{\lambda_1\phi} + e^{\lambda_2\phi}]. \tag{4.3}$$

From conservation of energy momentum we have

$$\nabla_\mu T^\mu_{(c)\nu} = \beta\phi_{,\nu}T_{(c)}, \tag{4.4}$$

$$\nabla_\mu T^\mu_{(q)\nu} = -\beta\phi_{,\nu}T_{(c)} \tag{4.5}$$

where $T_{(q)}$ is the trace of the quintessence energy momentum tensor, and this leads to

$$\dot{\rho}_c = -\,3H\rho_c + \beta\dot{\phi}\rho_c, \tag{4.6}$$

$$\dot{\rho}_q = -\,3H(1+w_q)\rho_q - \beta\dot{\phi}\rho_c, \tag{4.7}$$

where $w_q = p_q/\rho_q$ is the quintessence equation of state.

As the initial conditions will be set at early times, during radiation domination, we have

$$a = H_0\sqrt{\Omega_r^{(0)}}\tau = \alpha\tau \quad \text{and} \quad H = \frac{\dot{a}}{a} = \frac{1}{\tau}\,, \tag{4.8}$$

where $\Omega_r^{(0)}$ is the fractional energy density of radiation today. We know that $\rho_\gamma \sim \rho_\nu \sim a^{-4}$ so that $\Omega_\gamma \sim \Omega_\nu \sim$ constant and $\rho_b \sim a^{-3}$ so that $\Omega_b \sim a \sim \tau$. We need

to determine how Ω_c and Ω_q evolve at early times. Solving Eq. (4.6) yields

$$\rho_c = \frac{\rho_c^* e^{\beta\phi}}{a^3}. \tag{4.9}$$

Using a version of CAMB [70], to which modifications have been made to incorporate the coupling between CDM and quintessence, we find that due to its small value (we consider $\beta = 0.1$) the coupling has a negligible effect on the time-dependence of the CDM density (see Fig. 4.1, top) so that $\rho_c \sim a^{-3}$ and therefore $\Omega_c \sim a$. For the quintessence field we can use Eq. (4.2) and assuming that $\frac{dV}{d\phi} \ll \beta\rho_c$ (see Fig. 4.1, bottom) we can write

$$\frac{d}{d\tau}(a^2\dot{\phi}) = -a^4\beta\rho_c \sim a, \tag{4.10}$$

which leads to $\dot{\phi} \sim$ constant (see Fig. 4.2, top). Also from CAMB we find that for both single and double exponential potentials, $w_q = 1$ until well into the matter dominated era (see Fig. 4.2, bottom). Therefore

$$\dot{\rho_q} = -6H\rho_q - \beta\dot{\phi}\rho_c, \tag{4.11}$$

and so

$$\frac{d}{d\tau}(a^6\rho_q) \sim a^3. \tag{4.12}$$

This gives $\rho_q \sim a^{-2}$ and $\Omega_q \sim a^2 \sim \tau^2$.

§ 4.3 Early Time Perturbation Equations

We require initial conditions for the adiabatic and isocurvature modes in order to solve the equations numerically. To obtain these we follow [48] and put the evolution equations for the perturbations into a first order differential matrix equation:

$$\frac{\mathrm{d}}{\mathrm{d}\,\ln x}\boldsymbol{U}(x) = A(x)\boldsymbol{U}(x)\,, \tag{4.13}$$

where $\boldsymbol{U}(x)$ is a vector containing the perturbation variables:

$$\boldsymbol{U}^T \equiv (\Delta_c, \tilde{V}_c, \Delta_\gamma, \tilde{V}_\gamma, \Delta_b, \Delta_\nu, \tilde{V}_\nu, \tilde{\Pi}_\nu, \Delta_q, \tilde{V}_q)\,, \tag{4.14}$$

$A(x)$ is the matrix of the coefficients in the equations and $x \equiv k\tau$ where k is the perturbation wavenumber. We shall also use gauge-invariant perturbation variables so that we need not concern ourselves with gauge modes. The gauge-invariant per-

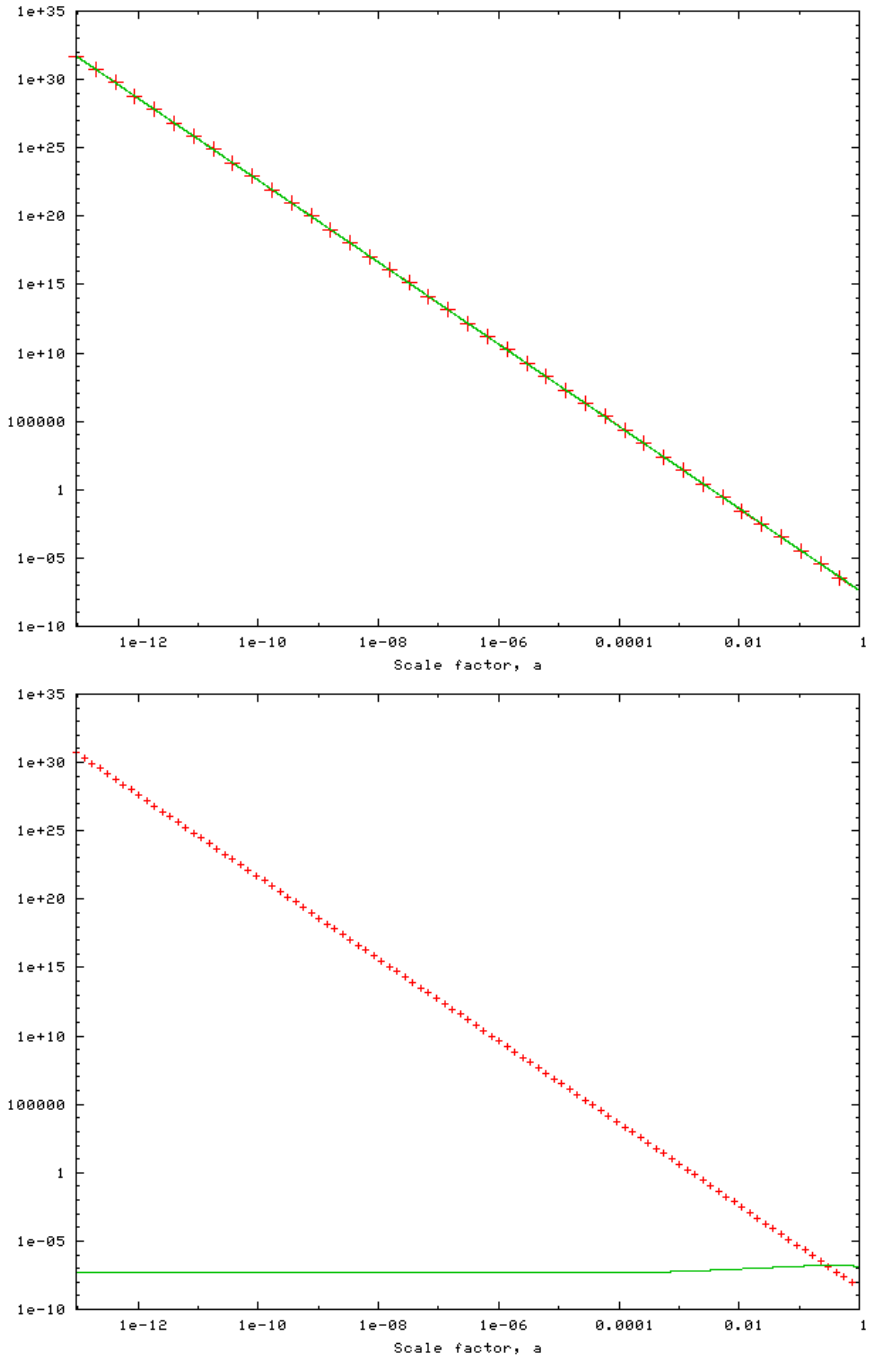

Figure 4.1: Top: evolution of ρ_c as given by Eq. (4.9) with $\beta = 0.1$ (red crosses) together with $\rho_c^* a^{-3}$ (green line). Bottom: evolution of $\beta\rho_c$ (red crosses) and $|\frac{dV}{d\phi}|$ (green line) for $\beta = 0.1$.

turbations are related to those in the conformal Newtonian gauge by

$$\Delta_\alpha = \delta_\alpha^{(Con)} + \frac{\dot{\rho_\alpha}}{H\rho_\alpha}\Phi\,, \qquad V_\alpha = v_\alpha^{(Con)}, \qquad \Pi_\alpha = \Pi_\alpha^{(Con)}, \tag{4.15}$$

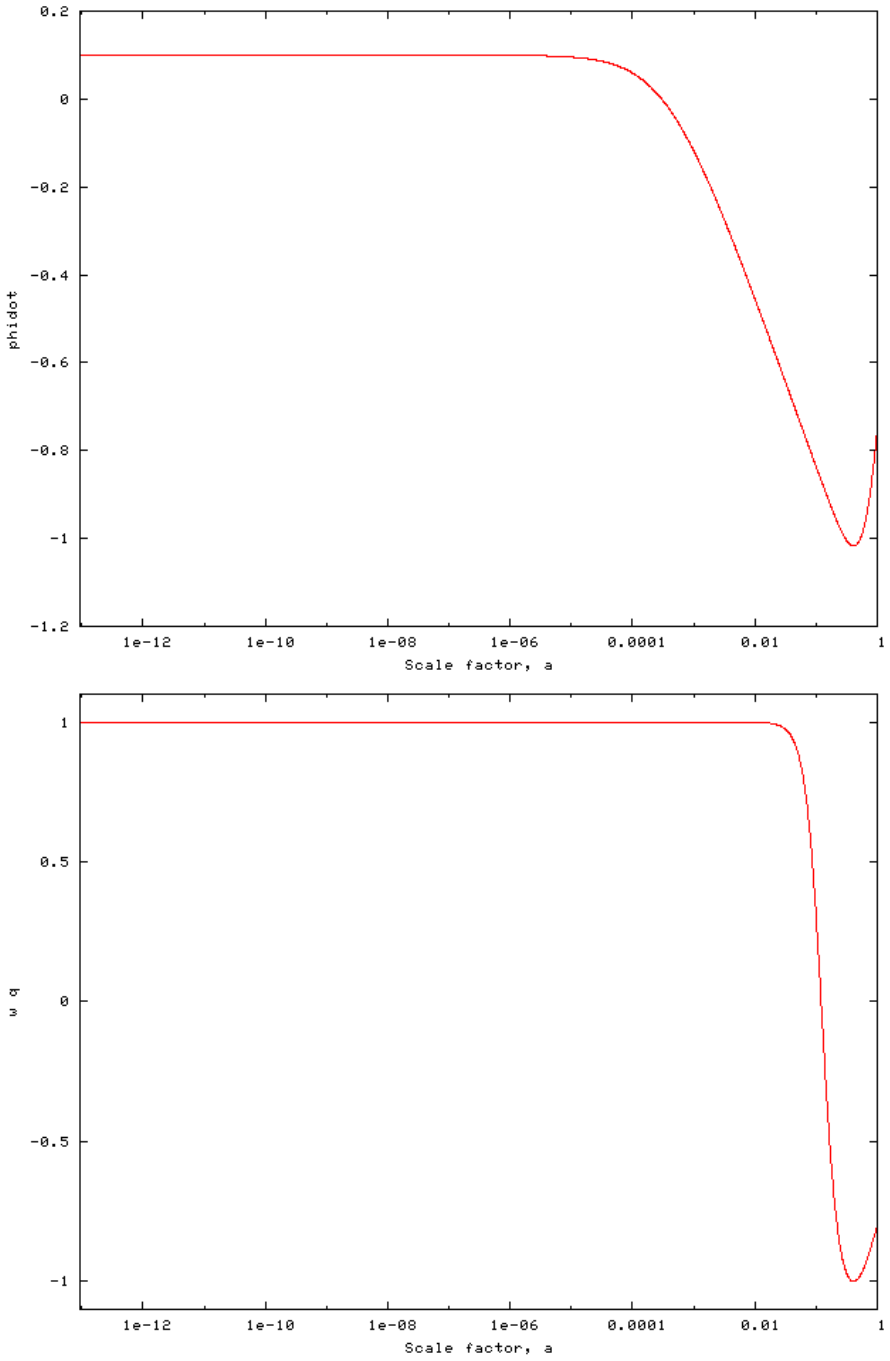

Figure 4.2: Top: evolution of $\dot{\phi}$ for $\beta = 0.1$. Bottom: evolution of the quintessence equation of state parameter w_q for $\beta = 0.1$. We can see that at late times w_q is close to -1 as required for consistency with the observed accelerated expansion.

where $\delta_\alpha = \delta\rho_\alpha/\rho_\alpha$ is the density contrast, v_α is the velocity and Π_α is the shear. We define our metric in the conformal Newtonian gauge as

$$ds^2 = a^2(\tau)[-(1+2\Psi)d\tau^2 + (1-2\Phi)\gamma_{ij}dx^i dx^j]\,. \tag{4.16}$$

Again following [48] the quintessence fluctuations will be dealt with using density and velocity perturbations in the same way as the matter and radiation fluids and we shall use $\tilde{V}_\alpha \equiv V_\alpha/x$ and $\tilde{\Pi}_\alpha \equiv \Pi_\alpha/x^2$ for our velocity and shear perturbations.

The equations for the photon, neutrino and baryon perturbations are unchanged from the uncoupled case and so we take those given by [48]. In the conformal Newtonian gauge the equations for the CDM density contrast and velocity are

$$\dot{\delta}_c = -kv_c + 3\dot{\Phi} + \beta\delta\dot{\phi}\,, \tag{4.17}$$

$$\dot{v}_c = -Hv_c + k\Psi + k\beta\delta\phi - \beta\dot{\phi}v_c\,. \tag{4.18}$$

Using Eqs. (4.15) and (4.6) we can rewrite these as

$$\dot{\Delta}_c = -kV_c + \beta\delta\dot{\phi} + \frac{\beta\dot{\phi}}{H}\dot{\Phi} + \beta\left(\dot{\phi} + \frac{\ddot{\phi}}{H}\right)\Phi\,, \tag{4.19}$$

$$\dot{V}_c = -HV_c + k\Psi + k\beta\delta\phi - \beta\dot{\phi}V_c\,. \tag{4.20}$$

The quintessence density and velocity perturbations can be found by perturbing the energy-momentum tensor for the field,

$$T^\mu_\nu = g^{\alpha\mu}\nabla_\mu\phi\nabla_\nu\phi - \delta^\mu_\nu[\tfrac{1}{2}g^{\rho\sigma}\nabla_\rho\nabla_\sigma\phi + V(\phi)], \tag{4.21}$$

to obtain

$$\delta_q = \frac{\dot{\phi}\delta\dot{\phi}}{a^2\rho_q} - \frac{\dot{\phi}^2\Psi}{a^2\rho_q} + \frac{V_{,\phi}\delta\phi}{\rho_q}\,, \tag{4.22}$$

which using our knowledge of the background evolution of the field can be simplified to

$$\delta_q = 2\left(\frac{\delta\dot{\phi}}{\dot{\phi}} - \Psi\right); \tag{4.23}$$

and

$$v_q = \frac{k\delta\phi}{\dot{\phi}}\,. \tag{4.24}$$

Transforming to gauge-invariant variables and differentiating with respect to τ we obtain

$$\dot{\Delta}_q = \frac{2\delta\ddot{\phi}}{\dot{\phi}} - \frac{2\ddot{\phi}\delta\dot{\phi}}{\dot{\phi}^2} - 2\dot{\Psi} - 6\dot{\Phi} - \frac{\beta\dot{\phi}\rho_c}{H\rho_q}\dot{\Phi} - \left(\frac{\beta\ddot{\phi}\rho_c}{H\rho_q} + \frac{\beta\dot{\phi}\dot{\rho}_c}{H\rho_q} - \frac{\beta\dot{\phi}\rho_c\dot{H}}{H^2\rho_q} - \frac{\beta\dot{\phi}\rho_c\dot{\rho}_q}{H\rho_q^2}\right)\Phi\,, \tag{4.25}$$

and

$$\dot{V}_q = \frac{k\delta\dot{\phi}}{\dot{\phi}} - \frac{k\ddot{\phi}\delta\phi}{\dot{\phi}^2}\,. \tag{4.26}$$

Perturbing Eq. (4.1) to first order yields an equation for the field fluctuations $\delta\phi$,

$$\delta\ddot{\phi}+2H\delta\dot{\phi}+\left(k^2+a^2\frac{d^2V}{d\phi^2}\right)\delta\phi-\dot{\phi}(\dot{\Psi}+3\dot{\Phi})+2a^2\left(\frac{dV}{d\phi}+\beta\rho_c\right)\Psi=-a^2\beta\delta\rho_c\,. \tag{4.27}$$

Using this and the background equations and then Einstein's equations we can rewrite Eqs. (4.19), (4.20), (4.25) and (4.26) as linear equations in the perturbation variables contained in $\boldsymbol{U}(x)$ and the gravitational potential Φ. It is convenient to define the constants

$$\tilde{\Omega}_c = \frac{\Omega_c}{x}\,, \qquad \tilde{\Omega}_b = \frac{\Omega_b}{x}\,, \qquad \tilde{\Omega}_q = \frac{\Omega_q}{x^2}\,, \tag{4.28}$$

so as to make all x dependence explicit. In these variables the perturbation equations are as follows:

$$\begin{aligned}
\Delta_c' =& -x^2\tilde{V}_c + \tfrac{1}{2}\sqrt{6}\beta\tilde{\Omega}_q^{1/2}x\left[3\tilde{\Omega}_c x\tilde{V}_c + (4\Omega_\gamma + 3\tilde{\Omega}_b x)\tilde{V}_\gamma + 4\Omega_\nu\tilde{V}_\nu + \Delta_q\right.\\
&\left. + 6\tilde{\Omega}_q x^2\tilde{V}_q + 4\Phi\right]\,, &(4.29)\\
\tilde{V}_c' =& -2\tilde{V}_c - \Omega_\nu\tilde{\Pi}_\nu + \Phi - \sqrt{6}\beta\tilde{\Omega}_q^{1/2}x\left[\tilde{V}_c - \tilde{V}_q\right]\,, &(4.30)\\
\Delta_\gamma' =& -\frac{4}{3}x^2\tilde{V}_\gamma\,, &(4.31)\\
\tilde{V}_\gamma' =& \frac{1}{4}\Delta_\gamma - \tilde{V}_\gamma - \Omega_\nu\tilde{\Pi}_\nu + 2\Phi\,, &(4.32)\\
\Delta_b' =& -x^2\tilde{V}_\gamma\,, &(4.33)\\
\Delta_\nu' =& -\frac{4}{3}x^2\tilde{V}_\nu\,, &(4.34)\\
\tilde{V}_\nu' =& \frac{1}{4}\Delta_\nu - \tilde{V}_\nu - \frac{1}{6}x^2\tilde{\Pi}_\nu - \Omega_\nu\tilde{\Pi}_\nu + 2\Phi\,, &(4.35)\\
\tilde{\Pi}_\nu' =& \frac{8}{5}\tilde{V}_\nu - 2\tilde{\Pi}_\nu\,, &(4.36)\\
\Delta_q' =& -2x^2\tilde{V}_q - \frac{\sqrt{6}\beta\tilde{\Omega}_c}{2\tilde{\Omega}_q^{1/2}}\left[2\Delta_c + 3\tilde{\Omega}_c x\tilde{V}_c + (4\Omega_\gamma + 3\tilde{\Omega}_b x)\tilde{V}_\gamma + 4\Omega_\nu\tilde{V}_\nu - \Delta_q\right.\\
&\left. + 6\tilde{\Omega}_q x^2\tilde{V}_q + 2\Phi\right]\,, &(4.37)\\
\tilde{V}_q' =& -\Omega_\nu\tilde{\Pi}_\nu + \tfrac{1}{2}\Delta_q + \tilde{V}_q + 4\Phi + \frac{\sqrt{6}\beta\tilde{\Omega}_c}{2\tilde{\Omega}_q^{1/2}}\left[\tilde{V}_q + \Phi\right]\,, &(4.38)
\end{aligned}$$

where the gravitational potential is

$$\Phi = -\frac{\sum_{\alpha=c,\gamma,b,\nu,q} \Omega_\alpha(\Delta_\alpha + 3(1+w_\alpha)\tilde{V}_\alpha)}{\sum_{\alpha=c,\gamma,b,\nu,q} 3(1+w_\alpha)\Omega_\alpha + \frac{2x^2}{3}}\,, \tag{4.39}$$

and the primes denote derivatives with respect to $\ln x$. We expand $A(x)$ and $\boldsymbol{U}$ as series in x:

$$A(x) = A_0 + xA_1 + x^2A_2 + x^3A_3 + ... \tag{4.40}$$

$$\boldsymbol{U}^{(i)}(x) = x^{\lambda_i}(\boldsymbol{U}_0^{(i)} + x\boldsymbol{U}_1^{(i)} + x^2\boldsymbol{U}_2^{(i)} + x^3\boldsymbol{U}_3^{(i)} + ...)\,. \tag{4.41}$$

Inserting these in matrix equation gives:

$$A_0\boldsymbol{U}_0^{(i)} = \lambda_i\boldsymbol{U}_0^{(i)} \tag{4.42}$$

$$\boldsymbol{U}_1^{(i)} = -\left[A_0 - (\lambda_i+1)\boldsymbol{I}\right]^{-1}A_1\boldsymbol{U}_0^{(i)} \tag{4.43}$$

$$\boldsymbol{U}_2^{(i)} = -\left[A_0 - (\lambda_i+2)\boldsymbol{I}\right]^{-1}(A_2\boldsymbol{U}_0^{(i)} + A_1\boldsymbol{U}_1^{(i)}) \tag{4.44}$$

$$\boldsymbol{U}_3^{(i)} = -\left[A_0 - (\lambda_i+3)\boldsymbol{I}\right]^{-1}(A_3\boldsymbol{U}_0^{(i)} + A_2\boldsymbol{U}_1^{(i)} + A_1\boldsymbol{U}_2^{(i)})\,. \tag{4.45}$$

Therefore λ_i are eigenvalues of A_0 and $\boldsymbol{U}_0^{(i)}$ are the corresponding eigenvectors. The eigenvalues of A_0 are

$$\lambda_i = \left(-2, -1, -\frac{5}{2} + \frac{\sqrt{1-32\Omega_\nu/5}}{2}, -\frac{5}{2} - \frac{\sqrt{1-32\Omega_\nu/5}}{2}, 0, 0, 0, 0, \lambda_g, \lambda_{g+}\right)\,, \tag{4.46}$$

where

$$\lambda_g = \frac{\sqrt{6}\beta\tilde{\Omega}_c}{2\tilde{\Omega}_q^{1/2}}\,, \qquad \lambda_{g+} = 1 + \frac{\sqrt{6}\beta\tilde{\Omega}_c}{2\tilde{\Omega}_q^{1/2}}\,. \tag{4.47}$$

The first four eigenvalues are negative so their corresponding modes will decay and can be neglected. There are four modes with $\lambda_i = 0$ and two growing modes which we shall refer to as $\boldsymbol{U}^{(g)}$ and $\boldsymbol{U}^{(g+)}$. In the next section we will seek to find solutions to Eqs. (4.29)-(4.38) corresponding to these last six modes.

§ 4.4 Mode Solutions

In sections 4.4.1 and 4.4.2 we solve the zero-order equations to get $\boldsymbol{U}_0$ for the constant modes and growing modes respectively. In section 4.4.3 we transform our solutions to the synchronous gauge and then in section 4.4.4 the full mode solutions

to be entered into CAMB are given.

4.4.1 Constant Modes

For the modes with $\lambda_i = 0$, Eq.(4.42) yields six non-trivial constraints for the components of $\boldsymbol{U}_0^{(i)}$:

$$2\tilde{V}_c + \Omega_\nu \tilde{\Pi}_\nu - \Phi = 0 \tag{4.48}$$

$$\frac{1}{4}\Delta_\gamma - \tilde{V}_\gamma - \Omega_\nu \tilde{\Pi}_\nu + 2\Phi = 0 \tag{4.49}$$

$$\frac{1}{4}\Delta_\nu - \tilde{V}_\nu - \Omega_\nu \tilde{\Pi}_\nu + 2\Phi = 0 \tag{4.50}$$

$$\frac{8}{5}\tilde{V}_\nu - 2\tilde{\Pi}_\nu = 0 \tag{4.51}$$

$$2\Delta_c + 4\Omega_\gamma \tilde{V}_\gamma + 4\Omega_\nu \tilde{V}_\nu - \Delta_q + 2\Phi = 0 \tag{4.52}$$

$$-\Omega_\nu \tilde{\Pi}_\nu + \tfrac{1}{2}\Delta_q + \tilde{V}_q + 4\Phi + \frac{\sqrt{6}\beta\tilde{\Omega}_c}{2\tilde{\Omega}_q^{1/2}}\left[\tilde{V}_q + \Phi\right] = 0\,. \tag{4.53}$$

As emphasized by [48], whilst one could specify initial conditions using any basis for the subspace spanned by the $\lambda_i = 0$ eigenvectors, it is still best to use physically meaningful modes. Physical choices are adiabatic and isocurvature modes. With adiabatic (curvature) perturbations the ratios of the densities of different species to one another are the same everywhere so that the entropy perturbations between them vanish. The gauge-invariant entropy perturbation between species α and β is defined as

$$\mathcal{S}_{\alpha:\beta} = -3H\left(\frac{\rho_\alpha \Delta_\alpha}{\dot{\rho_\alpha}} - \frac{\rho_\beta \Delta_\beta}{\dot{\rho_\beta}}\right)\,. \tag{4.54}$$

In contrast, isocurvature (entropy) perturbations do not give rise to perturbations in the curvature of spacetime. This is because an overdensity in one species is balanced by an underdensity in the others. The gauge-invariant curvature perturbation on hyper-surfaces of uniform total energy density is defined as

$$\zeta_{tot} = -\Phi + \frac{\sum_\alpha \delta_\alpha}{\sum_\alpha 3(1+w_\alpha)\rho_\alpha}\,. \tag{4.55}$$

In terms of the gauge-invariant perturbation variables this is

$$\zeta_{tot} = \frac{\sum_\alpha \Omega_\alpha \Delta_\alpha}{\sum_\alpha 3(1+w_\alpha)\Omega_\alpha} \,. \tag{4.56}$$

Non-Adiabatic Curvature Mode

The natural first choice is an adiabatic mode for which $\mathcal{S}_{\alpha:\beta} = 0$ for all pairs of species. However this would result in eleven constraints for the ten components of $\boldsymbol{U}_0^{(i)}$ (six from Eqs.(4.48)-(4.53), four from adiabaticity and one from overall normalisation). Therefore we choose to require adiabaticity between photons, neutrinos, baryons and CDM:

$$\Delta_c = \Delta_b = \frac{3}{4}\Delta_\nu = \frac{3}{4}\Delta_\gamma \,. \tag{4.57}$$

We obtain

$$\boldsymbol{U}_0^{(ad)} = C_{ad} \begin{pmatrix} \frac{3}{4} \\ -\frac{5}{4(15+4\Omega_\nu)} \\ 1 \\ -\frac{5}{4(15+4\Omega_\nu)} \\ \frac{3}{4} \\ 1 \\ -\frac{5}{4(15+4\Omega_\nu)} \\ -\frac{1}{15+4\Omega_\nu} \\ \frac{35-10\Omega_\gamma-2\Omega_\nu}{2(15+4\Omega_\nu)} \\ \frac{(10+4\Omega_\nu)\lambda_g+5+10\Omega_\gamma+14\Omega_\nu}{4\lambda_{g+}(15+4\Omega_\nu)} \end{pmatrix} \tag{4.58}$$

where C_{ad} is the normalisation constant. It can be seen that quintessence is not adiabatic with respect to the other components. Therefore this mode is not truly adiabatic. This is in contrast with the uncoupled case of [48] and the interacting dark energy model of [74] and is a result of coupling terms appearing at zero-order in the perturbation equations. In the model of [74] the equations at zero-order in x contain no coupling terms and so at this level there is no difference with the uncoupled case.

Neutrino Isocurvature Mode

An isocurvature mode is one for which $\zeta_{tot} = 0$. For the neutrino isocurvature mode we require adiabaticity between photons, baryons and CDM but that $\mathcal{S}_{\nu:\gamma} \neq 0$ and that the gauge-invariant curvature perturbation vanishes:

$$\zeta_{tot} = 0, \quad \Delta_c = \Delta_b = \tfrac{3}{4}\Delta_\gamma \,. \tag{4.59}$$

We obtain

$$\boldsymbol{U}_0^{(\nu\, iso)} = C_{\nu\, iso} \begin{pmatrix} \frac{3}{4} \\ \frac{\Omega_\gamma}{15+4\Omega_\nu} \\ 1 \\ \frac{4\Omega_\gamma+4\Omega_\nu+15}{4(15+4\Omega_\nu)} \\ \frac{3}{4} \\ -\frac{\Omega_\gamma}{\Omega_\nu} \\ -\frac{15\Omega_\gamma}{4\Omega_\nu(15+4\Omega_\nu)} \\ -\frac{3\Omega_\gamma}{\Omega_\nu(15+4\Omega_\nu)} \\ \frac{3}{2} + \frac{2\Omega_\gamma(2\Omega_\gamma+2\Omega_\nu-1)}{15+4\Omega_\nu} \\ \frac{4\Omega_\gamma(2+\lambda_g-2\Omega_\gamma-2\Omega_\nu)-45-12\Omega_\nu}{4\lambda_{g+}(15+4\Omega_\nu)} \end{pmatrix} \tag{4.60}$$

CDM Isocurvature Mode

We require that photons, neutrinos and baryons are adiabatic with respect to one another whilst $\mathcal{S}_{c:\gamma} \neq 0$ and the gauge-invariant curvature perturbation vanishes:

$$\zeta_{tot} = 0, \quad \Delta_b = \tfrac{3}{4}\Delta_\nu = \tfrac{3}{4}\Delta_\gamma \,. \tag{4.61}$$

We obtain

$$\boldsymbol{U}_0^{(c\, iso)} = C_{c\, iso} \left(1, 0, 0, 0, 0, 0, 0, 0, 0, 2, -\tfrac{1}{\lambda_{g+}}\right) \,. \tag{4.62}$$

Baryon Isocurvature Mode

We require adiabaticity between photons, neutrinos and CDM but that $\mathcal{S}_{b:\gamma} \neq 0$ and that the gauge-invariant curvature perturbation vanishes:

$$\zeta_{tot} = 0, \quad \Delta_c = \tfrac{3}{4}\Delta_\nu = \tfrac{3}{4}\Delta_\gamma \,. \tag{4.63}$$

We obtain

$$\boldsymbol{U}_0^{(biso)} = C_{biso}\,(0,0,0,0,1,0,0,0,0,0)\ . \tag{4.64}$$

4.4.2 Growing Modes

Eq.(4.42) provides ten constraint equations for modes with non-zero eigenvalues:

$$\lambda_i\Delta_c = 0 \tag{4.65}$$

$$\lambda_i\tilde{V}_c = -2\tilde{V}_c - \Omega_\nu\tilde{\Pi}_\nu + \Phi \tag{4.66}$$

$$\lambda_i\Delta_\gamma = 0 \tag{4.67}$$

$$\lambda_i\tilde{V}_\gamma = \frac{1}{4}\Delta_\gamma - \tilde{V}_\gamma - \Omega_\nu\tilde{\Pi}_\nu + 2\Phi \tag{4.68}$$

$$\lambda_i\Delta_b = 0 \tag{4.69}$$

$$\lambda_i\Delta_\nu = 0 \tag{4.70}$$

$$\lambda_i\tilde{V}_\nu = \frac{1}{4}\Delta_\nu - \tilde{V}_\nu - \Omega_\nu\tilde{\Pi}_\nu + 2\Phi \tag{4.71}$$

$$\lambda_i\tilde{\Pi}_\nu = \frac{8}{5}\tilde{V}_\nu - 2\tilde{\Pi}_\nu \tag{4.72}$$

$$\lambda_i\Delta_q = -\frac{\sqrt{6}\beta\tilde{\Omega}_c}{2\tilde{\Omega}_q^{1/2}}\left[2\Delta_c + 4\Omega_\gamma\tilde{V}_\gamma + 4\Omega_\nu\tilde{V}_\nu + 4\Omega_\nu\tilde{\Pi}_\nu - \Delta_q\right] \tag{4.73}$$

$$\lambda_i\tilde{V}_q = -\Omega_\nu\tilde{\Pi}_\nu + \tfrac{1}{2}\Delta_q + \tilde{V}_q + 4\Phi + \frac{\sqrt{6}\beta\tilde{\Omega}_c}{2\tilde{\Omega}_q^{1/2}}\left[\tilde{V}_q + \Phi\right] \tag{4.74}$$

We consider the growing modes $\boldsymbol{U}_0^{(g)}$ and $\boldsymbol{U}_0^{(g+)}$. Solving for these, we obtain

$$\boldsymbol{U}_0^{(g)} = C_g\left(0,0,0,0,0,0,0,0,1,-\tfrac{1}{2}\right)\ . \tag{4.75}$$

and

$$\boldsymbol{U}_0^{(g+)} = C_{g+}\,(0,0,0,0,0,0,0,0,0,1)\ . \tag{4.76}$$

For the constant modes and the second growing mode we obtained higher order corrections to $\boldsymbol{U}^{(i)}$ using Eqs.(4.43)-(4.45). However, in the case of the first growing mode $\boldsymbol{U}_0^{(g)}$ this was not possible since the matrix $[A_0 - (\lambda_g + 1)\boldsymbol{I}]$ is singular and therefore cannot be inverted. We decided to neglect this mode and do not consider it here any further.

4.4.3 Transforming to Synchronous Gauge

Since CAMB uses synchronous gauge variables we need to transform the initial conditions obtained above to this gauge. The synchronous gauge perturbations are related to the gauge-invariant ones by

$$\delta_\alpha^{(Syn)} = \Delta_\alpha - \frac{\dot{\rho_\alpha}}{H\rho_\alpha}\eta\,, \tag{4.77}$$

$$v_\alpha^{(Syn)} = x\tilde{V}_\alpha - \frac{1}{2k}\left(\dot{h} + 3\dot{\eta}\right)\,, \tag{4.78}$$

$$\Pi_\alpha^{(Syn)} = x^2\tilde{\Pi}_\alpha\,. \tag{4.79}$$

Therefore the first step is to obtain the synchronous potentials h and η (defined in Eq. (1.22)) for each mode. They are related to the Newtonian ones by [73]:

$$\Psi = \frac{1}{2k^2}\left[\ddot{h} + 6\ddot{\eta} + \frac{\dot{a}}{a}(\dot{h} + 6\dot{\eta})\right]\,, \tag{4.80}$$

$$\Phi = \eta - \frac{1}{2k^2}\frac{\dot{a}}{a}(\dot{h} + 6\dot{\eta})\,. \tag{4.81}$$

We expand h, η, Ψ and Φ in the following manner

$$h = h_0 + h_1\tau + h_2\tau^2 + h_3\tau^3 + ... \tag{4.82}$$

and substitute in Eqs.(4.80)-(4.81). Then equating orders in τ we find, for $n > 1$, that

$$\Psi_{n-2} = \frac{n^2}{2k^2}(h_n + 6\eta_n)\,, \tag{4.83}$$

$$\Phi_{n-2} = \eta_{n-2} - \frac{1}{n}\Psi_{n-2}\,, \tag{4.84}$$

from which we get

$$\eta_n = (1 + \tfrac{1}{n+2})\Phi_n - \tfrac{1}{n+2}\Omega_\nu\tilde{\Pi}_{\nu,n}\,, \tag{4.85}$$

$$h_1 = -6\eta_1\,, \tag{4.86}$$

$$h_n = 2(\tfrac{k}{n})^2\Phi_{n-2} - 6(1 + \tfrac{1}{n+2})\Phi_n - 2(\tfrac{k}{n})^2\Omega_\nu\tilde{\Pi}_{\nu,n-2} + \tfrac{6}{n+2}\Omega_\nu\tilde{\Pi}_{\nu,n} \quad \text{for } n > 1\,, \tag{4.87}$$

having used the fact that $\Psi = \Phi - \Omega_\nu\tilde{\Pi}_\nu$. Using (4.39) we can now transform our initial conditions to the synchronous gauge.

4.4.4 Initial Conditions for Modes in Synchronous Gauge

CAMB uses some slightly different perturbation variables. Heat fluxes q_α are used instead of the radiation velocities and the shear is defined differently:

$$q_\alpha = (1 + w_\alpha)v_\alpha \qquad \text{and} \qquad \pi_\alpha = w_\alpha \Pi_\alpha, \tag{4.88}$$

so that

$$q_\gamma = \tfrac{4}{3}v_\gamma, \qquad q_\nu = \tfrac{4}{3}v_\nu, \qquad \pi_\nu = \tfrac{1}{3}\Pi_\nu. \tag{4.89}$$

For quintessence the field fluctuation and its time derivative are used. The former is

$$\delta\phi = \frac{\dot{\phi} v_q}{k}, \tag{4.90}$$

and the latter is simply obtained by differentiating $\delta\phi$. Finally CAMB also requires initial conditions for $v_b = v_\gamma$ and the neutrino octupole. We set the latter to zero since the neutrino distribution function was truncated beyond the quadrupole to get our perturbation equations. This is reasonable at early times.

Curvature Mode

The curvature mode is as follows. We have set $C_{ad} = -4$ so that at zero-order $\eta = 1$. Clearly these algebraic expressions are rather complicated and opaque. Despite this a few points can be made. Firstly, the modifications to the initial conditions appear as terms containing the coupling strength β. However, we cannot regain the expressions for the uncoupled case by simply setting $\beta = 0$ because frequently β appears in the denominator of these terms. This is the case for all of the modes. For the curvature mode the only variable unchanged by the coupling is the neutrino shear π_ν. Several variables are related simply to the metric perturbation η and like it are only modified at second order in τ. $\delta\dot{\phi}$ is modified at zero-order; $\delta\phi$ and δ_c at first order. At early times when these initial conditions are set these will be the most significant modifications.

$$\eta = 1 + \left(\frac{9\tilde{\Omega}_q - 1}{12(\Omega_\gamma + \Omega_\nu)} + \frac{10 - 45\sqrt{6}\beta\tilde{\Omega}_c\tilde{\Omega}_q^{1/2}}{12(15 + 4\Omega_\nu)} + \frac{15\sqrt{6}\beta\tilde{\Omega}_c\tilde{\Omega}_q^{1/2}}{2(\Omega_\gamma + \Omega_\nu)(15 + 4\Omega_\nu)} \right.$$
$$+ \frac{15\tilde{\Omega}_q^{3/2}}{(15 + 4\Omega_\nu)(\sqrt{6}\beta\tilde{\Omega}_c + 2\tilde{\Omega}_q^{1/2})} + \frac{3\tilde{\Omega}_q^{3/2}}{2(\Omega_\gamma + \Omega_\nu)(\sqrt{6}\beta\tilde{\Omega}_c + 2\tilde{\Omega}_q^{1/2})}$$
$$\left. - \frac{45\tilde{\Omega}_q^{3/2}}{(\Omega_\gamma + \Omega_\nu)(15 + 4\Omega_\nu)(\sqrt{6}\beta\tilde{\Omega}_c + 2\tilde{\Omega}_q^{1/2})} \right) (k\tau)^2 + O(\tau^3) \tag{4.91}$$

$$\delta_\gamma = \delta_\nu = -4 - \frac{10(k\tau)^2}{3(15 + 4\Omega_\nu)} + 4\eta \tag{4.92}$$

$$q_\gamma = \tfrac{1}{9}k\tau\delta_\gamma \tag{4.93}$$

$$q_\nu = q_\gamma - \frac{8(k\tau)^3}{27(15 + 4\Omega_\nu)} \tag{4.94}$$

$$\pi_\nu = \frac{4(k\tau)^2}{3(15 + 4\Omega_\nu)} \tag{4.95}$$

$$\delta_b = \tfrac{3}{4}\delta_\gamma \tag{4.96}$$

$$\delta_c = \delta_b + \frac{20(\Omega_\gamma + \Omega_\nu - 2)\sqrt{6}\beta\tilde{\Omega}_q^{1/2}}{15 + 4\Omega_\nu}k\tau + \left(\frac{15\sqrt{6}\beta\tilde{\Omega}_c\tilde{\Omega}_q^{1/2}}{2(15 + 4\Omega_\nu)} - \frac{9\beta^3\tilde{\Omega}_c\tilde{\Omega}_q}{\sqrt{6}\tilde{\Omega}_q^{1/2} - 3\beta\tilde{\Omega}_c} \right.$$
$$\left. - \frac{45\beta\tilde{\Omega}_q(\tilde{\Omega}_c - \tilde{\Omega}_b + 8\beta^2\tilde{\Omega}_c(\Omega_\gamma + \Omega_\nu - 2))}{2(15 + 4\Omega_\nu)(\sqrt{6}\tilde{\Omega}_q^{1/2} - 3\beta\tilde{\Omega}_c)} \right) (k\tau)^2 + O(\tau^3) \tag{4.97}$$

$$v_c = - \left(\frac{1}{3} + \frac{2}{3(\sqrt{6}\beta\tilde{\Omega}_c + 2\tilde{\Omega}_q^{1/2})} + \frac{20\tilde{\Omega}_q^{1/2}(\Omega_\gamma + \Omega_\nu - 3)}{3(15 + 4\Omega_\nu)(\sqrt{6}\beta\tilde{\Omega}_c + 2\tilde{\Omega}_q^{1/2})} \right) \sqrt{6}\beta\tilde{\Omega}_q^{1/2}(k\tau)^2$$
$$+ \left(\frac{7\sqrt{6}\beta^2\tilde{\Omega}_q^{3/2}}{4(\sqrt{6}\tilde{\Omega}_q^{1/2} - 3\beta\tilde{\Omega}_c)} + \frac{3\beta^2\tilde{\Omega}_q^{3/2}}{2(\sqrt{6}\beta\tilde{\Omega}_c + 2\tilde{\Omega}_q^{1/2})} + \frac{10(\Omega_\gamma + \Omega_\nu - 3)\beta^2\tilde{\Omega}_q^{3/2}}{(15 + 4\Omega_\nu)(\sqrt{6}\beta\tilde{\Omega}_c + 2\tilde{\Omega}_q^{1/2})} \right.$$
$$+ \frac{15\beta\tilde{\Omega}_q(8\sqrt{6}\beta\tilde{\Omega}_q^{1/2}(\Omega_\gamma + \Omega_\nu - 2) + 3(\tilde{\Omega}_c - \tilde{\Omega}_b))}{4(15 + 4\Omega_\nu)(\sqrt{6}\tilde{\Omega}_q^{1/2} - 3\beta\tilde{\Omega}_c)}$$
$$\left. - \frac{3\sqrt{6}\beta^4\tilde{\Omega}_c^2\tilde{\Omega}_q}{2(\sqrt{6}\beta\tilde{\Omega}_c + 2\tilde{\Omega}_q^{1/2})(\sqrt{6}\tilde{\Omega}_q^{1/2} - 3\beta\tilde{\Omega}_c)} \right) (k\tau)^3 \tag{4.98}$$

$$\delta\phi = - \left(1 + \frac{2}{\sqrt{6}\beta\tilde{\Omega}_c + 2\tilde{\Omega}_q^{1/2}} + \frac{20\tilde{\Omega}_q^{1/2}(\Omega_\gamma + \Omega_\nu - 3)}{(15 + 4\Omega_\nu)(\sqrt{6}\beta\tilde{\Omega}_c + 2\tilde{\Omega}_q^{1/2})} \right) \sqrt{6}\tilde{\Omega}_q^{1/2}k\tau$$
$$+ \frac{((20\Omega_\gamma + \Omega_\nu + 15 + 4\Omega_\nu - 40)2\sqrt{6}\beta\tilde{\Omega}_q^{1/2} + 15(\tilde{\Omega}_c - \tilde{\Omega}_b))3\tilde{\Omega}_q}{(15 + 4\Omega_\nu)(\sqrt{6}\tilde{\Omega}_q^{1/2} - 3\beta\tilde{\Omega}_c)}(k\tau)^2 \tag{4.99}$$

$$\delta\dot{\phi} = -\left(1 + \frac{2}{\sqrt{6}\beta\tilde{\Omega}_c + 2\tilde{\Omega}_q^{1/2}} + \frac{20\tilde{\Omega}_q^{1/2}(\Omega_\gamma + \Omega_\nu - 3)}{(15 + 4\Omega_\nu)(\sqrt{6}\beta\tilde{\Omega}_c + 2\tilde{\Omega}_q^{1/2})}\right)\sqrt{6}\tilde{\Omega}_q^{1/2}k$$
$$+ \frac{((20\Omega_\gamma + \Omega_\nu + 15 + 4\Omega_\nu - 40)2\sqrt{6}\beta\tilde{\Omega}_q^{1/2} + 15(\tilde{\Omega}_c - \tilde{\Omega}_b))6\tilde{\Omega}_q}{(15 + 4\Omega_\nu)(\sqrt{6}\tilde{\Omega}_q^{1/2} - 3\beta\tilde{\Omega}_c)}k^2\tau \quad (4.100)$$

CDM Isocurvature Mode

The CDM isocurvature mode is as follows. We set $C_c = 1$ in order to have $\delta_c = 1$ at zero-order. As with the curvature mode π_ν is the only unchanged variable and $\delta\dot{\phi}$, $\delta\phi$ and δ_c are the only variables receiving corrections at zeroth or first order.

$$\eta = -\frac{\tilde{\Omega}_c}{6(\Omega_\gamma+\Omega_\nu)}k\tau + \left(\frac{3\tilde{\Omega}_c(2\tilde{\Omega}_c+3\tilde{\Omega}_b)}{64(\Omega_\gamma+\Omega_\nu)^2} - \frac{3\tilde{\Omega}_q^{1/2}(\sqrt{6}\beta\tilde{\Omega}_c+2\tilde{\Omega}_q^{1/2})}{16(\Omega_\gamma+\Omega_\nu)} + \frac{9\tilde{\Omega}_q^{3/2}}{4(\Omega_\gamma+\Omega_\nu)(\sqrt{6}\beta\tilde{\Omega}_c+2\tilde{\Omega}_q^{1/2})}\right)(k\tau)^2 + O(\tau^3) \tag{4.101}$$

$$\delta_\gamma = \delta_\nu = 4\eta \tag{4.102}$$

$$\delta_b = \tfrac{3}{4}\delta_\gamma \tag{4.103}$$

$$\pi_\nu = -\frac{\tilde{\Omega}_c}{(\Omega_\gamma+\Omega_\nu)(15+2\Omega_\nu)}(k\tau)^3 \tag{4.104}$$

$$q_\gamma = q_\nu = -\frac{\tilde{\Omega}_c}{9(\Omega_\gamma+\Omega_\nu)}(k\tau)^2 + \left(\frac{\tilde{\Omega}_c(2\tilde{\Omega}_c+3\tilde{\Omega}_b)}{48(\Omega_\gamma+\Omega_\nu)^2} - \frac{\tilde{\Omega}_q^{1/2}(\sqrt{6}\beta\tilde{\Omega}_c+2\tilde{\Omega}_q^{1/2})}{12(\Omega_\gamma+\Omega_\nu)} + \frac{\tilde{\Omega}_q^{3/2}}{(\Omega_\gamma+\Omega_\nu)(\sqrt{6}\beta\tilde{\Omega}_c+2\tilde{\Omega}_q^{1/2})}\right)(k\tau)^3 \tag{4.105}$$

$$\delta_c = 1 + \sqrt{6}\beta\tilde{\Omega}_q^{1/2}k\tau + \left(\frac{15}{8(\Omega_\gamma+\Omega_\nu)(15+2\Omega_\nu)} - \frac{3\sqrt{6}\beta^2\tilde{\Omega}_q^{1/2}}{2(\sqrt{6}\tilde{\Omega}_q^{1/2}-3\beta\tilde{\Omega}_c)} - \frac{15}{8(15+2\Omega_\nu)} - \frac{1}{12(\Omega_\gamma+\Omega_\nu)} + \frac{45\beta\tilde{\Omega}_c}{8(15+2\Omega_\nu)(\sqrt{6}\tilde{\Omega}_q^{1/2}-3\beta\tilde{\Omega}_c)} - \frac{45\beta\tilde{\Omega}_c}{2(\Omega_\gamma+\Omega_\nu)(15+2\Omega_\nu)(\sqrt{6}\tilde{\Omega}_q^{1/2}-3\beta\tilde{\Omega}_c)} + \frac{3\beta\tilde{\Omega}_c}{2(\Omega_\gamma+\Omega_\nu)(\sqrt{6}\tilde{\Omega}_q^{1/2}-3\beta\tilde{\Omega}_c)}\right)\sqrt{6}\beta\tilde{\Omega}_c\tilde{\Omega}_q^{1/2}(k\tau)^2 + 3\eta + O(\tau^3) \tag{4.106}$$

$$v_c = -\frac{2\sqrt{6}\beta\tilde{\Omega}_q}{3(\sqrt{6}\beta\tilde{\Omega}_c+2\tilde{\Omega}_q^{1/2})}(k\tau)^2 + \left(\frac{\beta\tilde{\Omega}_c(2\tilde{\Omega}_q-3\beta^2\tilde{\Omega}_c^2)}{4(\Omega_\gamma+\Omega_\nu)(\sqrt{6}\beta\tilde{\Omega}_c+2\tilde{\Omega}_q^{1/2})(\sqrt{6}\tilde{\Omega}_q^{1/2}-3\beta\tilde{\Omega}_c)} + \frac{45\beta\tilde{\Omega}_c\tilde{\Omega}_q^{1/2}}{2(\Omega_\gamma+\Omega_\nu)(15+2\Omega_\nu)(\sqrt{6}\tilde{\Omega}_q^{1/2}-3\beta\tilde{\Omega}_c)} + \frac{2\sqrt{6}\beta^2\tilde{\Omega}_q^{3/2}}{(\sqrt{6}\beta\tilde{\Omega}_c+2\tilde{\Omega}_q^{1/2})(\sqrt{6}\tilde{\Omega}_q^{1/2}-3\beta\tilde{\Omega}_c)} - \frac{45\beta\tilde{\Omega}_c\tilde{\Omega}_q^{1/2}}{8(15+2\Omega_\nu)(\sqrt{6}\tilde{\Omega}_q^{1/2}-3\beta\tilde{\Omega}_c)} + \frac{\tilde{\Omega}_q^{1/2}}{4(\Omega_\gamma+\Omega_\nu)} - \frac{3\beta\tilde{\Omega}_c\tilde{\Omega}_q^{1/2}}{2(\Omega_\gamma+\Omega_\nu)(\sqrt{6}\tilde{\Omega}_q^{1/2}-3\beta\tilde{\Omega}_c)} + \frac{\sqrt{6}\beta^2\tilde{\Omega}_q}{\sqrt{6}\tilde{\Omega}_q^{1/2}-3\beta\tilde{\Omega}_c}\right)\tilde{\Omega}_q^{1/2}(k\tau)^3 \tag{4.107}$$

$$\delta\phi = -\frac{2\sqrt{6}\tilde{\Omega}_q}{\sqrt{6}\beta\tilde{\Omega}_c + 2\tilde{\Omega}_q^{1/2}}k\tau - \left(\frac{4\sqrt{6}\tilde{\Omega}_c\tilde{\Omega}_q^{1/2}}{3(\Omega_\gamma+\Omega_\nu)} + \frac{6\sqrt{6}\beta\tilde{\Omega}_q^{3/2}}{\sqrt{6}\tilde{\Omega}_q^{1/2} - 3\beta\tilde{\Omega}_c} - \frac{30\tilde{\Omega}_q}{\beta(\Omega_\gamma+\Omega_\nu)(15+2\Omega_\nu)}\right.$$
$$-\frac{45\tilde{\Omega}_c\tilde{\Omega}_q}{2(15+2\Omega_\nu)(\sqrt{6}\tilde{\Omega}_q^{1/2} - 3\beta\tilde{\Omega}_c)} - \frac{\sqrt{6}\tilde{\Omega}_q^{1/2}(54\beta^2\tilde{\Omega}_c^2 - 12\tilde{\Omega}_q)}{12\beta(\Omega_\gamma+\Omega_\nu)(\sqrt{6}\tilde{\Omega}_q^{1/2} - 3\beta\tilde{\Omega}_c)}$$
$$\left.+\frac{30\sqrt{6}\tilde{\Omega}_q^{3/2}}{\beta(\Omega_\gamma+\Omega_\nu)(15+2\Omega_\nu)(\sqrt{6}\tilde{\Omega}_q^{1/2} - 3\beta\tilde{\Omega}_c)}\right)(k\tau)^2 \tag{4.108}$$

$$\delta\dot{\phi} = -\frac{2\sqrt{6}k\tilde{\Omega}_q}{\sqrt{6}\beta\tilde{\Omega}_c + 2\tilde{\Omega}_q^{1/2}} - \left(\frac{8\sqrt{6}\tilde{\Omega}_c\tilde{\Omega}_q^{1/2}}{3(\Omega_\gamma+\Omega_\nu)} + \frac{12\sqrt{6}\beta\tilde{\Omega}_q^{3/2}}{\sqrt{6}\tilde{\Omega}_q^{1/2} - 3\beta\tilde{\Omega}_c} - \frac{60\tilde{\Omega}_q}{\beta(\Omega_\gamma+\Omega_\nu)(15+2\Omega_\nu)}\right.$$
$$-\frac{45\tilde{\Omega}_c\tilde{\Omega}_q}{(15+2\Omega_\nu)(\sqrt{6}\tilde{\Omega}_q^{1/2} - 3\beta\tilde{\Omega}_c)} - \frac{\sqrt{6}\tilde{\Omega}_q^{1/2}(54\beta^2\tilde{\Omega}_c^2 - 12\tilde{\Omega}_q)}{6\beta(\Omega_\gamma+\Omega_\nu)(\sqrt{6}\tilde{\Omega}_q^{1/2} - 3\beta\tilde{\Omega}_c)}$$
$$\left.+\frac{60\sqrt{6}\tilde{\Omega}_q^{3/2}}{\beta(\Omega_\gamma+\Omega_\nu)(15+2\Omega_\nu)(\sqrt{6}\tilde{\Omega}_q^{1/2} - 3\beta\tilde{\Omega}_c)}\right)k^2\tau \tag{4.109}$$

Baryon Isocurvature Mode

The baryon isocurvature mode is as follows. We set $C_b = 1$ so as to get $\delta_b = 1$ at zero-order. For this mode $\delta\dot{\phi}$ is the only variable modified at first order and most are unmodified to third order and higher.

$$\eta = -\frac{\tilde{\Omega}_b}{6(\Omega_\gamma+\Omega_\nu)}k\tau + \frac{3\tilde{\Omega}_b(2\tilde{\Omega}_c+3\tilde{\Omega}_b)}{64(\Omega_\gamma+\Omega_\nu)^2}(k\tau)^2 + O(\tau^3) \tag{4.110}$$

$$\delta_\gamma = \delta_\nu = 4\eta + O(\tau^3) \tag{4.111}$$

$$\delta_b = 1 + \tfrac{3}{4}\delta_\gamma \tag{4.112}$$

$$q_\gamma = q_\nu = -\frac{\tilde{\Omega}_b}{9(\Omega_\gamma+\Omega_\nu)}(k\tau)^2 + \frac{\tilde{\Omega}_b(2\tilde{\Omega}_c+3\tilde{\Omega}_b)}{48(\Omega_\gamma+\Omega_\nu)^2}(k\tau)^3 \tag{4.113}$$

$$\pi_\nu = -\frac{\tilde{\Omega}_b}{(\Omega_\gamma+\Omega_\nu)(15+2\Omega_\nu)}(k\tau)^3 \tag{4.114}$$

$$\begin{aligned}\delta_c = 3\eta + \Bigg(&\frac{15}{8(\Omega_\gamma+\Omega_\nu)(15+2\Omega_\nu)} - \frac{15}{8(15+2\Omega_\nu)} \\ &+\frac{45\beta\tilde{\Omega}_c}{8(15+2\Omega_\nu)(\sqrt{6}\tilde{\Omega}_q^{1/2}-3\beta\tilde{\Omega}_c)} - \frac{1}{12(\Omega_\gamma+\Omega_\nu)} \\ &+\frac{3\beta\Omega_\nu\tilde{\Omega}_c}{(\Omega_\gamma+\Omega_\nu)(15+2\Omega_\nu)(\sqrt{6}\tilde{\Omega}_q^{1/2}-3\beta\tilde{\Omega}_c)}\Bigg)\sqrt{6}\beta\Omega_b\tilde{\Omega}_q^{1/2}(k\tau)^2 + O(\tau^3)\end{aligned} \tag{4.115}$$

$$\begin{aligned}v_c = -\Bigg(&\frac{15\sqrt{6}\beta\tilde{\Omega}_q^{1/2}}{16(15+2\Omega_\nu)(\sqrt{6}\tilde{\Omega}_q^{1/2}-3\beta\tilde{\Omega}_c)} + \frac{\sqrt{6}\beta\Omega_\nu\tilde{\Omega}_q^{1/2}}{2(\Omega_\gamma+\Omega_\nu)(15+2\Omega_\nu)(\sqrt{6}\tilde{\Omega}_q^{1/2}-3\beta\tilde{\Omega}_c)} \\ &+\frac{(3\beta^2\tilde{\Omega}_c^2+2\sqrt{6}\beta\tilde{\Omega}_c\tilde{\Omega}_q^{1/2}-6\tilde{\Omega}_q)}{24\tilde{\Omega}_c(\Omega_\gamma+\Omega_\nu)(\sqrt{6}\tilde{\Omega}_q^{1/2}-3\beta\tilde{\Omega}_c)}\Bigg)\sqrt{6}\tilde{\Omega}_b\tilde{\Omega}_q^{1/2}(k\tau)^3\end{aligned} \tag{4.116}$$

$$\begin{aligned}\delta\phi = -\Bigg(&\frac{15\sqrt{6}\tilde{\Omega}_q^{1/2}}{4(15+2\Omega_\nu)(\sqrt{6}\tilde{\Omega}_q^{1/2}-3\beta\tilde{\Omega}_c)} + \frac{2\sqrt{6}\Omega_\nu\tilde{\Omega}_q^{1/2}}{(\Omega_\gamma+\Omega_\nu)(15+2\Omega_\nu)(\sqrt{6}\tilde{\Omega}_q^{1/2}-3\beta\tilde{\Omega}_c)} \\ &+\frac{(3\beta^2\tilde{\Omega}_c^2+2\sqrt{6}\beta\tilde{\Omega}_c\tilde{\Omega}_q^{1/2}-6\tilde{\Omega}_q)}{6\beta\tilde{\Omega}_c(\Omega_\gamma+\Omega_\nu)(\sqrt{6}\tilde{\Omega}_q^{1/2}-3\beta\tilde{\Omega}_c)}\Bigg)\sqrt{6}\tilde{\Omega}_b\tilde{\Omega}_q^{1/2}(k\tau)^2\end{aligned} \tag{4.117}$$

$$\begin{aligned}\delta\dot{\phi} = -\Bigg(&\frac{15\sqrt{6}\tilde{\Omega}_q^{1/2}}{2(15+2\Omega_\nu)(\sqrt{6}\tilde{\Omega}_q^{1/2}-3\beta\tilde{\Omega}_c)} + \frac{4\sqrt{6}\Omega_\nu\tilde{\Omega}_q^{1/2}}{(\Omega_\gamma+\Omega_\nu)(15+2\Omega_\nu)(\sqrt{6}\tilde{\Omega}_q^{1/2}-3\beta\tilde{\Omega}_c)} \\ &+\frac{(3\beta^2\tilde{\Omega}_c^2+2\sqrt{6}\beta\tilde{\Omega}_c\tilde{\Omega}_q^{1/2}-6\tilde{\Omega}_q)}{3\beta\tilde{\Omega}_c(\Omega_\gamma+\Omega_\nu)(\sqrt{6}\tilde{\Omega}_q^{1/2}-3\beta\tilde{\Omega}_c)}\Bigg)\sqrt{6}\tilde{\Omega}_b\tilde{\Omega}_q^{1/2}k^2\tau\end{aligned} \tag{4.118}$$

Neutrino Isocurvature Mode

The neutrino isocurvature mode is as follows. We set $C_\nu = -\Omega_\nu/\Omega_\gamma$ so that $\delta_\nu = 1$ at zero-order. As with the baryon isocurvature mode most variables are unmodified at lower orders. The exceptions are $\delta\dot{\phi}$ and $\delta\phi$ which receive corrections at zeroth and first order respectively.

$$\eta = \frac{\Omega_\nu(\tilde{\Omega}_c + 2\tilde{\Omega}_b)}{8\Omega_\gamma(\Omega_\gamma + \Omega_\nu)}k\tau + O(\tau^2) \tag{4.119}$$

$$\delta_\gamma = -\frac{\Omega_\nu}{\Omega_\gamma} + 4\eta + O(\tau^2) \tag{4.120}$$

$$\delta_\nu = 1 + 4\eta + O(\tau^2) \tag{4.121}$$

$$\delta_b = \tfrac{3}{4}\delta_\gamma \tag{4.122}$$

$$\delta_c = -\frac{3\Omega_\nu}{4\Omega_\gamma} - \left(\frac{4\Omega_\gamma(\Omega_\gamma + \Omega_\nu - 2)}{15 + 4\Omega_\nu} + \frac{3}{4}\right)\frac{\sqrt{6}\Omega_\nu\tilde{\Omega}_q^{1/2}}{\Omega_\gamma}k\tau + 3\eta + O(\tau^2) \tag{4.123}$$

$$q_\gamma = -\frac{\Omega_\nu}{3\Omega_\gamma}k\tau + \frac{\Omega_\nu(\tilde{\Omega}_c + 2\tilde{\Omega}_b)}{12\Omega_\gamma(\Omega_\gamma + \Omega_\nu)}(k\tau)^2 + O(\tau^3) \tag{4.124}$$

$$q_\nu = \tfrac{1}{3}k\tau + \frac{\Omega_\nu(\tilde{\Omega}_c + 2\tilde{\Omega}_b)}{12\Omega_\gamma(\Omega_\gamma + \Omega_\nu)}(k\tau)^2 + O(\tau^3) \tag{4.125}$$

$$v_c = \left(1 + \frac{8\Omega_\gamma(\Omega_\gamma + \Omega_\nu - 3)}{3(15 + 4\Omega_\nu)}\right)\frac{\sqrt{6}\beta\Omega_\nu\tilde{\Omega}_q}{2\Omega_\gamma(\sqrt{6}\beta\tilde{\Omega}_c + 2\tilde{\Omega}_q^{1/2})}(k\tau)^2 + O(\tau^3) \tag{4.126}$$

$$\pi_\nu = \frac{3}{15 + 4\Omega_\nu}(k\tau)^2 + O(\tau^3) \tag{4.127}$$

$$\delta\phi = \left(1 + \frac{8\Omega_\gamma(\Omega_\gamma + \Omega_\nu - 3)}{3(15 + 4\Omega_\nu)}\right)\frac{3\sqrt{6}\Omega_\nu\tilde{\Omega}_q}{2\Omega_\gamma(\sqrt{6}\beta\tilde{\Omega}_c + 2\tilde{\Omega}_q^{1/2})}k\tau + O(\tau^2) \tag{4.128}$$

$$\delta\dot{\phi} = \left(1 + \frac{8\Omega_\gamma(\Omega_\gamma + \Omega_\nu - 3)}{3(15 + 4\Omega_\nu)}\right)\frac{3\sqrt{6}\Omega_\nu\tilde{\Omega}_q}{2\Omega_\gamma(\sqrt{6}\beta\tilde{\Omega}_c + 2\tilde{\Omega}_q^{1/2})}k + O(\tau) \tag{4.129}$$

Growing Mode

The growing mode is as follows. We set $C_{g+} = 1$. This mode does not exist in the uncoupled mode and so we cannot look for modified terms. It is worth noting though that all variables except $\delta\phi$ and $\delta\dot{\phi}$ are zero up until second order.

$$\eta = \left(\frac{128\Omega_\gamma\Omega_\nu\tilde{\Omega}_q^2}{G(\Omega_\gamma+\Omega_\nu)(4\sqrt{6}\tilde{\Omega}_q^{1/2}+3\beta\tilde{\Omega}_c)(6\sqrt{6}\Omega_\gamma\tilde{\Omega}_q^{1/2}+4\sqrt{6}\Omega_\nu\tilde{\Omega}_q^{1/2}+3\beta\Omega_\gamma\tilde{\Omega}_c+3\beta\Omega_\nu\tilde{\Omega}_c)} \right.$$
$$- \frac{(75\beta^2\tilde{\Omega}_c^2+175\sqrt{6}\beta\tilde{\Omega}_c\tilde{\Omega}_q^{1/2}+500\tilde{\Omega}_q+48\Omega_\nu\tilde{\Omega}_q)}{9G(\Omega_\gamma+\Omega_\nu)}$$
$$\left. + \frac{32\sqrt{6}\Omega_\nu\tilde{\Omega}_q^{3/2}}{3G(6\sqrt{6}\Omega_\gamma\tilde{\Omega}_q^{1/2}+4\sqrt{6}\Omega_\nu\tilde{\Omega}_q^{1/2}+3\beta\Omega_\gamma\tilde{\Omega}_c+3\beta\Omega_\nu\tilde{\Omega}_c)} \right) \frac{27\tilde{\Omega}_q}{4}(k\tau)^2 \tag{4.130}$$

$$\delta_\gamma = \delta_\nu = 4\eta \tag{4.131}$$

$$\delta_b = 3\eta \tag{4.132}$$

$$\delta_c = 3\eta + O(\tau^3) \tag{4.133}$$

$$q_\gamma = q_\nu = \left(15\beta^2\tilde{\Omega}_c^2 - 5\sqrt{6}\beta\tilde{\Omega}_c\tilde{\Omega}_q^{1/2} - 140\tilde{\Omega}_q - 16\Omega_\nu\tilde{\Omega}_q \right.$$
$$\left. + \frac{32\sqrt{6}\tilde{\Omega}_q^{3/2}(5+\Omega_\nu)}{(4\sqrt{6}\tilde{\Omega}_q+3\beta\tilde{\Omega}_c)} \right) \frac{\tilde{\Omega}_q}{G(\Omega_\gamma+\Omega_\nu)}(k\tau)^3 \tag{4.134}$$

$$v_c = \frac{6\beta\tilde{\Omega}_q}{(4\sqrt{6}\tilde{\Omega}_q+3\beta\tilde{\Omega}_c)}(k\tau)^2 + O(\tau^3) \tag{4.135}$$

$$\pi_\nu = O(\tau^4) \tag{4.136}$$

$$\delta\phi = \dot{\phi}\tau \tag{4.137}$$

$$\delta\dot{\phi} = \dot{\phi} \tag{4.138}$$

where $G = (15\beta^2\tilde{\Omega}_c^2 + 55\sqrt{6}\beta\tilde{\Omega}_c\tilde{\Omega}_q^{1/2} + 300\tilde{\Omega}_q + 16\Omega_\nu\tilde{\Omega}_q)$.

§ 4.5 Numerical Results for CMB Angular Power Spectrum

In order to observe the effects of the coupling on the different modes we used our modified CAMB code to numerically integrate all the perturbation equations. The initial conditions for the modes given in the previous section were used to obtain the resulting CMB angular power spectra. These are shown in Fig. 4.3 together with the spectra of the corresponding uncoupled modes. In each case the essential shape of the spectrum is unchanged by a small coupling. For the adiabatic and neutrino isocurvature modes the coupling results in a relative suppression of power that is

most noticeable on intermediate scales around the first two peaks. In contrast the spectrum for the coupled CDM isocurvature mode is enhanced on all but the largest scales compared to its uncoupled counterpart. The coupling has least effect on the baryon isocurvature mode. Between $l \approx 10$ and $l \approx 700$ the spectrum is slightly suppressed but on the smallest and largest scales it is enhanced. Additionally, when the coupling is increased a shift in the peaks to smaller scales becomes visible.

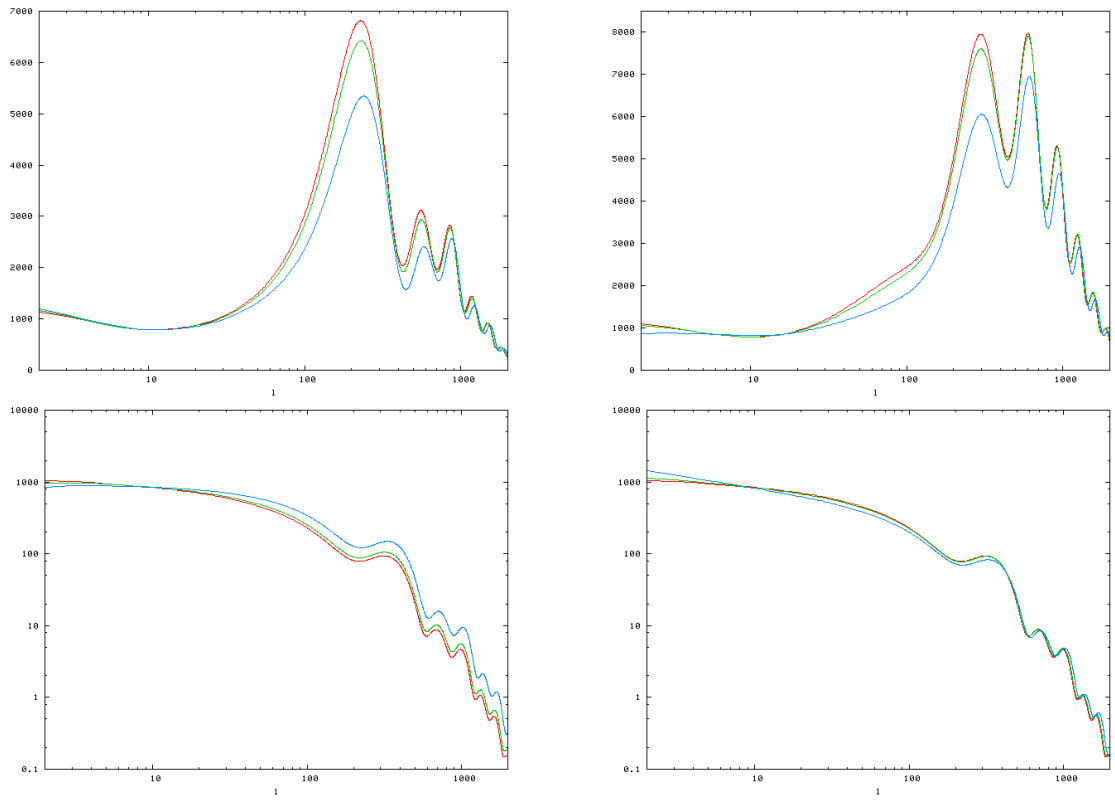

Figure 4.3: COBE normalised temperature angular power spectra as a function of multipole l. Top left: adiabatic/curvature. Top right: neutrino isocurvature. Bottom left: CDM isocurvature. Bottom right: baryon isocurvature. In each case we plot the uncoupled mode (red) and the coupled mode with $\beta = 0.1$ (green) and $\beta = 0.2$ (blue) and we use $h = 0.695, \Omega_b h^2 = 0.023$ and $\Omega_c h^2 = 0.083$ ($H_0 = 100h\,\mathrm{km\,s^{-1}Mpc^{-1}}$).

§ 4.6 Conclusions

In this chapter we have considered the effect of a coupling between quintessence and CDM on the possible perturbation modes. In particular the aim has been to determine the consequences of allowing for isocurvature modes in addition to the dominant adiabatic/curvature mode on constraints on the strength of the coupling arising from

observations of the CMB. Firstly the effect of the coupling on the background evolution at early times has been investigated. We have found that for exponential potentials and positive β the field is kinetically dominated ($w_q = 1$) until well into the matter dominated epoch, that the growth rate of Ω_c is the same as in the uncoupled case but that of Ω_q goes as a^2. Using these results evolution equations for the gauge-invariant CDM and quintessence perturbations at early times have been derived. These have then been solved analytically together with those governing the photon, neutrino and baryon evolution to give initial conditions for regular perturbation modes, both curvature and isocurvature. We have found that there exists no pure adiabatic mode but there is a growing mode. The initial conditions for the constant modes have been entered into CAMB and plots of the resulting angular power spectra produced. We find that the spectra for the coupled modes follow those for the uncoupled modes closely but whereas for the coupled CDM isocurvature mode the spectrum is enhanced on all but the largest scales, for the other modes there is a reduction in power on intermediate scales. This provides further motivation for considering mixtures of curvature and isocurvature modes and using Bayesian likelihood analysis to constrain the coupling strength β.

Chapter 5

Conclusions

In this thesis we have considered scalar-tensor theories as models of dark energy. The work done has been motivated by two broad questions. Firstly, what new observable effects might these models have in the early universe? And secondly, how are the constraints that have been placed on such models affected if we relax certain assumptions typically made about the early universe?

In addressing the first question we consider the modified evolution of perturbations in contrast to the majority of previous work which has focused on either the background evolution or late-time perturbations. In Chapter 2 we initially considered a general scalar-tensor theory with disformal couplings and derived for the first time the evolution equations for perturbation equations of a fluid, either relativistic or non-relativistic, coupled to the scalar field. For the case of a coupling only to baryons the modified sound-speed of the photon-baryon plasma was then derived. As an application of this we then looked at the effect on the CMB μ-distortion. Being created at high redshifts this is in fact the earliest direct probe of modified gravity and has not been considered before. For the case of a purely conformal coupling we found that the sound-speed and therefore the μ-distortion is smaller than in General Relativity and that a very large value for the coupling was required to generate significant deviations. This is possible if the coupling strength is allowed to vary with time and this might generally be expected in disformal theories where, as we have found, the effective coupling is a much more complicated function than in the conformal case.

In Chapter 3 we considered the screened models of modified gravity that satisfy a tomographic description in terms of the effective mass of the scalar field, $m(a)$, and the coupling strength, $\beta(a)$, and which are purely conformal scalar-tensor theories. We investigated the possible effects on the CMB angular power spectrum, again find-

ing that very large couplings were necessary in order to see deviations from ΛCDM. We therefore considered two phenomenological models where the coupling strength decreases with time: "generalised chameleons" with a power-law coupling and a transition model in which the coupling rapidly changes from a large value to a small one at some point before decoupling. For these models we applied the constraints that arise from local tests of gravity, in particular the lunar laser ranging experiment, and the variation of particle masses since BBN. For parameters satisfying these constraints we found that the generalised chameleons do not generate observable deviations from ΛCDM but the transition models may do so for sufficiently large couplings. We found that the effects took the form of alternating increases and decreases in power which could provide a distinctive signature of modified gravity.

In Chapter 4 we addressed our second question and chose to consider the effect of allowing for isocurvature perturbations on the constraints on coupled quintessence coming from CMB data. To do this we derived the initial conditions for the possible modes in a coupled quintessence universe. The resulting CMB spectra for adiabatic and isocurvature modes were computed and compared to the equivalent ones in ΛCDM. It was found that while a coupling causes an enhancement of the CDM isocurvature spectrum, there is a reduction in power for the other modes. It is left to future work to use these results to perform a Bayesian likelihood analysis of the cosmological parameters with CosmoMC, a Monte Carlo Markov Chain code, and determine whether the constraints on the coupling strength are modified by the inclusion of isocurvature perturbations.

In searching for an explanation of the dark energy phenomenon cosmologists have generated a great many different theories and models. Discriminating between these using observational data of improving quality and quantity is now a complicated task. It is therefore useful to discover what effects the different classes of theory could have on all available probes of cosmology and if possible identify characteristic features. In this thesis we have concentrated on models where the scalar field responsible for the late-time accelerated expansion interacts with some of the other forms of matter. For such models we have considered the possibility of using the CMB to constrain their parameters and potentially differentiate them from other types of theory. This work complements the investigations into the effects of these models on other observables such as those related to the distributions of galaxies. It is also important to investigate how uncertainties about other aspects of cosmology could affect the conclusions drawn from the analysis of observational data. In this thesis we looked at isocurvature perturbations but other possibilities include non-Gaussianity

(the initial perturbations not obeying Gaussian statistics), the number of neutrino species and the properties of dark matter (another major unresolved problem in cosmology).

Bibliography

[1] P. A. R. Ade *et al.*, [Planck Collaboration], (2013), [arXiv:1303.5076 [astro-ph.CO]].

[2] P. A. R. Ade *et al.*, [Planck Collaboration], (2013), [arXiv:1303.5082 [astro-ph.CO]].

[3] E. G. Adelberger [EOT-WASH Group Collaboration], (2002), [arXiv:hep-ex/0202008].

[4] E. G. Adelberger, B. R. Heckel and A. E. Nelson, Ann. Rev. Nucl. Part. Sci. **53** (2003), 77. [arXiv:hep-ph/0307284].

[5] L. Amendola, Phys. Rev. D **62** (2000), 043511.

[6] L. Amendola and C. Quercellini, Phys. Rev. D **68** (2003), 023514.

[7] L. Amendola, V. Pettorino, C. Quercellini and A. Vollmer, Phys. Rev. D **85** (2012), 103008.

[8] L. Amendola and S. Tsujikawa, *Dark Energy: Theory and Observations*, Cambridge University Press (2010).

[9] S. A. Appleby and R. A. Battye, Phys. Lett. B **654** (2007), 7. [arXiv:0705.3199 [astro-ph]].

[10] T. Barreiro, E. J. Copeland, and N. J. Nunes, Phys. Rev. D **61** (2000), 127301.

[11] R. Bean, E. E. Flanagan, I. Laszlo and M. Trodden, Phys. Rev. D **78** (2008), 123514.

[12] P. F. Bedaque, T. Luu and L. Platter, Phys. Rev. C **83** (2011), 045803. [arXiv:1012.3840 [nucl-th]].

[13] J. D. Bekenstein, Phys. Rev. D **48** (1993), 3641. [gr-qc/9211017].

[14] C. L. Bennett *et al.* [WMAP Collaboration], Astrophys. J. Suppl. **208** (2013), 20.

[15] J. C. Berengut, V. V. Flambaum and V. F. Dmitriev, Phys. Lett. B **683** (2010), 114. [arXiv:0907.2288 [nucl-th]].

[16] B. Bertotti, L. Iess and P. Tortora, Nature **425** (2003), 374.

[17] C. Brans and R. H. Dicke, Phys. Rev. **124** (1961), 925.

[18] P. Brax, Phys. Lett. B **712** (2012), 155. [arXiv:1202.0740 [hep-ph]].

[19] P. Brax, C. van de Bruck, S. Clesse, A. -C. Davis and G. Sculthorpe, Phys. Rev. D **89**, 123507 (2014). arxiv:1312.3361 [astro-ph.CO]

[20] P. Brax, C. van de Bruck, A. -C. Davis, J. Khoury and A. Weltman, Phys. Rev. D **70** (2004), 123518. [arXiv: astro-ph/0408415]

[21] P. Brax, C. van de Bruck, A. -C. Davis, B. Li, B. Schmauch and D. J. Shaw, Phys. Rev. D **84** (2011), 123524. [arXiv:1108.3082 [astro-ph.CO]].

[22] P. Brax, C. van de Bruck, A. -C. Davis, B. Li and D. J. Shaw, Phys. Rev. D **83** (2011), 104026. [arXiv:1102.3692 [astro-ph.CO]].

[23] P. Brax, C. van de Bruck, A. -C. Davis and D. J. Shaw, Phys. Rev. D **78** (2008), 104021. [arXiv:0806.3415 [astro-ph]].

[24] P. Brax, C. van de Bruck, A. -C. Davis and D. J. Shaw, Phys. Rev. D **82** (2010), 063519. [arXiv:1005.3735 [astro-ph.CO]].

[25] P. Brax, C. Burrage and A. -C. Davis, JCAP **1210** (2012), 016. arXiv:1206.1809 [hep-th].

[26] P. Brax, S. Clesse and A. -C. Davis, JCAP **1301** (2013), 003. [arXiv:1207.1273 [astro-ph.CO]].

[27] P. Brax and A. -C. Davis, Phys. Rev. D **85** (2012), 023513.

[28] P. Brax, A. -C. Davis and B. Li, Phys. Lett. B **715** (2012), 38. [arXiv:1111.6613 [astro-ph.CO]].

[29] P. Brax, A. -C. Davis, B. Li and H. A. Winther, Phys. Rev. D **86** (2012), 044015. [arXiv:1203.4812 [astro-ph.CO]].

[30] P. Brax, A. -C. Davis, B. Li, H. A. Winther and G. -B. Zhao, JCAP **1210** (2012), 002. [arXiv:1206.3568 [astro-ph.CO]].

[31] P. Brax, A. -C. Davis, B. Li, H. A. Winther and G. -B. Zhao, JCAP **1304** (2013), 029. [arXiv:1303.0007 [astro-ph.CO]].

[32] A. W. Brookfield, C. van de Bruck and L. M. H. Hall, Phys. Rev. D **74** (2006), 064028. [hep-th/0608015].

[33] C. van de Bruck and G. Sculthorpe, Phys. Rev. D **87** (2013), 044004. [arXiv:1210.2168 [astro-ph.CO]].

[34] R. R. Caldwell, R. Dave and P. J. Steinhardt, Phys. Rev. Lett. **80** (1998), 1582.

[35] E. Carretta, R. G. Gratton, G. Clementini and F. Fusi Pecci, Astrophys. J. **533** (2000), 215.

[36] S. M. Carroll, Phys. Rev. Lett. **81** (1998), 3067.

[37] J. Chluba, A. L. Erickcek and I. Ben-Dayan, Astrophys. J. **758** (2012), 76. arXiv:1203.2681 [astro-ph.CO].

[38] J. Chluba, R. Khatri and R. A. Sunyaev, Mon. Not. Roy. Astron. Soc. **425** (2012), 1129. arXiv:1202.0057 [astro-ph.CO].

[39] S. Clesse, L. Lopez-Honorez, C. Ringeval, H. Tashiro and M. H. G. Tytgat, Phys. Rev. D **86** (2012), 123506. [arXiv:1208.4277 [astro-ph.CO]].

[40] T. Clifton, P. G. Ferreira, A. Padilla and C. Skordis, Phys. Rept. **513** (2012), 1. [arXiv:1106.2476 [astro-ph.CO]].

[41] E. J. Copeland, M. Sami and S. Tsujikawa, Int. J. Mod. Phys. D **15** (2006), 1753. [hep-th/0603057].

[42] T. Damour and K. Nordtvedt, Phys. Rev. D **48** (1993), 3436.

[43] T. Damour and A. M. Polyakov, Nucl. Phys. B **423** (1994), 532.

[44] S. Das, P. S. Corasaniti and J. Khoury, Phys. Rev. D **73** (2006), 083509.

[45] A. -C. Davis, B. Li, D. F. Mota and H. A. Winther, Astrophys. J. **748** (2012), 61. [arXiv:1108.3081 [astro-ph.CO]].

[46] J. B. Dent, D. A. Easson and H. Tashiro, Phys. Rev. D **86** (2012), 023514. arXiv:1202.6066 [astro-ph.CO].

[47] S. Dodelson, *Modern Cosmology*, Academic Press (Elsevier), New York (2003).

[48] M. Doran, C. M. Müller, G. Schäfer and C. Wetterich, Phys. Rev. D **68** (2003), 063505.

[49] D. J. Eisenstein *et al.* [SDSS Collaboration], Astrophys. J. **633** (2005), 560.

[50] T. Faulkner, M. Tegmark, E. F. Bunn and Y. Mao, Phys. Rev. D **76** (2007), 063505. [astro-ph/0612569].

[51] W. Freedman *et al.* [HST Collaboration], Astrophys. J. **553** (2001), 47.

[52] S. Furlanetto *et al.*, science white paper submitted to the US Astro2010 Decadal Survey "Cosmology and Fundamental Physics" Science Frontier Panel. [arXiv:0902.3259 [astro-ph.CO]].

[53] J. Garcia-Bellido and D. Wands, Phys. Rev. D **53** (1996), 5437.

[54] M. Hamuy *et al.*, Astron. J. **112** (1996), 2391.

[55] K. Hinterbichler and J. Khoury, Phys. Rev. Lett. **104** (2010), 231301. [arXiv:1001.4525 [hep-th]].

[56] K. Hinterbichler, J. Khoury, A. Levy and A. Matas, Phys. Rev. D **84** (2011), 103521. [arXiv:1107.2112 [astro-ph.CO]].

[57] W. Hu and I. Sawicki, Phys. Rev. D **76** (2007), 064004. [arXiv:0705.1158 [astro-ph]].

[58] W. Hu, D. Scott and J. Silk, Astrophys. J. Lett. **430** (1994), 5.

[59] W. Hu and J. Silk, Phys. Rev. D **48** (1993), 485.

[60] W. Hu and N. Sugiyama, Astrophys. J. **471** (1996), 542. [astro-ph/9510117].

[61] E. Hubble, Proceedings of the National Academy of Sciences **15** (1929), 168.

[62] B. Jain, V. Vikram and J. Sakstein, Astrophys. J. **779** (2013), 39. [arXiv:1204.6044 [astro-ph.CO]].

[63] R. Jimenez *et al.*, Mon. Not. Roy. Astron. Soc. **282** (1996), 926.

[64] R. Khatri, R. A. Sunyaev, J. Chluba, Astron. Astrophys. **540** (2012), A124.

[65] J. Khoury and A. Weltman, Phys. Rev. Lett. **93** (2004), 171104. [arXiv:astro-ph/0309300].

[66] J. Khoury and A. Weltman, Phys. Rev. D **69** (2004), 044026. [arXiv:astro-ph/0309411].

[67] S. Kim, A. R. Liddle and S. Tsujikawa, Phys. Rev. D **72** (2005), 043506.

[68] A. Kogut *et al.*, JCAP **1107** (2011), 025.

[69] C. F. Kolda and D. H. Lyth, Phys. Lett. B **458** (1999), 197.

[70] A. Lewis and A. Challinor, CAMB Code Home Page, http://camb.info/.

[71] A. R. Liddle, A. Mazumdar and F. E. Schunck, Phys. Rev. D **58** (1998), 061301.

[72] A. R. Linde, Phys. Lett. B **158** (1985), 375.

[73] C.-P. Ma and E. Bertschinger, Astrophys. J. **455** (1995), 7.

[74] E. Majerotto, J. Valiviita and R. Maartens, Mon. Not. Roy. Astron. Soc. **402** (2010), 2344.

[75] J. C. Mather *et al.*, Astrophys. J. **420** (1994), 439.

[76] I. Navarro and K. Van Acoleyen JCAP **0702** (2007), 022.

[77] S. Nesseris and A. Mazumdar, Phys. Rev. D **79** (2009), 104006. [arXiv:0902.1185 [astro-ph.CO]].

[78] J. Noller, JCAP **1207** (2012), 013. [arXiv:1203.6639 [gr-qc]].

[79] K. A. Olive and M. Pospelov, Phys. Rev. D **77** (2008), 043524. [arXiv:0709.3825 [hep-ph]].

[80] E. Pajer and M. Zaldarriaga, JCAP **1302** (2013), 036. arXiv:1206.4479v1 [astro-ph.CO].

[81] S. Perlmutter *et al.* [Supernova Cosmology Project Collaboration], Astrophys. J. **517** (1999), 565. [astro-ph/9812133].

[82] P. Peter and J. -P. Uzan, *Primordial Cosmology*, Oxford University Press (2009).

[83] V. Pettorino, Phys. Rev. D **88** (2013), 063519.

[84] V. Pettorino, L. Amendola, C. Baccigalupi and C. Quercellini, Phys. Rev. D **86** (2012), 103507.

[85] D. Polarski and A. A. Starobinsky, Phys. Rev. D **50** (1994), 6123.

[86] R. Pourhasan, N. Afshordi, R. B. Mann and A. C. Davis, JCAP **1112** (2011), 005. [arXiv:1109.0538 [astro-ph.CO]].

[87] J. R. Pritchard and A. Loeb, Rept. Prog. Phys. **75** (2012), 086901. [arXiv:1109.6012 [astro-ph.CO]].

[88] C. de Rham, G. Gabadadze and A. J. Tolley, Phys. Rev. Lett. **106** (2011), 231101.

[89] A. G. Riess *et al.* [Supernova Search Team Collaboration], Astron. J. **116** (1998), 1009. [astro-ph/9805201].

[90] U. Seljak and M. Zaldarriaga, Astrophys. J. **469** (1996), 437.

[91] G. F. Smoot *et al.*, Astrophys. J. **396** (1992), L1-L5.

[92] T. P. Sotiriou and V. Faraoni, Rev. Mod. Phys. **82** (2010), 451.

[93] A. A. Starobinsky, Phys. Lett. B **91** (1980), 99.

[94] T. Tamaki and S. Tsujikawa, Phys. Rev. D **78** (2008), 084028. [arXiv:0808.2284 [gr-qc]]

[95] J. Valiviita, M. Savelainen, M. Talvitie, H. Kurki-Tuonio and S. Rusak, Astrophys. J. **753** (2012), 151.

[96] S. Weinberg, Phys. Rev. Lett. **59** (1987), 2607.

[97] J. G. Williams, S. G. Turyshev and D. H. Boggs, Phys. Rev. Lett. **93** (2004), 261101. [gr-qc/0411113].

[98] J. G. Williams, S. G. Turyshev and D. H. Boggs, Int. J. Mod. Phys. D **18** (2009), 1129. [gr-qc/0507083].

[99] J. G. Williams, S. G. Turyshev and D. Boggs, Class. Quant. Grav. **29** (2012), 184004. [arXiv:1203.2150 [gr-qc]].

[100] J. G. Williams, S. G. Turyshev and T. W. Murphy, Jr., Int. J. Mod. Phys. D **13** (2004), 567. [gr-qc/0311021].

[101] J. -Q. Xia, Phys. Rev. D **80** (2009), 103514.

[102] J. -Q. Xia, JCAP **1311** (2013), 022.

[103] I. Zlatev, L. M. Wang and P. J. Steinhardt, Phys. Rev. Lett. **82** (1999), 896.

[104] M. Zumalacarregui, T. S. Koivisto and D. F. Mota, Phys. Rev. D **87** (2013), 083010. arXiv:1210.8016 [astro-ph.CO].